INVESTIGATION ON THE EFFECT OF ADDITION OF SOME RARE EARTH ELEMENTS ON THE MECHANICAL BEHAVIOR FORMABILITY, AND WEAR RESISTANCE OF ALUMINUM

By
Safwan Mohammad A. Al Qawabah

Supervisor
Dr. Adnan I. Zaid Al-Kilani, Prof.

This Dissertation was Submitted in Partial Fulfillment of the Requirements of the Doctor of Philosophy Degree in Mechanical Engineering

Faculty of Graduate Studies
University of Jordan

December, 2007

This Dissertation (Investigation on the Effect of Addition of Some Rare Earth Elements on the Mechanical Behavior, Formability, and Wear Resistance of Aluminum) Was Successfully Defended and Approved on 16 /12 / 2007

Examination Committee	**Signature**
Dr. Adnan I. Zaid Al-Kilani, Chairman Prof. of Industrial Engineering.	
Dr. Saad Mohammad Habali, Member Prof. of Mechanical Engineering.	
Dr. Naser S. Al-Huniti, Member Prof. of Mechanical Engineering.	
Dr. Osama Mahmoud Abuzeid, Member Asso. Prof. of Mechanical Engineering	
Dr. Wa'il Radwan Tyfour, Member Asso. Prof. of Production Engineering (Mutah University)	

تعتمد كلية الدراسات العليا
هذه النسخة من الرسالة
التوقيع.....التاريخ.....

Dedication

TO MY GREAT FAMILY, WIFE, ORWA, BAR'A AND YAMAN

TO MY BIG FAMILY, MY PARENTS, SISTERS AND BROTHERS

ACKNOWLEDMENTS

I would like to express my special thanks and appreciation to my supervisor Prof. Dr. Adnan I. Zaid Al-Kilani for his supervision, guidance, cooperation and advice. I would like also to thank the examination committee members, Prof. Dr. Saad Mohammad Habali, Prof. Dr. Naser Al Huniti, Dr. Wa'il Radwan Tayfour and Dr. Usamah Mahmoud Abo Zaid. Also I would like to thank Prof. Dr. Sultan Abo Urabee (The President of Tafila Technical University) for his cooperation and guidance, Dr. Mahamoud Al-Banaa, Dr. Ubedullah Al Qawabeha, Mr. Fuad Karaman, Mr. Mohammad Araydah, Mr. Majed abo Quader, Eng. Hani Al-rawashdeh, Eng. Jamal Amayreh, Eng. Mohammad Ebedat, Mr. Mahamoud Al-Najdawee.

Finally I would like to thank the following firms:

1- Royal Scientific Society of Jordan (RSS)
2- Jordan University of Science and Technology.
3- Tafila Technical University
4- Karaman Factory.

List of Contents

List of Tables

LIST OF FIGURES

List of Abbreviation

σ : stress
d_o : average grain size
$\dot{\varepsilon}$: strain rate
σ_D : dynamic stress
σ_s : static stress
T_M : homologous temperature
P_i : extrusion pressure
$Y_{extruded}$: yield stress of extruded material
R : Extrusion ratio
A_o : initial area
A_f : final area
D_o : initial diameter of extruded billet
D_f ; final diameter of extruded billet
n* : factor of safety
n: engineering hardening index
Y: yield stress of punch material
$P_{critical}$: critical buckling load
E: modulus of elasticity
I: moment of inertia
L*: length of punch
d : smallest diameter of the plunger
σ_t : tangential stress
σr : radial stress
r_o: external radius of container
r_i : internal radius of container
$\bar{\sigma}$: representative stress
$\bar{\varepsilon}$: representative strain
$\bar{K}$: resistance to deformation
Y_{aver} : average flow stress
P: load
L : sliding distance
W_s: work of shear
V : worn volume
τ : shear stress
γ : shear strain
Wp : plastic work
K : strength coefficient
H : Hardness
K*: Wear rate coefficient
Δh : decrease in height

List of Appendices

INVESTIGATION ON THE EFFECT OF ADDITION OF SOME RARE EARTH ELEMENTS ON THE MECHANICAL BEHAVIOR, FORMABILITY AND WEAR RESISTANCE OF ALUMINUM

By
Safwan Mohammad A. Al-Qawabah

Supervisor
Dr. Adnan I. Zaid Al-Kilani, Prof.

ABSTRACT

Aluminum and its alloys solidify with a coarse columnar structure in the absence of grain refiners which tends to reduce their mechanical strength and surface quality. However, fine and equiaxed grain structure is achieved by the addition of small amounts of titanium (Ti) or titanium + boron, (Ti+B), into the melt before solidification.

Review of the available literature reveals that most of the published research work on the grain refinement of Al and its alloys is directed towards the effect of these refiners on the metallurgical aspects and little work is published on their effect on the mechanical behavior, fatigue strength and wear resistance. No work was carried out on the formability of aluminum or any of its alloys. This formed the main objective of this thesis.

As it has become customary in today's aluminum foundry to grain refine the aluminum melt before solidification by Ti or Ti+B to improve its surface quality and its mechanical behavior. The effect of addition of these two grain refiners commercially pure Al (at the rate which is normally used in industry) in addition to the effect of Zr addition on the grain size, general microstructure, mechanical characteristics, wear resistance and formability from extrusion and free upsetting is investigated. Furthermore, the effect of zirconium addition at a rate of 0.1 weight percentage to aluminum and Al grain refined by Ti or Ti+B from the metallurgical aspects, mechanical characteristics, formability and wear resistance is investigated and the obtained results are presented and discussed. It was found that Ti+B is better grain refiner than Ti although boron itself when added alone is not a grain refiner and the weight percentage of Ti when added with B is third its weight percentage when added alone.

Furthermore, it was found that addition of Zr at a rate of 0.1 wt % to Al resulted in poisoning of its grain size i.e. coarsening of the grains, whereas resulted in enhancement of the grain size when added to Al grain refined by Ti or Ti+B hence it improve of the grain refining efficiency of both Ti and Ti+B, being more pronounced in case of Ti+B.

Regarding the effect of Ti and Ti+B on the hardness and mechanical characteristics of Al, it was found that both of them resulted in improvement of its hardness; however Ti addition resulted in decrease of its mechanical characteristics e.g. its flow stress, ultimate tensile strength and its ductility, whereas addition of Ti+B resulted in improvement of its mechanical characteristics except its ductility which was reduced.

Addition of Zr to Al or Al grain refined by Ti resulted in decease of its hardness and its mechanical characteristics except its ductility which was enhanced. Addition of Zr to Al grain refined by Ti+B resulted in decrease of its hardness and its ductility but pronounced enhancement in its ultimate tensile strength.

The results obtained on the effect of addition of these elements on formability (extrusion) of commercially pure aluminum revealed that the extrusion process resulted in very pronounced grain refinement for Al and its five microalloys being maximum in the case of Al grain refined by Ti or Ti+B. Similarly, addition of Zr to Al or Al grain refined by Ti or Ti+B has been also grain refined by the extrusion process.

The extrusion also resulted in enhancement of the hardness of Al and its microalloys and their mechanical characteristics found that it improved the flow stress, ultimate tensile of Al and Al grain refined by Ti or Ti+B. Similarly when Zr addition resulted in improvement of hardness, flow stress and ultimate tensile strength. Regarding the effect of extrusion on ductility it was found that it was improved in case of Al-Ti, Al-Ti-B and Al-Ti-B-Zr microslloys and decrease of the ductility of Al, Al-Zr and Al-Ti-Zr.

The effect of Zr addition on the wear resistance of Al and Al grain refined by Ti or Ti+B using either the accumulated mass loss or the wear coefficient criterion revealed that they do not represent the wear data because they do not consider the plastic deformation at the worn end. A new model is suggested that based on shearing or chipping resulting in mass loss and the plastic deformation at the worn end is presented and discussed and found to assess the wear resistance, and found to be more realistic than the previously used methods.

1. INTRODUCTION

1.1 Aluminum

Aluminum is the second widely used metal due to it's desirable chemical, physical and mechanical properties. Wohler, in 1945, succeeded in preparing aluminum in slightly large quantities and indicated the relationship of aluminum to other metals and compounds and provided the awareness of remarkable lightness of aluminum,(Vanttron, 1967).

Due to it's high strength-to-weight ratio, besides other desirable properties e.g. desirable appearance, non toxic, non sparking , non magnetic, high corrosion resistance, high electrical and thermal conductivities and ease fabrication stimulated the developing of different Al-alloys in the last forty years, (Polmear, 1981).

These properties led to the association of aluminum and its alloys with transportation particularly with aircraft and space vehicles, construction and building, containers and packaging and electrical transmission lines.

1.1.1 Aluminum Alloys

Aluminum is a soft metal therefore; it is alloyed with other elements to form several alloys to improve its mechanical properties, wear resistance, and corrosion resistance. Aluminum alloys are classified into four categories:

1- Non-heat treatable casting alloys: These alloys are essentially binary alloys containing aluminum silicon. Non-heat treatable alloys do not respond significantly to heat treatment beyond annealing.

2- Non-heat treatable wrought alloys: These alloys contain trace of manganese or trace of magnesium. Aluminum-magnesium alloys are highly resistance to corrosion. Their mechanical properties allow them to be formed by variety of processes including forging, rolling, extrusion and drawing.

3- Heat-treatable casting alloys: these are complex alloys containing copper or nickel or both in a significant amount plus other alloying elements in lesser amounts. They respond to heat treatment and in particular to solution treatment and precipitation hardening.

4- Heat-treatable wrought alloys: These are complex alloys of aluminum together with alloying elements such as copper, magnesium, silicon and zinc, (Arthar, Elizabath, 1966).

1.1.2 Aluminum Micro Alloys

Rare earth materials, e.g. titanium, boron, zirconium, tantalum and hafnium some times exist on micron level (< 0.1 % weight) in metals and their alloys. Before 1952, if these elements existed in the metals and their alloys in this level were considered inclusions and their effect was neglected.

In 1952, Cibula found that the addition of titanium Ti or boron B or both Ti+B in micron level < 0.1% wt to commercially pure aluminum resulted in refinement of the grains of its microstructure and enhancement of its surface quality. Ever since, it became customary in the aluminum foundry to add Ti or Ti+B to the aluminum melt before solidification to refine its surface quality and several aluminum-titanium, Al-Ti, and aluminum-titanium-boron, Al-Ti-B, master alloys were developed and now commercially available for this purpose e.g. (Al-5% Ti- 1 % B), (Zaid, 2003).

Over the subsequent years and until the beginning of this century most of the reported work was directed towards the effect of rare earth materials on the metallurgical aspects of the grain refinement phenomenon and very rarely work was reported on the effect of addition of these elements on the mechanical behavior or wear resistance of aluminum and its alloys, (Zaid, 2003).

The available research work reveals that the addition of some of these elements, e.g. Ti or Ti+B, Zr or Ta to aluminum or its alloys resulted in refinement of the structure whereas elements Ti +Zr existed together resulted in the poisoning of the structure i.e. causes coarsening of the grains, which means that the effect of existence of these elements if exists results in larger grain size than if they were absent, (Abdel-Hamid and Zaid, 2000).

As the main goal of developing new materials or alloys is to be used in practice in industrial and engineering applications and this requires knowledge about their mechanical behavior, formability, machinability and wear resistance and due to the lack of available information, regarding these important characteristics it is anticipated that investigating the effect of addition of some of these elements e.g. Ti, Ti+ B, Zr on the formability and wear resistance of aluminum is worthwhile investigating.

1.2 Mechanisms of strengthening in metals

Understanding of the strengthening mechanisms require knowing the relation between dislocation motion and mechanical behavior of metals. Virtually all strengthening techniques rely on simple principal : restricting or hindering dislocation motion which renders the material harder and stronger.

The strengthening mechanisms can be introduced by solid solution, strain hardening, precipitation hardening and grain size reduction, (Callister, 1993).

Fine grain size is often desired for high strength. Fine particles may be added to increase strength and phase transformations may be utilized to increase strength, (Dieter, 1986).

1.2.1 Solid Solution Hardening

The introduction of the solute atoms into solid solution in the solvent-atom lattice invariably produces an alloy, which is stronger than the pure metal. There are two types of solid-solution hardening : substitutional and interstitial solid solutions.

The main aim is to raise the yield stress and the level of stress-strain curve. In multiphase alloy, each phase contributes certain characteristics to the over all properties of the aggregate, (Dieter, 1986).

1.2.2 Strain Hardening

A cold working process is used to harden metals or alloys that do not respond to heat treatment. Cold work produces elongation of the grains in the principal direction of the working, severe deformation produces a reorientation of the grains into a preferred orientation.The final strength of the cold worked solid solution alloy is almost greater than that of the pure metal cold worked to the same extent, (Dieter, 1986).

The free movement of the dislocations is impeded by the interaction with each other in the cross slip, in which a dislocation changes from one slip plane to another intersecting slip plane and with other barriers such as grain boundaries and precipitates. This produces strain hardening, (Rollason, 1989).

1.2.3 Strengthening by Grain Size Reduction

The size of the grains, or average grain diameter, in polycrystalline metal influences the mechanical properties. Adjacent grains normally have different crystallographic orientations and, of course, a common grain boundary, as indicated in figure (1)

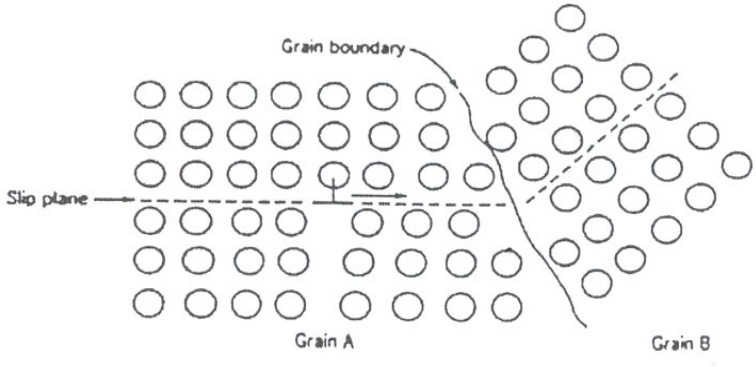

Fig. 1: The motion of the dislocation as it is encounters a grain boundary (Callister, 1993)

During plastic deformation, slip or dislocation motion must take place across this common boundary, say, from grain A to grain B, the boundary acts as a barrier to dislocation motion for two reasons:

1- Since the two grains are of different orientations, a dislocation passing into grain B will have change of its direction of motion; this becomes more difficult as crystallographic disorientation increases.

2- The atomic disorder within a grain boundary region will result in a discontinuity of the slip planes from one region into another.

A fine-grained material is harder and stronger than the one which is coarse grained, since the former has greater total grain boundary area to impeded dislocation motion. For many materials, the yield strength σ_y varies with grain size according to:

$$\sigma_y = \sigma_o + k_y d^{-1/2} \qquad (1.1)$$

In this expression, d is the average grain diameter, and σ_o and k_y are constants for a particular material, (Callister, 1993).

A more recent method of reducing the grain size is the grain refinement by additions of a very small amount of some refractory metals (Ta, Zr, Ti, B, V, Mo, Hf,….) on micron level in the order of 0.1 % weight percent to the melt before solidification.

1.3 The Formability of Aluminum

The formability of a material is the extent to which it can be deformed in a particular process before the onset of failure. Aluminum and its alloys are among the most readily formable metals. Aluminum alloy sheet usually fails during forming either by localized necking or by ductile fracture. Necking is governed largely by material properties such as work hardening and strain rate hardening which depends critically on the strain path followed by forming process. Ductile fracture occurs as a result of the nucleation and linking of microscopic voids particles and the concentration of the strain in narrow shear bands, (ASM, Vol. 14, 1998).

The formability of aluminum and its microalloys were studied through extrusion and free upsetting processes. Cold extrusion competes with such alternative metal forming processes as hot forging, hot extrusion, machining and some times casting. Cold extrusion is used when the process is economically feasible because of :

1- Saving in material.
2- Reduction or elimination of machining and grinding operations, because of the good surface finish and dimensional accuracy achieved of cold extruded parts.
3- Elimination of heat – treating operations.

The compression test is a small scale prototype of forging process (upsetting), so it was also used in this investigation.

To study the formability by extrusion, a forward extrusion die has been designed and manufactured, as it will be discussed later.

1.3.1 Extrusion

Extrusion is one of the forming processes where the material is compressed and pushed through a die of a certain geometrical shape and takes its shape while compressed above its elastic limit, i.e. within its plastic region. Cold extrusion is competitive with deep

drawing to form sheet metal. It has the advantage of requiring fewer steps, and the shell may be extruded with thick bottoms or flanges and walls. Extrusion is also competitive with casting and forging for producing the same parts.

1.3.1.1 Extrusion Types:

Four main types of extrusion exist:

1.3.1.1.1 Direct Extrusion (Forward Extrusion)

The billet slides relative to the container wall; the wall friction increases the ram force considerably, figure (2).

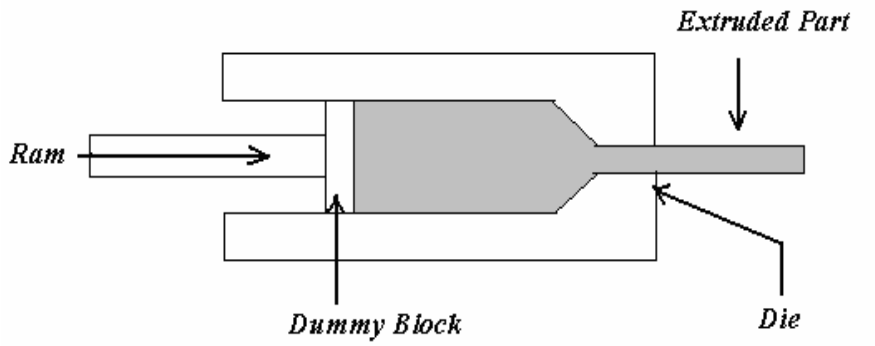

Fig. 2: Schematic diagram for direct extrusion.

Direct extrusion is used in the manufacturing of solid and hollow cylinder products as well as structural shapes which can not be obtained by any other metal-forming process. Obviously, the efficiency of material utilization in this case is usually low, and the waste can amount to 10 or even 15 percent, as opposed to rolling, where the waste is only 1 to 3 percent. This makes the productivity of direct extrusion much inferior to that of rolling in this respect, (Zaid, 1990).

It is worth mentioning that the conventional extrusion process has the advantages of high-dimensional accuracy and the possibility of producing complex sections from materials having poor plasticity.

On the other hand, its disadvantages include low productivity, short tool life and expensive tooling. Therefore, the process is usually employed for the manufacture of complex shapes with high-dimensional accuracy, especially when the material of the product has low plasticity.

1.3.1.1.2 Indirect Extrusion (Reverse, Inverted, or Backwards Extrusion)

Here the die moves toward the billet; thus, except at the die, there is no relative motion at the billet-container interface. As shown in figure (3), the metal flows out of the die opening in a direction opposite to the ram motion. There is almost no sliding motion between the billet and the container walls. This eliminates friction, and the extrusion load will be lower than that required in forward or direct extrusion by about 30 percent. In addition, the amount of waste scrap is reduced to only 5 percent. Nevertheless, indirect extrusion finds only limited application due to the complexity and the cost of tooling and press arrangement required.

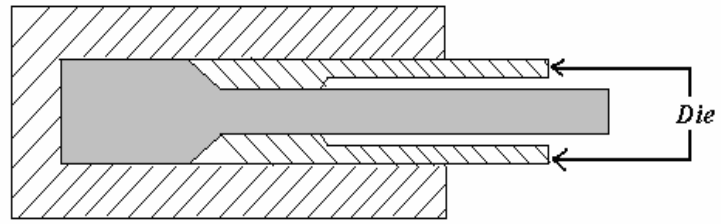

Fig. 3: Schematic diagram for indirect extrusion.

Another application of indirect-extrusion method is the manufacturing of hollow sections. In this case, the metal is extruded through the gap between the ram and the container; as in the indirect-extrusion method, the ram and the product travel in opposite directions.

1.3.1.1.3 Hydrostatic Extrusion

A radical development that eliminates the disadvantages of cold extrusion such as higher loads due to high friction involves hydrostatic extrusion. In this process, the

chamber is filled with a fluid that transmits the pressure to the billet, which is then extruded through the die. There is practically no friction along the container walls.

Figure (4) illustrates the basic principles of this process, where the billet is shaped to fit the die and surrounded by a high-pressure hydraulic fluid inside a container.

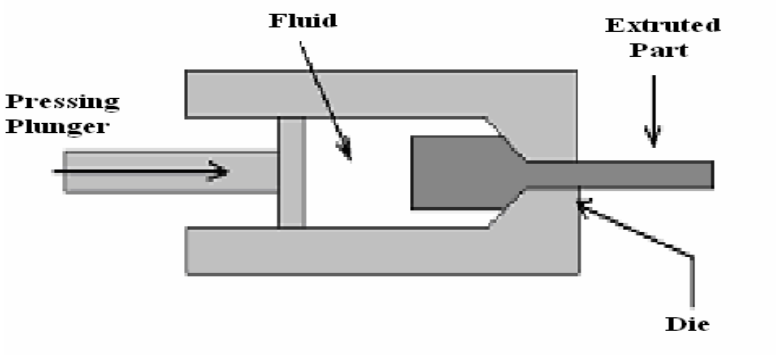

Fig. 4: Schematic diagram for hydrostatic extrusion.

When the plunger is pressed, it increases the pressure inside the container, and the resulting high pressure forces the billet to flow through the die. Friction between the billet and the container walls is thus eliminated, whereas friction between the billet and the die is markedly reduced. Also, the buckling effect of longer billets is eliminated, since all the length of the billet is subjected to hydrostatic pressure. This makes it possible to extrude very long billets. (Arnold, 1987)

1.3.1.1.4 Impact Extrusion

It is a form of indirect extrusion and is particularly suitable for hollow shapes. In impact extrusion, the punch descends at high speed and strikes the billet (slug), extruding it upward. The thickness of extruded tubular section is a function of the clearance between the punch and the die cavity.

There are three types of impact-extrusion process, forward, reverse, and combination; the names refer to the direction of motion of the deforming metal relative to that of punch. Figure (5) indicates the process of reverse impact extrusion. It is used for manufacturing hollow parts with forged bases and extruded sidewalls.

The process of forward impact extrusion is mainly employed in producing hollow or semi hollow products with heavy flanges and multiple diameters formed on the inside and outside.

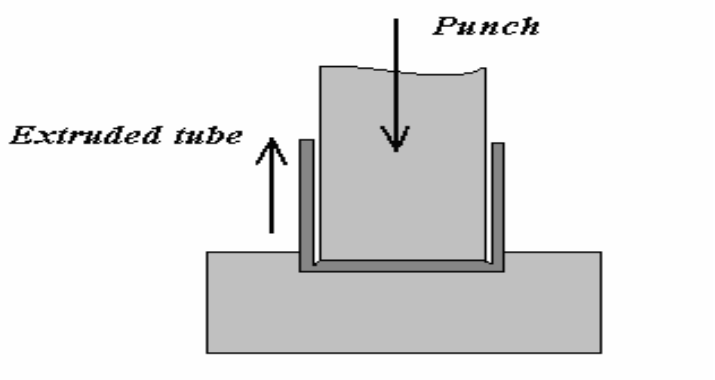

Fig. 5: Schematic diagram for impact extrusion.

Complex shapes can be produced by a combination of the two preceding processes, which are performed simultaneously in the same single stroke. Like the other impact extrusion methods, this process has the advantage of cleaner product surface, elimination of the need for trimming or further machining operations, and higher strength of the produced parts is obtained, (Arnold, 1987).

1.3.1.2 Load Variation and Pipe Formation in Extrusion

Figure (6) shows the general shape of the typical autographic record, (load-displacement diagram) observed for direct and indirect extrusion. There are at least three distinct regions associated with direct extrusion, these are:

1) Initial and rapid rise in load from O to A is due to the initial compression of the billet to fill the container, plus some extrusion of relatively undeformed material. When the load reaches point A, The metal begins to exit from the die under steady-state conditions.

2) The drop in load from A to B results from a steadily decreasing frictional effect at the billet-container interface. As more metal is extruded, the contact area at that interface

steadily decreases, thereby lowering the total frictional force. At point B, a non-steady situation begins accompanying load drop.

(Note that for indirect extrusion there is no relative motion at the billet-container interface and if frictional effects are constant, the steady-state load is constant as shown in Fig (6).

3) Somewhere between B and C a small cavity, called a pipe, forms at the centerline on the back face of the billet. C is the crucial point.

Pipe formation occurs when the radial compressive stress becomes large enough to induce buckling of the disc-like material still contained within the extrusion chamber. As displacement is continues, the pipe becomes larger. Eventually, the remainder of the billet, now an annular-like form, is subjected to direct compression, and a rapid load increase, illustrated by point C, occurs. The operation must cease before this load becomes too large and equipment damage will result.

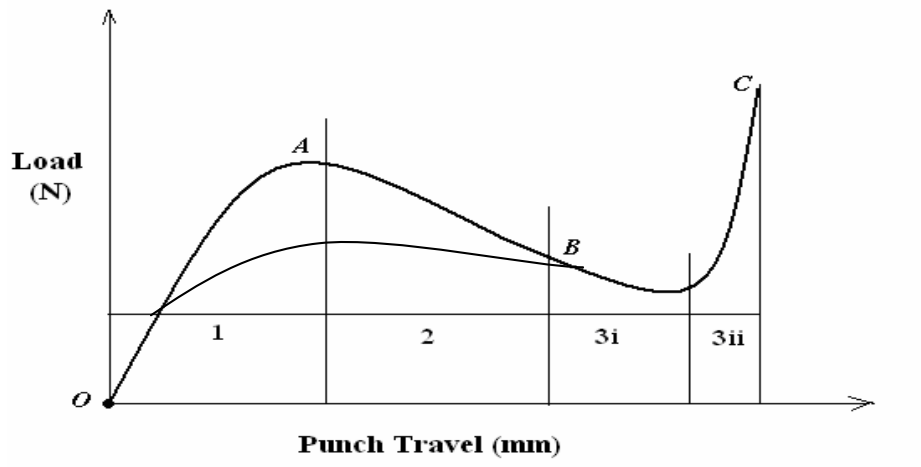

Fig. 6: Autographic record for direct and indirect extrusion.(Johnson, 1985)

1.3.1.3 Extrusion Classification

Like any other forming process, extrusion may be classified according to the temperature, and strain rate.

1.3.1.3.1 According to Temperature:

Extrusion is classified with respect to temperature, homologous temperature (H.T) defined as the ratio of working temperature (^{o}K) to melting temperature (^{o}K) of the billet material into:

1) Hot Extrusion

If H.T. > 0.5

Hot extrusion enables the metal to be easily supported, handled and forced from equipment. It is mostly used in large metallic pieces and aluminum. Most hot extrusion is done on horizontal hydraulic presses for common sizes rated from (150-25000 tons).

One of the major problems in hot extrusion is how to protect the equipment from high temperature (340-480 ^{o}C for Al), and (1200-1325 ^{o}C for steel).

2) Cold Extrusion

If: H.T. < 0.5

It is normally carried out at room temperature for most metals and metallic alloys, and at a speed ranging from 0.25 to 1.25 m/s, which generate heat that raises the temperature few hundreds of degrees, which causes reduction in extrusion force than if it is done slowly.

Cold extrusion requires higher force and energy than hot extrusion. Its advantages are that it is fast, improves mechanical properties, saves heat treatment and has little or no wastes. It can make parts with small radius and no draft, and can produce parts with small tolerances of about ±25μm and save machining as it has no oxidation. Cans fire extinguisher cases, are normally produced by cold extrusion.

3) Worm Extrusion:

If H.T. = 0.5

This type of extrusion works on moderate temperature, and is classified between cold and hot extrusion as a process and a product property.

1.3.1.3.2 Strain Rate

According to deformation in tension test the specimen may be manufactured according to low or high speeds, i.e. strained at different rates.

Deformation rate may be defined as function of speed as $\acute{\varepsilon}$ = V/L (one per second).

Where έ is the strain rate, V is a speed of deformation, and L is the specimen length.

The strain rate will decrease when specimen becomes longer. Increasing the strain rate will cause increase in yield stress, flow stress, ultimate stress, and fracture stress, also it increases work hardening characteristics and reduce the ductility of material.

Force in hot extrusion is difficult to calculate, because of strain rate sensitivity of metal at elevated temperature, figure (7).

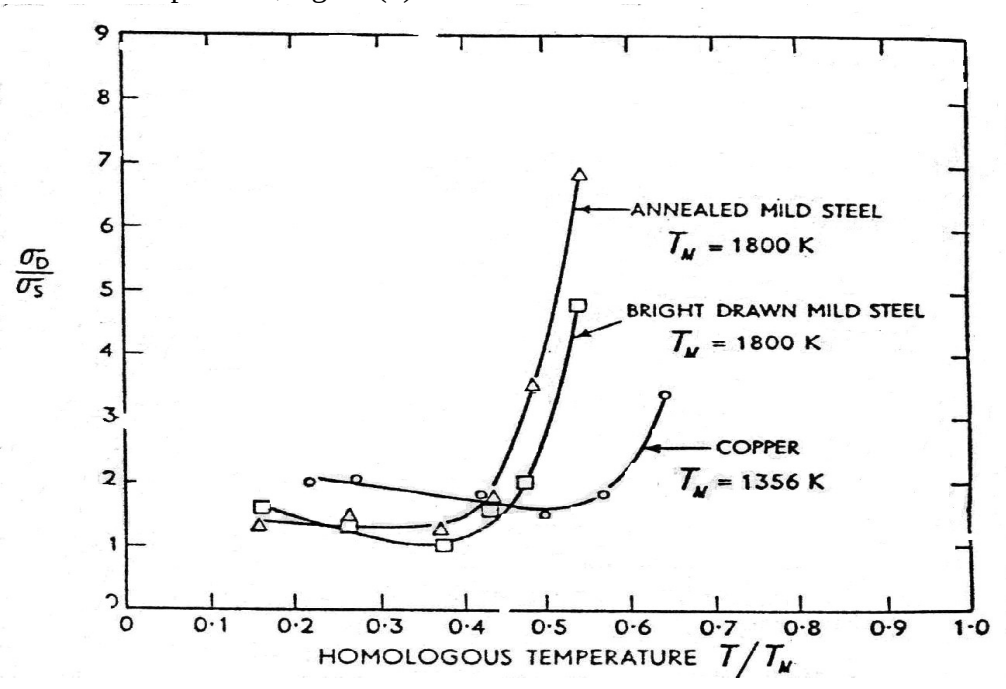

Fig. 7 : Showing the variation of dynamic /static mean yield stress ratios with homologous temperature (T/T_M), (Johnson, 1969)

The average strain rate is given by $\dot{\varepsilon} / t$ Where, $\bar{\varepsilon}$ is the representative strain in the process, and t is the forming time. Loading processes in general and forming processes in particular are classified with respect to strain rate into:

1) Quasi Static ($\dot{\varepsilon} = 10^{-4}/s - 10^{0}/s$):

In these processes, the time ranges from seconds to few minutes e.g. all presses mechanical, hydraulic or servomotor types fall within this range.

2) Intermediate Rate ($\dot{\varepsilon} = 10^{0}/s - 10^{2}/s$):

The time in these processes is in the order of milliseconds e.g. all types of hammers, whether of the falling weight (drop hammers), spring hammers or hydraulic hammers.

3) Dynamic or High Strain Rate-Impact on Dynamic Processes ($\dot{\varepsilon} = 10^{2}/s - 10^{4}/s$):

The time in these processes is of the order of microsecond e.g. all high-energy rate forming processes (HERF) e.g. explosive forming and gas forming processes.

4) Shock Loading ($\dot{\varepsilon} > 10^{4}/s$):

In general, increasing the strain rate will cause increase in yield stress, flow stress, ultimate tensile strength, and fracture stress. In addition, it increases the work hardening characteristics of the material and reduces its ductility.

1.3.1.4 Metal Flow in Extrusion:

There are three different patterns of flow in direct extrusion as shown in figure (8). The conditions leading to these different flow patterns are :

1) The most homogenous flow pattern is obtained when there is no friction at billet-container-die interfaces. This type of flow occurs when the lubricant is very effective or with indirect extrusion, figure (8.a).

2) When the friction along all interfaces is high, a dead-metal zone develops, where the high-shear area as the material flows into the die exist, some what like liquid following into funnel. This configuration may indicate that the billet surfaces (with there oxide

layer and lubricant) could enter this high-shear zone and be extruded, causing defects in the extruded product, figure (8.b).

3) In the third configuration, the high-shear zone extends farther back. This extension can result from high container-wall friction, which retards the flow of the billet, or from materials in which the flow stress drops rapidly while increasing temperature. In hot working, the material near the container walls cool rapidly and hence increases in strength; thus, the material in the center regions flow toward the die more easily than that at the outer regions. As a result, a large dead-metal zone forms, and the flow is inhomogeneous. This flow leads to a defect known as a pipe, or extrusion, defect, figure (8.c).

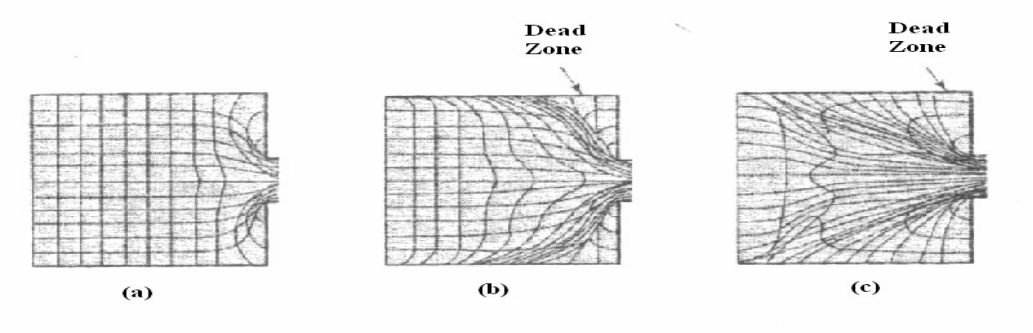

Fig. 8 : Schematic illustration of three different types of metal flow in direct extrusion (Kalpakjian, 2003)

1.3.1.5 Extrusion Defects

Metal forming is indeed the most useful production tool in manufacture of metal products and is less expensive than cutting methods when large number of parts is required. Cold forging and extrusion of steel and the plastic forming of brittle materials are recent example. One of the major limitations in metal forming is the creation of defects in the product.

There are three principal defects in extrusion: surface cracking, extrusion defect, and internal cracking. These defects are described as follows:

1.3.1.5.1 Surface Cracking:

These defects occurs if the extrusion temperature, friction, or extrusion speed is too high, surface temperatures rise significantly, this can lead to surface cracking and tearing. This situation can be avoided by using lower temperatures and speeds.

1.3.1.5.2 Pipe Defect:

This type tends to draw surface oxides and impurities towards the center of the billet, much like a funnel. This defect is known as extrusion defect, pipe, tailpipe, and fishtailing. This defect can be reduced by modifying the flow pattern to a less inhomogeneous one, such as by controlling friction and minimizing temperature gradients. Another method to avoid this defect is to machine the surface of the billet prior to extrusion to eliminate scale and impurities. The extrusion defect can also be avoided by using a dummy block that is smaller in diameter than the container, thus leaving a thin shell along the container wall as extrusion progresses.

1.3.1.5.3 Internal Cracking:

Some times referred to as central burst, these situations are attributed to a state of hydrostatic tensile stress at the center line of deformation zone in the die. This situation is similar to the necked region in an uniaxial, (Zaid, 1990).

1.3.1.6 Cold Extrusion of Aluminum Alloy Parts

Aluminum alloys are well adapted to cold (impact) extrusion. The lower- strength, more ductile alloys, such as 1100 and 3003, are the easiest to extrude. When higher mechanical properties are required in the final product, heat-treatable grades are used. The cold extrusion process should be considered for aluminum parts for the following reasons. High production rates - up to 4000 pieces per hour- can be achieved. However, even when parts are large and complex shape, lower production rates may be still economical. Although nearly all aluminum alloys can be cold

extruded, the easiest alloy to extrude (1100) has been assigned an arbitrary value of 1.0 in the comparison, (ASM, Vol.14, 1998).

1.4 Wear of metals

Wear is defined as the erosion of material from a solid surface by the action of another solid. The study of the process of wear is part of the discipline of tribology. Tribology is the science and technology of friction, lubrication and wear derived from the Greek tribo meaning (I rub), defined as the science and technology of interacting surfaces in relative motion and all practices related thereto. The study of tribology is commonly applied in bearing design. Basically any product where one material slides or rubs over another is affected by complex tribological interactions, whether lubricated (i.e. hip implants and other artificial prosthesis) or unlubricated (some studies, for examples, have looked at high temperature sliding wear in which conventional lubricants can no longer be used and the formulation of complicated oxide layer glazes have been observed to protect against wear).

The mechanism of wear is very complex so there are theories attempting to explain the wear process on a microscopic scale and to relate the magnitude of wear to the material properties, and the number and nature of encounters. The first theory was proposed by Holm (1946), who related wear rate to the number of inter-atomic encounters between opposing surfaces. However, the idea of the material removal from solids by plucking of atoms has not been generally accepted. The more realistic assumption is that wear occurs as a results of interaction between surface asperities. It should be understood that the real area of contact between two solid surfaces compared with the apparent area of contact is invariably very small, being limited to the points of contacts between surface asperities. The load applied to the surfaces will be transferred through these points of contacts and the localized forces can be very large. The

material properties such as hardness, strength, ductility, work hardening etc. are very important factors for wear resistance, but other factors like surfaces finish, lubrication, load, speed, corrosion, temperature and properties of the opposing surfaces etc. are equally important. Wear can occur through many mechanisms: adhesion, abrasion, third body, surfaces fatigue and corrosion, from which the different types of wear existing in engineering applications are attributed to, which will briefly reviewed in this section.

1.4.1 Adhesive wear

Adhesive wear is also known as scoring, galling, or seizing. It occurs when two solid surfaces slide over one another under pressure. Surface projections, or asperities, are plastically deformed and eventually welded together by the high local pressure. As sliding continues, these bonds are broken, producing cavities on the surface, projections on the second surface, and frequently tiny, abrasive particles, all of which contribute to future wear of surfaces.For example, when there is relative motion between two surfaces, bonding of asperities occurs. Continued motion of the surfaces results in breaking the bond junctions. Each time a bond junction is broken, a wear particle is created, usually from the weaker material. In the theory of adhesive wear, it was assumed that surfaces were rough and the contact occurred between asperities which were assumed to be hemispherical and the particles removed were equi-axed and directly related to the size of the asperity. This leads to the relationship :

$$V= (KPL)/3H \qquad (1.2)$$

Where: V is the worn volume, P is the load, L is the sliding distance. H is the hardness, and K is a constant which was interpreted as the probability that a particular asperity contact could produce a wear particle. In some cases when tangential motion imposed to cause the slider to move across the surfaces, the adhesion bonds at the interface are

stronger than the cohesive bonds across the slip or cleavage planes and fracture then occurs. Surfaces which are held apart by lubricating films, oxides films etc. reduce the tendency for adhesion to occur. The mechanism of adhesive wear is shown below in figure (9).

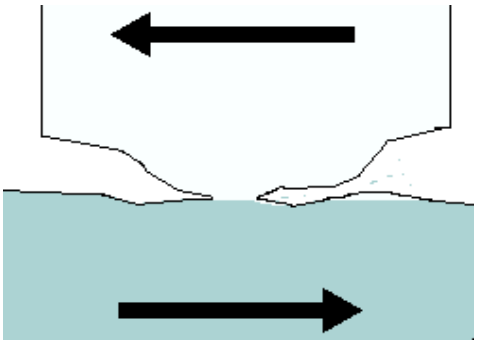

Fig. 9: Adhesive wear mechanism

1.4.2 Abrasive wear

Abrasive wear can be defined as wear in which hard asperities on one body, moving across a softer surface, under some load, penetrate and remove material from the surface body, leaving a groove**.** The mechanism of abrasive wear is shown below in figure (10)**.**

Abrasive wear occurs between surfaces of different relative hardness. In an abrasive wear mechanism, micro roughened regions and small asperities on the harder surface locally plow through the softer surface. Abrasive wear results in the softer material being moved from the track traced by the asperity during the motion of the harder surface.These hard particles either may be present at the surface of a second material or may exist as loose particles between two surfaces. The most obvious manifestation of this kind of wear is the grooves produced in the surface, and for this reason abrasive wear has also been termed ‘grooving wear'.

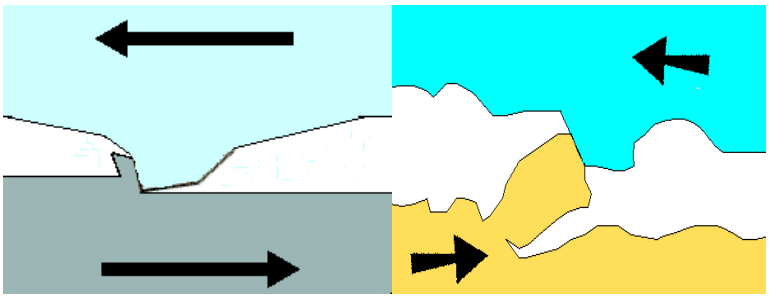

a) Two body abrasion

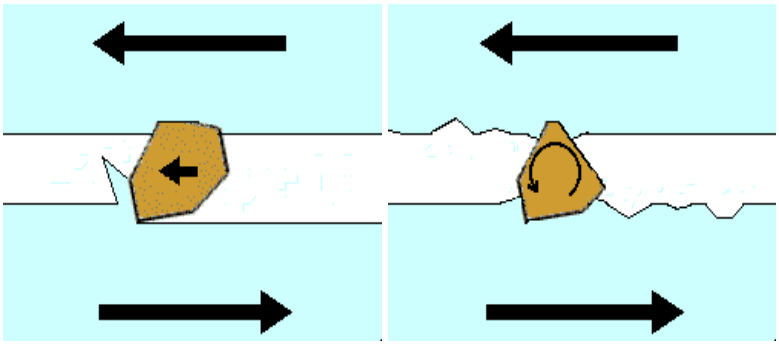

b) Three body abrasion

Fig. 10 : Abrasive wear mechanisms

1.4.3 Surface fatigue

Surface fatigue is a process by which the surface of a material is weakened by cyclic loading, which is one type of general material fatigue. It was until quite recently, generally considered in rolling contacts only, but localized fatigue in an asperity scale is now being increasingly recognized as a significant factor in sliding.

1.4.4 Delaminating wear

Delaminating wear is a results of cracks forming the surface and propagating to link up with other cracks. They are the results of the sub-surface strain gradients caused by the load and the anti-adhesion force and are aggravated by fatigue or defective material. As a result, sub-surface deformation occurs and the material becomes detached as wear

debris of a platelet or laminated form. The structure of the debris therefore reflect that of the sub-surface structures from which they originated. If the sub-surface structure of the alloy is itself of a laminar type, it is more vulnerable to this kind of wear.

1.4.5 Third body wear

Is a form of abrasive wear that occurs when hard particles become embedded in a soft surface. figure (11).

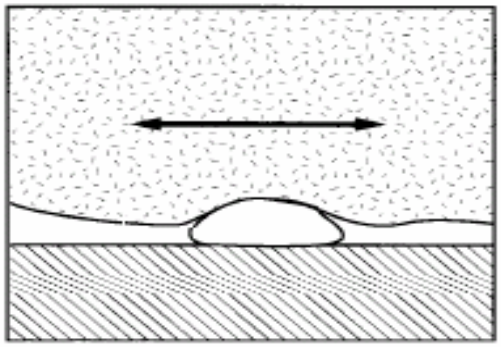

Fig. 11: Third Body Wear

1.4.6 Corrosive wear

Corrosive wear is an indirect wear mechanism, defined as the deterioration of useful properties in a material due to reactions with its environment. It is of third body wear, where the liberated corrosive debris acts as an abrasive third body. Corrosive wear can also be considered an accelerating mechanism of corrosion itself.

1.4.7 Fretting Wear

Fretting is a small amplitude oscillatory motion, usually tangential, between two solid surfaces in contact. Fretting wear occurs when repeated loading and unloading causes cyclic stresses which induce surface or subsurface break-up and loss of material. Vibration is a common cause of fretting wear.

1.5 Parameters Affecting Wear

There are many factors that affect wear, which should be considered, they are classified in three groups: Operating conditions, Material structure and properties and Environmental conditions.

1.5.1 Operating conditions

1.5.1.1 Load

Depending on the application, the applied load may be low, medium or high. It may be unidirectional or reversing, continuous or intermittent. It governs the friction and adhesion resistance and consequently the rate of wear. It has therefore a pronounced influence on wear. The resistance of metal to severe wear under high load conditions does not always correlate with their wear resistance under less severe conditions. In a sliding wear situation, wear rate increases with load and sliding distance although not necessarily in a linear manner. This indicates that there can be more than one wear mechanism operative.

1.5.1.2 Velocity

Velocity, like loading, can be varying from low to high, unidirectional or reversing, continuous or intermittent. It is one of the factors that affect the wear rate although, in some cases, speed has little effect on wear. In other cases it increases the rate of wear and yet in other cases it reduces it. This is because the effect of speed is related to other factors such as lubrication and the temperature which generate from friction.

1.5.1.3 Lubrication

The object of lubrication is to reduce friction and the tendency to adhesion and to mitigate their effects. There are five types of lubrication:

- Hydrodynamic lubrication in which the mating surfaces are separated by a fluid film; in this case adhesion is prevented and little surface distortion occurs.
- Hydrostatic lubrication in which the lubricant is supplied under pressure and is able to sustain higher load without contact taking place between the surfaces.
- Elasto-hydrodynamic lubrication in which the pressure between the surfaces is so high and the lubricant film is so thin that elastic deformation of the surfaces is likely to occur and is a feature of this kind of lubrication.

- Boundary lubrication in which an oil or grease, containing a suitable boundary lubricant, separates the surfaces by what is known as ‘adsorbed molecular films’; appreciable contact between asperities and formation of junctions may occur.
- Solid lubricants which provide a solid low shear strength film between the surfaces.

It may not always be possible to lubricate in a given wear situation and there are many demanding unlubricated sliding systems in various industries. In other cases, it may be necessary to adapt to a lubricant dictated by circumstances, such as water.

1.5.1.4 Surface finish

Surface finish affects wear. A well-polished surface finish - say less than about 0.25 µm- provides more intimate contact between the surfaces. This results in more interaction between them and may lead to forming local weld junctions and therefore a

greater susceptibility to galling. Lubricants also tend to be swept away between smooth surfaces whereas shot peening of the surface helps to retain a lubricant. If, on the other hand, the surfaces are too rough - say 2 µm - the asperities will tend to interlock resulting in severe tearing and galling. Most machined finish, however, fall within an intermediate range of surface finish. It is advisable to give the harder of the two surfaces a finer finish to eliminate asperities that can plough into the softer material.

1.5.1.5 Material structure and properties

Among the most important factors affecting wear are those relating to the structure and properties of the mating materials themselves.

1- Microstructure and space lattice structure.
2- Oxide film.
3- Tribological compatibility and adhesion.
4- Coefficient of friction.
5- Tensile properties.
6- Elastic properties.
7- Thermal conductivity.
8- Hardness.
9- Metal defects.

1.5.1.6 Environmental conditions

1.5.1.6.1 Inter-face temperature

Inter-face temperature also influences wear performance. It may result either from ambient conditions or from frictional heating caused by heavy loads and high speeds.

High temperature has an effect on the oxide film which adversely affects wear performance. It also affects mechanical properties, reduces hardness and increases the tendency to galling and to surface deformation due to plastic flow.

1.5.1.6 .2 Corrosion

In many cases, the apparent 'wear' of a metal surface is the result of corrosion followed by mechanical wear of the corrosion product. The corroding agent varies widely, from sulphuric acid, originating from products of combustion, to atmospheric contamination in industrial or marine environments. The proportion of wear attributable to corrosion is impossible to assess, but it is advisable to use a corrosion-resistant material. Because corrosion is liable to attack both the surface and sub-surface layers of an alloy, it is liable to undermine its wear performance.

1.5.1.6 .3 Foreign particles

Hard foreign particles finding their way between the mating surfaces can plough grooves into the softer surface and cause severe abrasive wear. Steps need to be taken, therefore, to prevent the ingress of hard foreign particles. Filtering systems normally only remove the coarser particles, and the resistance of the material to abrasion therefore assumes considerable importance for most bearing applications.

1.6 Objective of the Work

Due to the attractive properties of aluminum, and its wide usage in our life, it is necessary to enhance its hardness and other mechanical properties to improve and expand its usage, so the proper method for this is the grain refinement by rare earth materials.

The main goal of developing new materials or alloys is to be used in practice in industrial and engineering applications. This requires knowledge about their mechanical behavior, formability, machinability and wear resistance; and due to the lack of available information regarding these important characteristics it is anticipated that investigating the effect of addition of some of these elements e.g. Ti, Ti+ B, Zr on the formability and wear resistance of aluminum is worthwhile investigating. This formed the research work. In this thesis, the effect of the addition of some of these elements when added alone or together on the mechanical behavior, formability and wear resistance of commercially pure aluminum is investigated. It is hoped this study will expand the existing knowledge of the state of grain refinement of metals in general and aluminum and its alloys in particular.

2. LITRETURE REVIW

2.1 Grain Refinement of Aluminum

Cibula (1949) showed that the presence of titanium, particularly in the presence of carbon or boron, produced a good refining effect in aluminum. Since then, it became an industrial practice to add titanium, either alone or with boron, to grain refine aluminum and its alloys. Originally, salt mixtures such as k_2TiF_6 with KBF_4 or borax were added for the Al melt for this purpose. However, this method gave variable recoveries of titanium and boron in addition to producing a troublesome slag. Furthermore, use of salts requires a high and costly addition rate to achieve a stationary grain refinement, for those reasons the use of salts was applied and subjected in the mix of master alloys. Al-Ti binary and Al-Ti-B ternary master alloys of different compositions have been developed for the grain refining of aluminum and its alloys.

Jones and Pearson (1976), the ternary Al-Ti-B master alloy in common use contains 5% Ti and 1% B, wt, and has two crystalline intermediate compounds, namely small crystallites of titanium diboride and large crystals of $TiAl_3$.

Cibula and Muriceau (1949, 1976) the increasing, and the increasingly efficient use of additions of Al-Ti-B master alloy has been justified from the technological and scientific point view. Although the mechanism of grain refining of Al and its alloys by these master alloys is still a controversial mater and further work needs to be carried out to verify the suggested mechanisms. It appears that more than one mechanism is reasonable for the grain refining, depending on the master alloy used, the cast alloy and the prevailing process conditions and other parameters. Several assumptions have been made to explain the mechanism.

Cibula (1949) It was reported that the grain refinement of aluminum is due to the nodular of α-Al by the aluminized particles.

Abdel-Hamid (1985) has discussed the mechanism and showed that a high local Ti-concentration exists in the vicinity of TiB_2 particles making high efficient nuclei for Al grains. Recently, others have also suggested the local Ti-enrichment associated with TiB2 particles, (Johnson and Cornish, 1980).

The grain refining showed that the efficiency of grain refinement depends upon:

a) The composition (Ti-concentration and Ti/B ratio) of the grain refining master alloys and its microstructure (size and morphology of $TiAl_3$ and TiB_2 particles).

b) The rate of addition of the master alloy (the level of Ti added).

c) The melt temperature and holding time (contact time) before casting.

d) The purity or composition of Al-cast i.e. the level of impurity such as Fe, Si or the presence of some alloying elements which can enhance the grain refining efficiency e.g. V, Mo, Nb or poison it e.g. Mn, Zr, Ta and Cr.

Zaid and Abdel-Hamid (2000) investigated the effect of microalloying aluminum and its alloys by different refractory metals on.

Most of the reported work on grain refinement was directed towards the effect of addition these elements on the grain size and microstructure and little attention has been given to their effect on the mechanical behavior, machinability and fatigue life of aluminum.

Zaid and Abdel-Hamid (1999) seems to be the first who reported the effect of addition of some rare earth materials namely V and Zr on the mechanical behavior and machinability of commercially pure aluminum.

Recently, Zaid and Al-Afsha (2001) reported the effect of Ta on the mechanical behavior and machinability of aluminum, Zaid and Al-Alami (2001) have investigated the effect of V, Mo elements on the fatigue life and strength of aluminum.

More recently, Zaid (2005) reported the metallurgical aspects of the fractured surfaces

2.1.1 Factors Affecting Grain Refinement

Jones and Pearson (1976) reported that the grain efficiency is affected by many factors these summarized in Table (1) under three headings namely:

i) Parameters related to Al or Al alloy melt.

ii) Parameters related to the grain refiner itself.

iii) Parameters related to the procedure followed in carrying out the grain refinement process. The effectiveness of the grain refinement depends on the purity of the Al melt. The presence of small amount of impurities or alloying elements can strongly affect the grain refining efficiency of the Al-Ti or Al-Ti-B master alloys.

Table (1): Summary of the Parameters Affecting Grain Refiner

I	Parameters Related to the Al and Al Alloy Melt	Purity : high or commercial chemical composition: wt% of each element, impurities and residuals, recycling % method of production: cast or formed
II	Parameters Related to the Grain Refiner	Chemical composition: Ti and B levels, Ti:B ratio, residuals or impurities, manufacturing process, form: salt, foil, sheet, rod or ingot. Grain size, uniformity of distribution of grain refining particles, addition level
III	Parameters Related to the Process of Grain Refinement	Method of addition: one set or more, furnace atmosphere, addition temp., holding or contact time (Fading), stirring time, pouring temperature, rate of cooling: inside the furnace, chilled, in air.

Abdel–Hamid (1989) showed that aluminum and most of its alloys solidify with a course columnar structure in the absence of grain refiner. Whereas, fine and equiaxed grain structure is obtained by the addition of small amounts of Ti or Ti+B into the melt before casting. When Ti is added alone, its presence in the melt must exceed the peritictic composition of about 0.15 % by weight, to obtain a satisfactory

grain refining. However, in the presence of boron, even in ppm order, an important refinement is obtained at Ti content as low as 0.005 %, although boron itself is not a grain refiner.

Thislethwaite and Birch (1985, 1986) experience, based on experimental results, have shown that optimum grain refining properties are achieved using Al-Ti-B master alloys with a Ti : B ratio of about 5:1.

Abdel-Hamid and Arjuna (1989, 1996) reported that the presence of some other alloying elements either as impurities or additives e.g. Zr, Cr may cause the grain refining effect to deteriorate. This generally referred to in the literature as "poisoning" and this term is also used when aluminum or its alloys are difficult to be grain refined due to the presence of a certain alloying element or when the grain size obtained in the alloy is much coarser in the presence of the alloying element than when it is absent.

Abdel–Hamid and Zaid (2000) reported that the grain refining efficiency deteriorates in the following cases :

i) Superheating of the Al melt i.e. high pouring temperatures.

ii) Prolonged (holding) or contact times after addition of the grain refiner, normally referred to this process as (fading).

iii) Passing certain gases (N2, Ar, Hz, or air) through the melt after the addition of grain refiner.

iv) Presence of certain elements, namely: Zn, Zr, Ta, and Cr and to lesser extent Mn, Ta, Li and high levels of Si. These elements are known as poisoning elements since they adversely affect the grain refining efficiency of the master alloy. The causes of the grain coarsening in the first three cases are well known and can be avoided.

The causes were attributed to the removal of the active nuclei from the bulk of Al melt by dissolution, gravity segregation/decantation or adherence of the nuclei with the floating gas bubbles. On the other hand, the exact reasons for grain coarsening caused by the presence of the poisoning elements, Zr and Cr are not established and are still a controversial matter, and needs clarification.

2.1.2 The Mechanisms Proposed for Grain Refinement and Poisoning

2.1.2.1 The Peritectic Reaction Theory: researchers of this theory Abdel-Hamid et al. (1985) attribute the grain refinement to the nucleation of aluminum by the compound $TiAl_3$ particles, in the Al-Ti system, according to the following peritectic temperature reaction at 1340 ˚C

$$\text{Liquid} + TiAl \text{ ===== } TiAl_3 \qquad (2.1)$$

The $TiAl_3$ compound has a tetragonal structure. The liquidus curve falls steeply from the peritectic temperature almost to the pure aluminum where there is reputed to be peritectic.

$$TiAl_3 + \text{liquid} \text{ ===== Al at } 650\ ^\circ C \qquad (2.2)$$

The phase digrame of Al-Ti binary system is shown on figure (12)

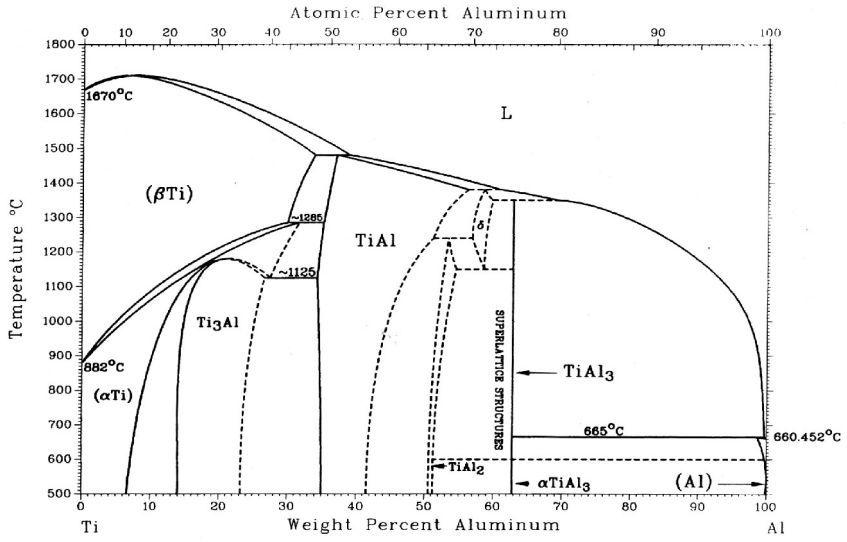

Fig. 12 : Phase digrame of Al-Ti binary system

The limit of the peritectic horizontal is placed at 0.15 % wt Ti. The titanium aluminize $TiAl_3$ crystals are presented in all commercial Al-Ti master alloys used to grain refine Al and it alloys. It was suggested by many authors that $TiAl_3$ is an active substrate for the nucleation of α–Al. It was reported that the nucleation efficiency of these Al-Ti alloys is affected by the presence of other elements in the Al melt.

Davies et al. (1970) has also investigated the grain refinement of aluminum by Al-Ti binary alloys.

Jones and Pearson (1976) in the second group theories, suggested that $TiAl_3$ particles acts as nuclei for the solidifying Al, and the role of the TiB_2 particles is to stabilize a form of $TiAl_3$ and extend the time it takes to dissolve. Recently Johnson et al (1994) reported that more than one mechanism are responsible for the grain refinement depending on the nucleant (master alloy) used, the chemical composition of the alloy cast and the processing conditions prevailing e.g. contact time, pouring temperature.

2.1.3 Advantages and Limitations of Grain Refinement:

2.1.3.1 Advantages of Grain Refinement

Since 1949, when Cibula reported that the presence of titanium particularly in combination with carbon or boron, produces a good grain refining effect in aluminum, which in turn enhances the mechanical behavior and surface finish, it became customary in the aluminum cast industry to add these elements to Al melt prior to solidification.

The grain refining of cast ingots in the aluminum industry is of prime importance as it provides a number of economical and technical advantages, namely (mollard,1985)

1- Reduces ingot cracking: fine grains provide an extensive network of grain boundaries reducing the tendency for crack initiation and propagation.

2- Improved soundness: fine grains promote the flow of the molten metal which feeds shrinkage during the final stages of solidifications. This gives smaller and uniformly dispersed shrinkage porosity. Also the fine grain structure promote a finer distribution of gas porosity.

3- Better mechanical deformation characteristics: it is well known that the fine equiaxed grains have greater capacity for uniform deformation than columnar grains. This leads to reduction of cracking during both hot and cold deformation.

4- Enhancement in mechanical behavior properties: grain boundaries are high energy areas along which fracture cracks initiate and propagate easily. Fine grain structure provides closely-knit grains and minimizes the tendency for crack initiation providing higher mechanical strength.

5- Reduced costs: the previous above improvements will lead to reduction in cost.

2.1.3.2 Limitations of Grain Refinement

Although grain refining of aluminum and its alloys has been proved to be essential in the aluminum industry and it became a common practice there are some limitations which should be considered in selecting the grain refiner. These include:

1- Ingot cracking, either during casting or subsequent hot and cold working when too little of the grain refiner is used. Conversely an excessive addition of grain refiner may lead to unusually fast filter loading undesirable amounts of Ti and /or B rich inclusions in the ingot which may result in defects in extruded products

2- Although the cost of the grain refiner as compared to the cost of aluminum ingot (e.g. a typical 2 % additions of Al-5Ti-B grain refiner per 1000 lbs of aluminum, corresponding to 0.01 %Ti addition will cost 0.4 cent per 1b of aluminum ingot, it may be extremely costly in some cases, especially it forces the use of slower casting rates, (Mollard,1985).

It can be seen from this chapter that most of the work is directed towards the metallurgical aspects of the grain refining process and little work is published on the effect of the process on mechanical behavior and wear resistance and no work is published on the effect of the process on the formability in general and aluminum in particular.

3. Materials, Equipments and Experimental Procedures

In this chapter, materials, equipment used and the experimental procedures will be discussed.

3.1 Materials

Different materials namely commercially pure aluminum, high purity titanium, boron, zirconium, D_2 tool steel, A_2 tool steel, Molykote-Gin metal assembly paste, pure graphite crucible and pure graphite rods were used in this work.

3.1.1 Aluminum

The base material used throughout this work is the commercially pure aluminum of (99.8 %) wt Al, obtained from Jordan Electricity Authority in the form of bundles of wires, the chemical analysis of this base metal is shown in Table 2.

Table (2) : The chemical analysis of pure aluminum

Element	Fe	Si	Cu	Mg	Ti	V	Zn	Mn	Na	Al
Wt %	0.09	0.05	0.005	0.004	0.004	0.008	0.005	0.001	0.005	Bal.

3.1.2 Titanium

Titanium (Ti) is used as an alloying element in part of this work, Ti is available in the form of cylindrical rod, sheet, wire and pure powder. Its melting point is 1668 ˚C, and its density is 4.5 g/cm^3 at 20 ˚C .

3.1.3 Boron

Boron (B) is a nontoxic material, black, its density is 2.3 g/cm^3 and its melting point is 2300 ˚C and 99 % purity used in rocket fuels. B in form of dust will slowly oxidize and should be kept under inert gas. It is a very powerful hardening agent, being 250 to 750 times as effective as molybdenum, (ASM Hand Book, V2, 1990).

3.1.4 Zirconium

The extraction, fabrication, and general metallurgy of zirconium are somewhat similar to those of titanium. The main uses of Zr are for cladding fuel elements, and for structural components in water-cooled systems, due to its corrosion resistance, (Rollason, 1989).

Zirconium density at 20 ˚C is 6.5 gm/cm^3, its melting point is 1852 ˚C and the atomic weight is 42. Zirconium exhibits strong anisotropy of two characteristics, Zr has a hexagonal closed packed (HCP) crystals structure at room temperature, and it undergoes allotropic transformation to BCC structure at 860 ˚C, (Lancaster,1987).

Zirconium was used as an alloying element in small weight percentages at a rate of 0.1%. It is available in the form of rod, wire, and sheet. It has a high corrosion resistance to high temperature water, resulting from the natural formation of a dense stable oxide on its surface of metal, (ASM, Handbook, V2, 1990).

3.1.5 D_2 steel

D_2 tool steel is a die steel, was used in the manufacturing of punch, die and the dummy block in the extrusion die set because of its high strength and toughness. Its composition is shown in Table (3).

Table (3) : Chemical composition of D_2 steel .

Element	C	Cr	Mo	V	Fe
Wt %	1.55	12	0.7	1.0	Remainder

To get appropriate mechanical properties of the, D_2 steel, it requires heat treatment which consisted of hardening followed by tempering to get red of residual stresses which results from the hardening process, due to the formation of martinsetic structure with high brittleness and lower toughness. The final hardness is 52 HRC which fulfills the requirements in this work.

3.1.6 A_2 steel

A_2 tool steel which is designated in the market by (Red/Green) steel was used in the manufacturing of the container of extrusion die**.** The chemical composition is shown in Table 4. Because the force exerted on the container is relatively small, no heat treatment processes was required. The hardness of A_2 steel is about 20 HRC.

Table (4) : Chemical composition of A_2 steel.

Element	C	Si	Mn	Cr	V	S	Fe
Wt %	1.0	0.2	0.8	5.3	0.2	0.1	Rem.

3.1.7 Molykote-Gin Metal Assembly Paste

This is an effective lubricant used especially for cold extrusion as recommended by the suppliers and was used for lubricating the billet and the extrusion die.

3.1.8 Master Alloys

Three master alloys were used to obtain the different micro alloys namely : the ternary Al 4.6%Ti-0.92%B ingot type alloy (A91445) of chemical composition shown in Table 5. This alloy is used in aluminum factories as a grain refiner of commercially pure aluminum. It was obtained from ARAL (aluminum factory in Amman) in the form of 10 mm rods.

Table (5): Chemical analysis of the Al 4.6 %Ti-0.92 %B by weight.

Element	Ti	B	Fe	Si	V	Al (A91445)	Grain Size(μ m)
Weight %	4.6	0.92	0.12	0.09	0.12	Remainder	179

The adequate quantities were cut from it and diluted in commercially pure aluminum to get the required percentages of Ti and B in the micro alloy.

The second-master alloy was the binary Al-2.92%Ti , which was prepared in the Material Laboratory at the Industrial Engineering Department, from commercially pure aluminum of the chemical analysis shown in Table 2 and the high purity 99.99 % titanium powder.

The third master was the binary Al-1.17 %Zr, which was also prepared in the Material Laboratory at the Industrial Engineering Department, as will be explained later.

3.1.9 Micro- Alloys

Five micro-alloys in addition to commercially pure aluminum were prepared. The chemical composition of each of these alloys is shown in Table 6, and given the numbers as shown in this table.

Table (6): Chemical composition of the different Al microalloys.

Sample	Alloys	Ti %	B%	Zr %	Balance
1	Al	0	0	0	Al
2	Al-Ti	0.15	0	0	Al
3	Al-Ti-Zr	0.15	0	0.1	Al
4	Al-Ti-B	0.046	0.0092	0	Al
5	Al-Zr	0	0	0.1	Al
6	Al-Ti-B-Zr	0.0046	0.0092	0.1	Al

3.2 Equipment

Electric resistance furnace (Carbolite) of 1200 ˚C maximum temperature was used for melting the master and micro alloys that used throughout this work which is shown in figure (13).

Fig. 13: Electric resistance furnace

The chemical composition, by weight of each of these alloys was determined using the scanning electron microscope, SEM, type DSM 950 in the Royal Scientific Society laboratories.

The grain size of each alloy was determined using Vickers optical microscope equipped with a microscopic micrometer. The micro hardness of each alloy was determined using standard Vickers micro hardness tester, whereas mechanical behavior was obtained from uniaxial tensile tests carried out on an Instron Universal Testing Machine type 1195 of 100 KN capacity. The tests were carried out in accordance with ASTM-Eq (II).

The extrusion and compression tests were carried out on Universal Testing Machine MTS of 250 KN capacity, shown in figure (14)

Fig. 14: Universal Testing Machine (MTS)

Wear tests were carried out using a pin-disk type wear tester at different rotational speeds and loads. The mass loss was determined using a balance HM-200 digital type of 200 grams capacity of 0.1 mg accuracy.

The reduction in length was measured using an electronic digital caliper of 0.01 mm accuracy whereas The profile of each specimen (mushrooming) was traced after every 15 min by shadowgraph instrument, contractor, at a magnification of 10x as shown in figure (15).

Fig. 15: Shadowgraph or contractor

At the end of each wear test i.e. after one hour monograph of each specimen was taken using a computerized microscope at a magnification of 40x as shown in figure (16)

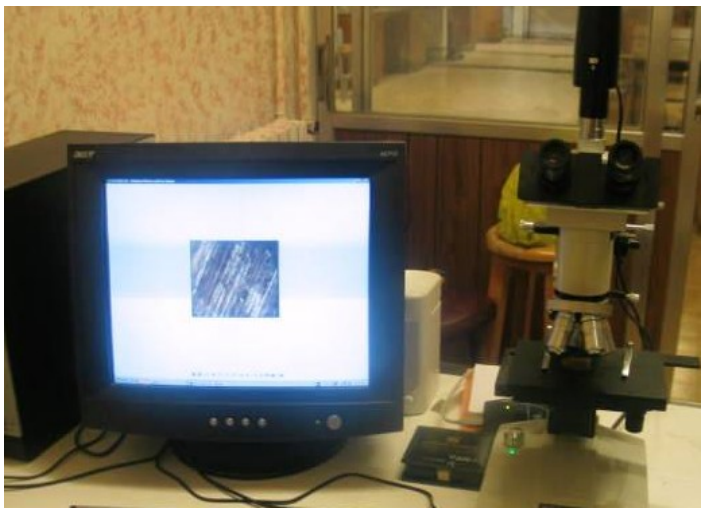

Fig. 16: The computerized microscope

The rotational speed of the motor was calibrated prior to testing using the digital tachometer shown in figure (17) from which the actual rotational speed was determined.

Fig. 17: The digital tachometer

3.3 Experimental Procedure

The experimental procedure was carried out in the following sequence:

1- Preparation of the commercially pure aluminum.

2- The preparation of the master alloys .

3- The preparation of the micro-alloys.

4- The chemical analysis of each of the master and micro-alloys was carried out.

5- Design and manufacturing of the extrusion die set.

6- Carrying out the extrusion test on the commercially pure aluminum, and the different microalloys specimens.

7- Determining the grain size of each micro alloy for both extruded and the as cast conditions.

8- Micro hardness was carried out on each micro alloys for both the extruded and the as casted conditions .

9- Tensile tests were carried out to investigate the mechanical behavior of each microalloy for both the extruded and the as casted conditions .

10- Compression tests were also carried out on each microalloy for both the extruded and the as casted conditions to determine their formability.

11- Finally, wear tests were carried out on each specimen from in the as cast condition microalloys at different rotational speeds and loads.

The rotational speeds were (31, 93, 215, 350) rpm corresponding to loads (5, 10, 15, 20) N.

3.3.1 Preparation of Pure Aluminum

The commercially pure aluminum cables were cut into wires of 6 cm length and 5 mm diameter, then cleaned by pickling in HNO_3 to remove any oxides layers and/or any other contaminants of the surface. The wires were melted in a pure graphite crucible of 90 mm internal diameter and 100 mm height in the electric furnace at a temperature 800 ˚C and finally stirred and poured to solidify in hollow brass cylinders of 18 mm internal diameter and 16 mm thickness. The graphite crucible and the rod are shown in figure (18).

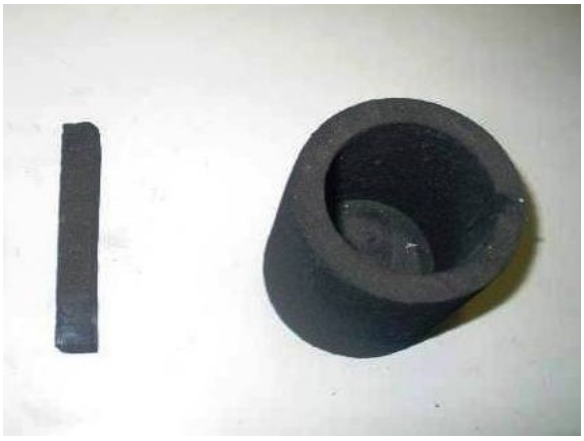

Fig. 18: Graphite crucible and graphite rod

These aluminum rods were then used to produce the master alloys, and the micro-alloys.

3.3.2 Preparation of The Master Alloys

All the master alloys were prepared in graphite crucible of internal diameter of 25 mm and 10 mm thickness. The selection of the pure graphite was used to ensure that no other elements would be introduced in the produced master alloy.

Pouring of the molten master alloys in a cylindrical hole in a ceramic block. Where the micro-alloys poured into the desired shapes were done in hollow, cylindrical brass dies of 13.5 mm internal diameter and 18 mm thickness. These dies were produced from 50 mm solid brass rods.

3.3.2.1 Al-2.92 %Ti Master Alloy

This master alloy was prepared by adding titanium powder to molten aluminum. A 47 gm aluminum were heated inside a graphite crucible in the furnace to 1100 ˚C, then a 3 gm titanium chips placed in aluminum foil were introduced to the melt, agitating the melt using a graphite rod. The crucible was introduced to the furnace for 30 minutes, and then poured in a cylindrical hole in a ceramic block. The microstructure is shown in figure (19).

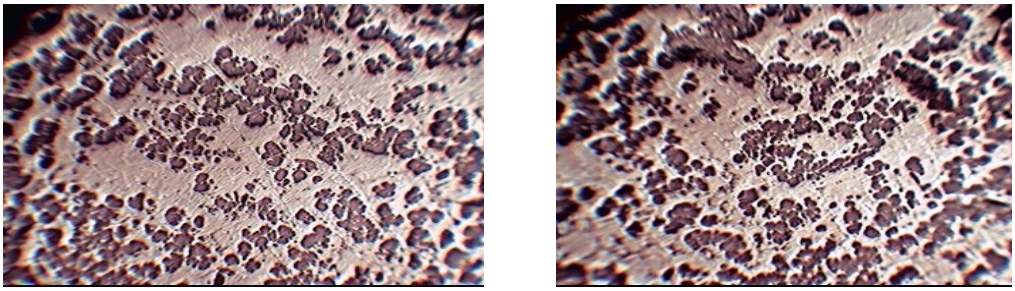

a) At 5 mm depth from top b) At 5 mm depth from bottom

Fig.19: Al-2.92 % Ti Master Alloy at Different Locations, X100

3.3.2.2 Al-1.17 % Zr

The binary Al-1.17 % Zr master alloy was prepared from pure metals of Al and Zr. Zirconium was added into molten aluminum at about 1100 ˚C and stirred under a cryolite flux. The temperature was kept constant for about 30 minutes then poured in a hollow cylindrical ceramic block. This master alloy was then compressed to reduce its thickness and finally cut into small pieces.

3.3.3 Preparation of Different Micro-Alloys

Five different micro-alloys were prepared, namely: Al-0.046%Ti-0.0092%B, Al-0.046%Ti-0.0092%B-0.1%Zr, Al-0.1%Zr, Al-0.15%Ti, and Al-0.15%Ti-0.1%Zr which

will replaced to as Al-Ti-B, Al-Ti-B-Zr, Al-Zr, Al-Ti and Al-Ti-Zr respectively. These microalloys were prepared as follows:

The predetermined amount of aluminum was weighed and placed in a crucible inside the electric furnace. the furnace is heated to 800 ˚C until the graphite crucible is red hot. The furnace temperature is then lowered to 750 ˚C where the predetermined amount of the grain refiner from the master alloy is weighted, wrapped in aluminum foil and added to the aluminum melt and stirred using a graphite rod and the crucible is placed again inside the furnace and its temperature raised to 800 ˚C for 5 minutes. Finally, the crucible is taken outside the furnace and the molten mix is agitated and poured to solidify in hollow cylindrical brass rods of 13.9 mm internal diameter and 70 mm height, figure (20).

Fig. 20: Brass die

3.3.4 Grain Size Determination

one specimen from each microalloy in the as cast and extruded condition were prepared for microscopic examination by sectioning, mounting and successive polishing with different grids of silicon carbide abrasive paper and finally with diamond paste, each specimen was etched in the solution of (0.5%-1% HF, 2.5% HNO_3, 1.5 % HCL and 95.5% distilled water).

The general microstructure of each of the prepared micro-alloys was obtained using optical microscope. The grain size was determined using the intercept method, in which straight lines in several directions all of the same length are drawn through the photograph that shows the grain structure. The number of grains intercepted by each line is determined; the average of six different lines for each specimen was obtained and considered to represent the number of grains, from which the grain size was obtained.

The grain size was also determined using the micro hardness tester HWDM-3, equipped with a unit for grain size determination from which the actual size in different directions was measured from which the average grain size was determined.

3.3.5 Mechanical Testing

3.3.5.1 Micro hardness measurements

The Vickers micro hardness of each micro alloy in the as cast and extruded was determined using HWDM-3 micro hardness tester at a load of 100 gm at Tafila Technical University, Six readings were taken on each specimen and the average of these readings was determined giving the average Vickers micro hardness of each microalloy.

3.3.5.2 Tensile tests

Tensile tests were performed for each microalloy both in the as cast and extruded conditions in accordance with ASTM-EII standard to determine their mechanical behavior. The tests were carried out on standard tensile specimens of 25 mm gauge length and 5.05 mm diameter, figure 3.8, using Instron 1195 Universal Testing Machine of 100 KN capacity at a cross head speed of 2 mm/min. at Jordan University of Science and Technology, JUST.

All the tensile specimens were machined on a Closter CNC-1000 machine at the same cutting conditions of 0.25 mm depth of cut, 750 rpm spindle speed and 120 mm/min feed rate. Figure (21)

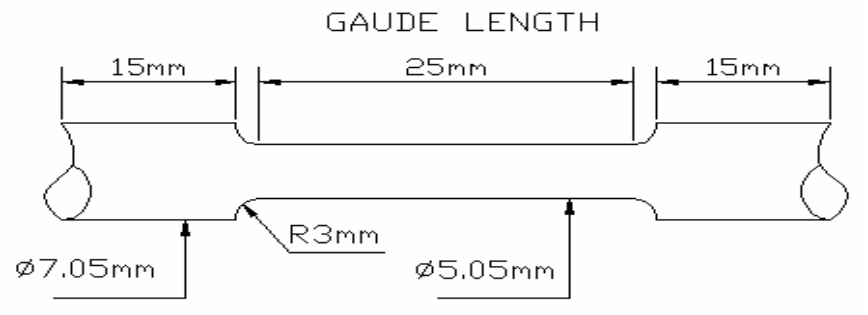

Fig. 21: Tensile test specimen (ASTM-E8, 1975)

Two specimen from each micro alloy were tested to ensure the repeatability of the results, and incase the variation more than 2 % a third test was carried out.

the autographic record (load- deflection curve) for each specimen was obtained from which the representative stress representative-strain diagram was plotted and the equation in the mechanical behavior at plastic region (K, n) were determined for both the extruded and the as cast conditions. micro alloys. Similarly the ductility, flow stress at 0.2 strain and the ultimate tensile strength were determined for each specimen.

3.3.5.3 Compression test

To investigate the effect of the rare earth materials (grain refiner)on the formability of aluminum under compressive loading, Twelve cylindrical specimens of height 10 mm and 10 mm diameter (H/D =1) of both extruded and as cast condition were prepared for compression tests.

The tests where performed on Universal Testing Machine (MTS) of 250 KN and 10 mm/min cross head speed, and the autographic record (load-deflection curve) was obtained for each alloy, then the true stress true strain for each alloy was plotted.

3.3.5.4 Extrusion test

After successful design and manufacturing of the extrusion die shown in figure (22), it was used in extrusion tests of aluminum and it's micro alloys.

Fig. 22 : Extrusion die

Two specimens from each micro alloys were prepared cylindrical shape of 13.9 mm diameter and 63 mm length were used as billet for extrusion tests. The billets were extruded to 10 mm in diameter. All the extrusion tests were carried out using the same lubricant MoS_2. For each micro alloyed extruded specimen there is an autographic record (load–ram travel curve) which is shown in appendix B, from which the maximum extrusion force and extrusion pressure were determined.

3.3.5.5 Wear resistance tests

To investigate the effect of the different grain refiner on the wear resistance of commercially pure aluminum, cylindrical pins of 7 mm diameter and 14 mm length were prepared from each microalloy in the as cast and extruded condition. The wear tests were carried out using the pin-rotating on disc assembly, figure 23, which is originally, a grinder–polisher (MeataServ) modified into a wear testing machine. This is achieved by adding an arm that holds the guided bushing, which

provides the load through a spring. The loading spring, supports the pin in a vertical position against the rotating disc. This apparatus can give different nominal rotational speeds (ranging from 50 to 500 rpm). The disk is made of carbon steel, hardened, tempered, and thermally sprayed with a hard compound of 65 HRC hardness. All the wear tests were carried out in the dry condition.

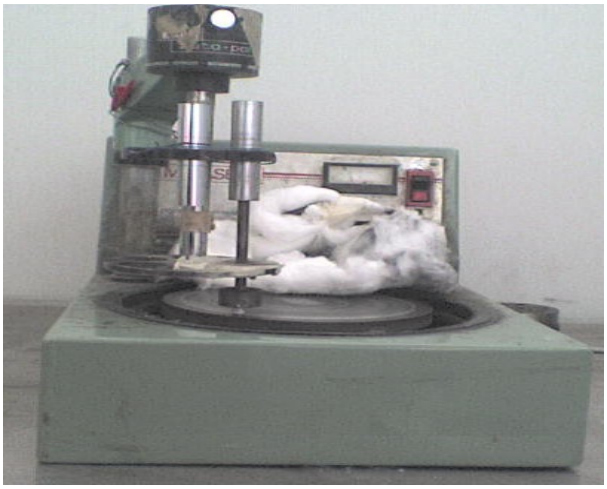

Fig. 23: Pin disk type wear tester

First the original length and mass of each sample were measured using the digital caliper and digital balance respectively. Each sample was mounted in position in the wear apparatus and the predetermined load is applied to the specimen and the speed was chosen and the test started. The test was interrupted every 15 minutes and the specimen removed, cleaned and weighed from which the mass loss is determined. The specimen was again mounted in position and the test started again under the same load and speed. The test was run for one hour.

Each test was repeated at four different loads namely: 5, 10, 15 and 20 N and at four different rotational speeds namely 31, 93, 215 and 350 rpm. The length of the specimen was measured and its profile was traced at the end of each test.

A photo macrograph at the worn end tip was taken for each specimen, results are plotted on a 3D graph (speed (rpm), accumulated mass loss (gm) and accumulated height reduction (mm)) at all loads and speeds using mat lab soft ware.

3.3.5.6 Formability tests

The formability tests were carried out using the extrusion die which was designed and manufactured for this purpose as will be discussed in the next chapter, under the Universal Testing Machine at cross head speed of 10 mm/min.

3.3.5.6.1 Heat Treatment of Punch and Die

Two heat treatment processes were carried out D_2 steel, the hardening process followed by tempering .

3.3.5.6.2 Hardening Process

D_2 steel was preheated to 600 ˚C for 30 minutes then the temperature was raised to 1050 ˚C for 120 minutes then quenched in oil. The hardening curve is shown in Fig. 24.

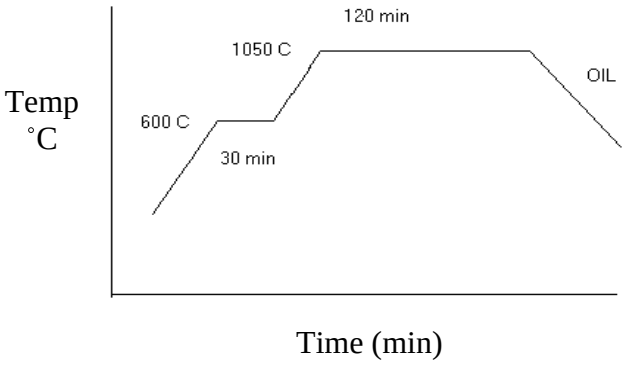

Fig. 24 : Hardening of D_2 Steel.

3.3.5.6.3 Tempering Process

D_2 steel heated to 600 ˚C for 100 minutes then the work piece was cooled in air. The Tempering is shown in Fig. (25).

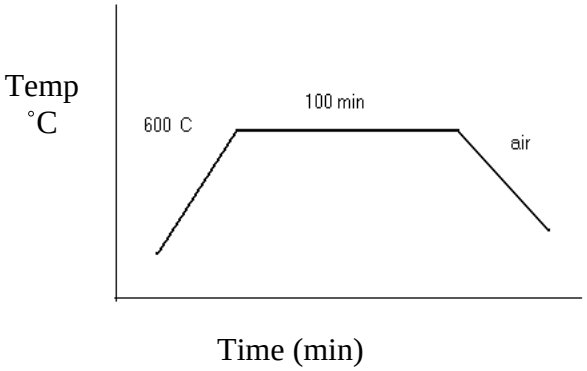

Fig. 25 : Tempering Regime of D_2 Steel

4. DESIGN OF EXTRUSION PUNCH AND DIE

4.1 Design of Extrusion Die

Design is not a one iteration process but is a closed loop process where it may repeat itself more than once until requirements are accomplished. Taking into consideration all the existing constraints.

In designing any die for any forming process, the starting point is to determine the maximum force which the die is going to be subjected to. In this project, the die material used in carrying out the experiments is die steel D2 of the general characteristics shown in Table (3) on extrusion of aluminum and it's micro alloys using an ASTM Universal testing machine of 250 KN capacity which exists in the manufacturing processes laboratory, in the Industrial Engineering Department.

4.2 The Maximum Extrusion Force

In general: Force = stress * cross sectional area.

$F_{max} = Pi\ A_o$ .....(4.1)

The billets to be used are of 13.5 mm diameters and will be extruded through a die of 10 mm diameter; the stress in equation (4.1) is the maximum of the material to be extruded. The extrusion force is estimated from the following equation: (Johnson, 1980)

$P_i = Y_{extruded} (a + b\ Ln\ R)$ …….. ……. (4.2)

Where

F_{max} = Maximum extrusion force

p_i = Extrusion Pressure or internal pressure

$Y_{extruded}$ = Yield stress of the extruded material

R = $\frac{A_0}{A_f}$ (Extrusion Ratio)

A_0 = Initial cross-sectional area of the billet

A_f = Final cross-sectional area of the extruded part

a and b are constants for the material to be extruded.

4.3 The Minimum Diameter of Punch

The minimum punch diameter is determined using the following well established design equation:

$$\frac{F_{max}}{\pi \frac{D_0^{\,2}}{4}} \le \frac{Y}{n^*} \quad \text{.....(4.3)}$$

Where

D_0 = Minimum punch diameter

n^* = Factor of safety

Y = Yield stress of the punch material

4.4 The Maximum Allowable Length of the Punch to Avoid Buckling

The maximum allowable length of the punch is determined using Euler's formula 4.4 to avoid buckling under the effect of the maximum used force:

$$P_{critical} = \frac{1.2\pi^2 EI}{L^2}, \text{ where } (P_{critical} < F_{max}) \quad \text{.....(4.4)}$$

(Shigliey, 1977)

Where

$P_{critical}$ = Critical buckling load

E = Modulus of elasticity

I = Moment of inertia = $\frac{\pi d^4}{64}$ (for cylindrical shapes)

L = Length of the punch

d = Smallest diameter of the plunger

4.5 Design of the Container

The container is a thick cylinder because the ratio t/r > 1/20:

$$\sigma_t = p_i \frac{r_0^2 + r_i^2}{r_0^2 - r_i^2} \quad \text{.....(4.5)}$$

$$\sigma_r = -p_i \quad \text{.....(4.6)}$$

$$\frac{\sigma_{y(die)}}{n} \geq (\sigma_t - \sigma_r) \quad , \left[Tresca's \quad Criterion \right] \quad \text{.....(4.7)}$$

Where

σ_t = Tangential stress

σ_r = Radial stress

p_i = Extrusion pressure or internal pressure

r_0 = External radius

r_i = Internal radius

Table (7): Properties and predefined parameters:

Parameter	Value
Y of Al	34 MPa
$Y_{D2Steel}$	400 MPa
E D2 steel	2 x 10^5 MPA
a	0.8
b	1.5

4.6 Calculations

4.6.1 Extrusion ratio, R

$$R = \frac{A_0}{A_f} = \frac{\frac{\pi * 14.02^2}{4}}{\frac{\pi * 10^2}{4}} = 1.9656$$

4.6.2 Evaluating the extrusion pressure

Substituting the value obtained for R and the values of the appropriate parameters in equation (4.2), to get

$$p_i = 34 * (0.8 + 1.5 * (0.6758)) = 61.6656\, MPa$$

4.6.3 Evaluating the maximum extrusion force

By substituting the values of the appropriate parameters in equation (4.1):

$$F_{\max} = p_i * A_0 = 61.6656 * (\frac{\pi (14.02)^2}{4}) = 61.6656 * 154.378 = 9394 N$$

4.6.4 Evaluating the minimum diameter of the punch:

Substituting the appropriate values of each parameter in equation (4.3):

$$\frac{9.394 * 10^3 N}{\pi \frac{D_0^{\,2}}{4}} \leq \frac{400 * 10^6 Pa}{3}$$

$$D_0^{\,2} \geq \frac{9.394 * 10^3 * 3}{\pi * 100 * 10^6} m^2 \rightarrow D_0 \geq 9.47 mm$$

The moment of inertia of the punch:

$$I = \frac{\pi D^4}{64} = \frac{\pi (9.47)^4 * 10^{-12}}{64} = 394.6 * 10^{-12}\, m^4$$

Substituting the appropriate value of each parameter in equation (4.4):

$$P_{critical} < 9.394\ KN$$

$$9.394 * 10^3 = \frac{1.2 * \pi^2 * 2 * 10^{11} N/m^2 * 394.6 * 10^{-12} m^4}{L^2}$$

L= 3171.8 mm

The maximum permissible length of the punch to avoid buckling is found to be 1098 mm

4.6.5 Checking whether the die sustains the load

Considering as thick cylinder where t/r = 4.22/14.02 > 1/10.

Substitute the values of the appropriate parameters in equations (4.5) and (4.6):

$$\sigma_t = 61.665 * \frac{14.02^2 + 10^2}{14.02^2 - 10^2} = 61.665 * 1.508 = 93.04\,MPa$$
$$\sigma_r = -p_i = -61.665\,MPa$$

The principle stresses results are (93.04, 0, -61.665)

Apply Tresca's criteria:

$$\frac{\sigma_{y(die)}}{2} > (93.04 - (-61.665))$$
$$\sigma_y > 309.40MPa$$
$$Y_{D2Steel} = 400MPa > 309.40MPa$$

So the die sustains safely the maximum load.

4.7 Finite Element Analysis (FEA)

Stress varies throughout the continuum of any part. By dividing the part into a mesh, one can obtain an approximation of the stress and strain within the part for any given set of boundary conditions and loads applied at various nodes in the structure.

The approximation can be improved by refining the mesh, i.e. using more elements of smaller size at the expense of increased computation time. Pro-wildfire software was used to do the FEA, for the punch and die. Figures 26 to 30 inclusive show the FEA analysis for the punch, where figures 31 to 35 inclusive give the FEA for the die.

4.7.1 Finite Element Analysis for the Punch:

It can be seen from the following figures that the finite element analysis (FEA) for the punch determines the distribution of the load, stress, displacement, and strain energy. Fig. 26 shows the load distribution per unit area. This load is the applied force from the universal testing machine to the punch. From FEA data the following are obtained:

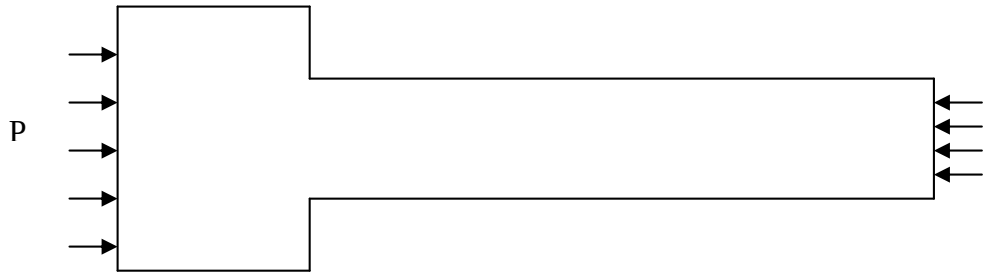

Fig. 26: Distribution of Load on the Punch (Cylinder).

- Stress distribution : the maximum stress concentration (red zone) can be seen at the perimeter of the punch, as indicated in Fig. 27.

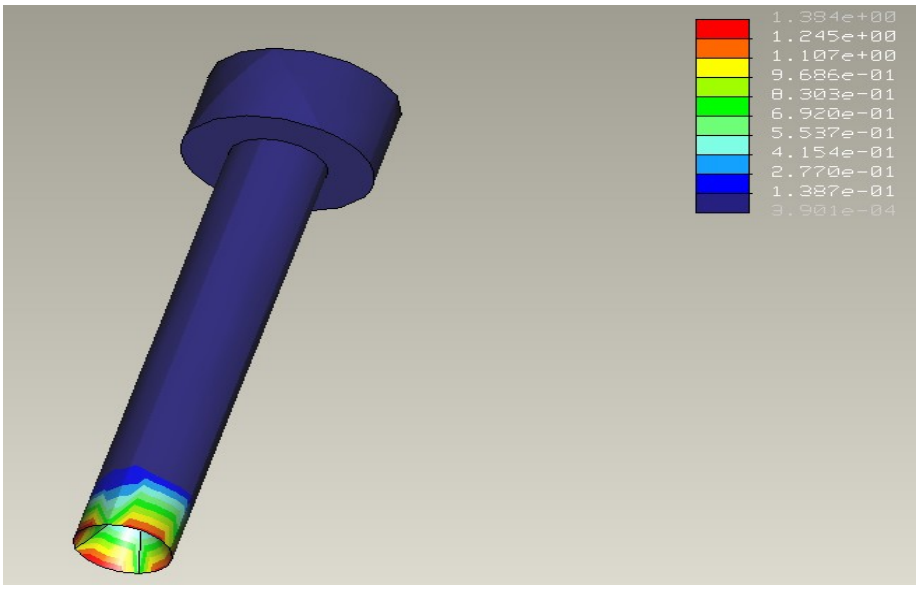

Fig. 27: Stress Distribution for the Punch. (Von Mises , MPa)

- Displacement distribution : the maximum displacement can be determined from the gradient scale, as shown in Fig. 28 and its location is at the center of the punch, exactly (red zone), because the maximum concentration of the applied load is centered at the ends of punch, this can be proved from the follows relation:

$$\Delta L = PL/EA \qquad (4.8)$$

Where:

ΔL: displacement (mm)

P: Applied load (N).

L: Length (mm).

E: Modulus of elasticity (N/mm²).

A: Cross Sectional area (mm²).

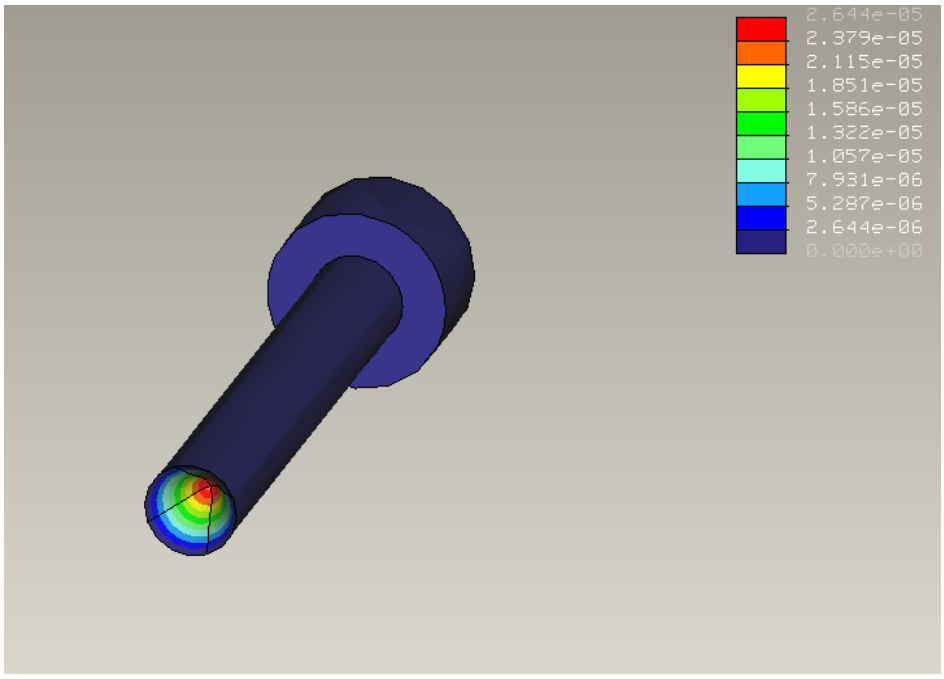

Fig. 28 : Displacement Distribution for the Punch (mm)

- Strain distribution : the maximum strain can be determined from the gradient scale, as shown in Fig.29 (red zone), and the location of the strain at the perimeter at small area of the punch, because the stress concentration is maximum at the same region, This can be proven from the following relationship :

$$\sigma = E * \varepsilon \, . \qquad (4.9)$$

σ : Stress (MPa).

E : Modulus of elasticity (N/mm²).

ε : Strain (mm/mm).

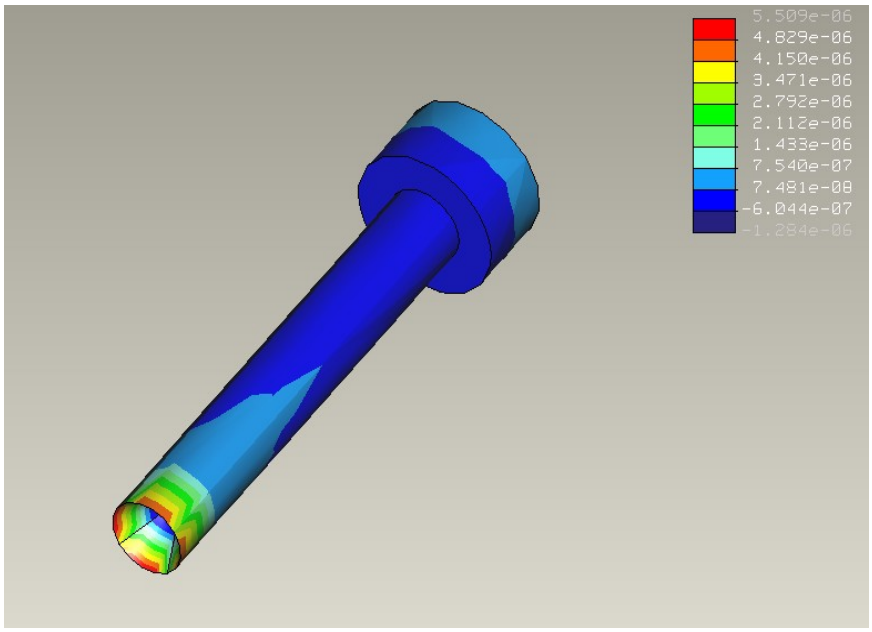

Fig. 29: Strain Distribution for the Punch (mm/mm)

- Strain energy : the maximum strain energy can be determined from the gradient scale, as shown in Fig.30 (green zone). The location of the maximum strain energy is at the perimeter too, because both the stress and the strain are maximum at this region.

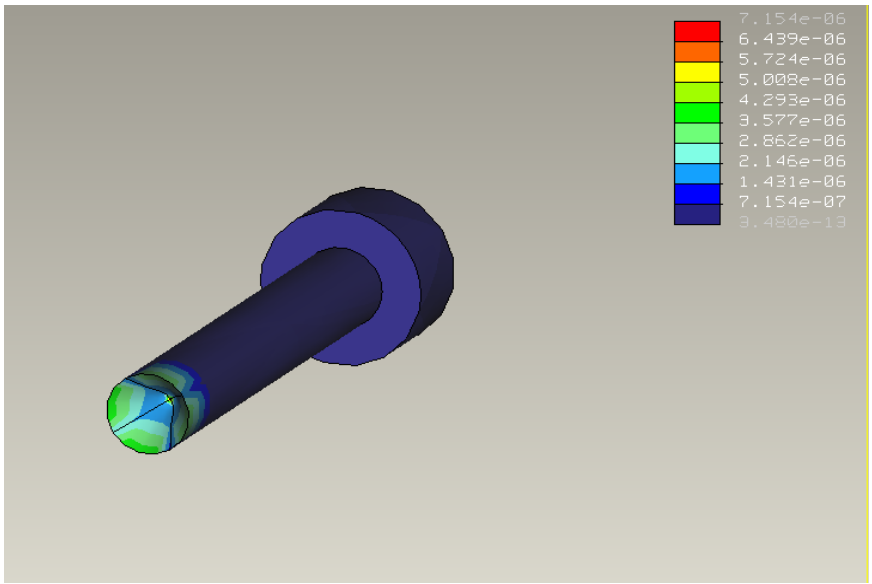

Fig. 30: Strain Energy Distribution for the Punch (N/mm^2).

4.7.2 Finite Element Analysis for the Die

Figure 31 shows the load distribution per unit area on the die. This load is an applied force on the cylindrical surface (entrance of metal zone), and is equal to the load applied on the punch, (regardless of the frictional force). The load distribution per unit area can be determined by dividing the applied load on the cylindrical surface area (contacting area between metal and entrance zone). From this distribution the following are obtained:

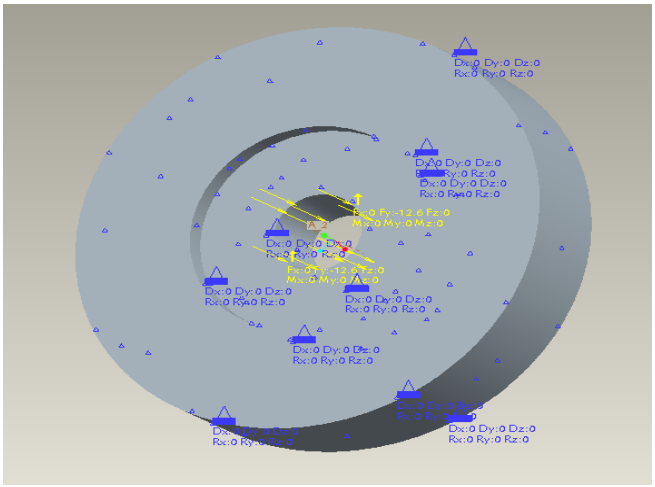

Fig. 31 : Distribution of Load on the Die.

- Stress distribution: The maximum stress concentration can be determined from the gradient scale and the location of the stress concentration is at the edge of the entrance zone (red zone), as indicated in Fig. 32, because the maximum force is concentrated at this region, and the high friction is at this region.

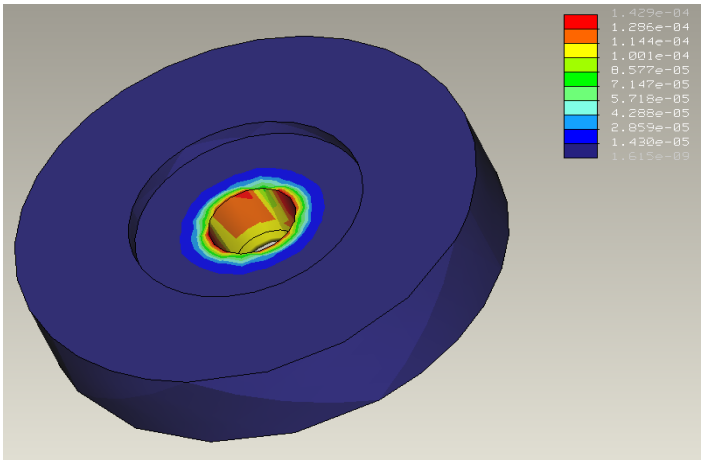

Fig. 32 : Stress Distribution for the Die.(Von Mises , MPa)

- Displacement distribution: The magnitude of the maximum displacement can be determined from the gradient scale, as shown in Fig. 33. The location of this distribution (red zone) is at the edge and along entrance zone, because the load is concentrated at this region.

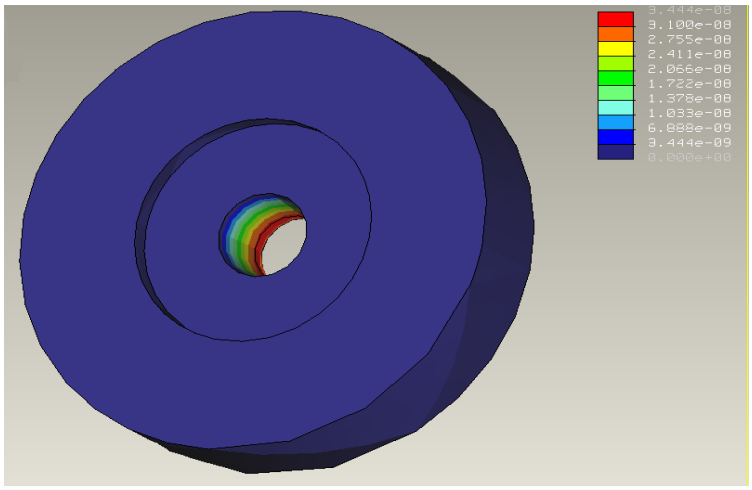

Fig. 33 : Displacement Distribution for the Die (mm).

- Strain distribution: The magnitude and location of strain concentration can be determined from Fig 34. The concentrated strain is in the same region of the concentrated stress.

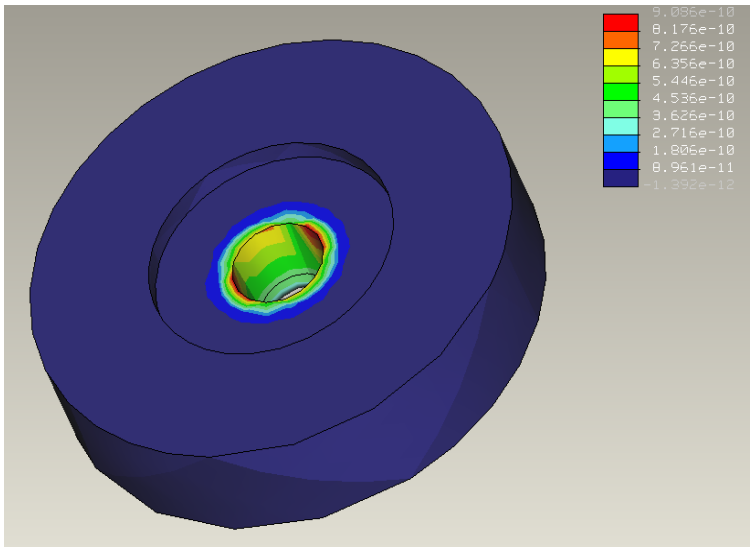

Fig. 34: Strain Distribution for the Die (mm/mm).

- Strain energy distribution: The magnitude and location of the concentration of strain energy are clearly shown in Fig. 35. The region of concentration of the strain energy is in the same region where the concentrated strain and stress exist.

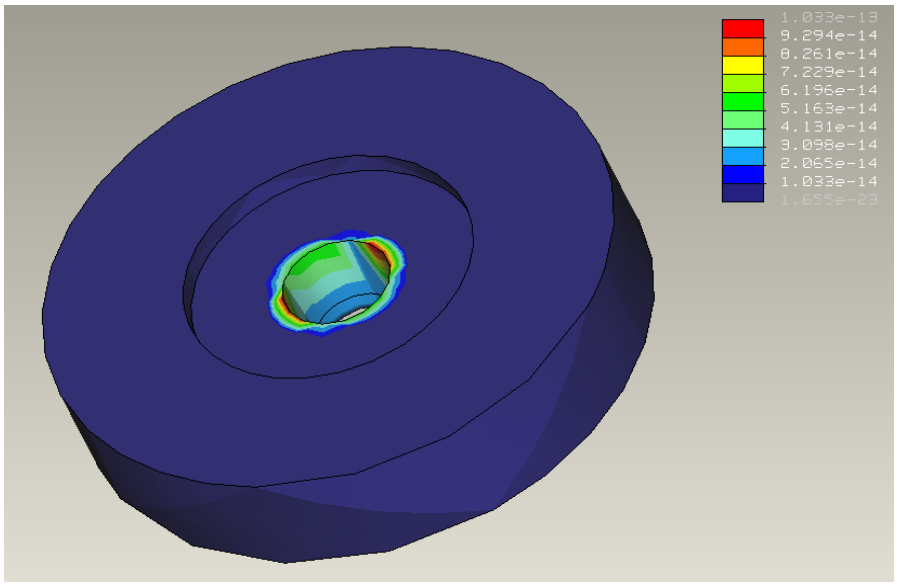

Fig.35 : Strain Energy Distribution for the Die (N/mm^2).

5. THEORETICAL CONSIDERATIONS

In this chapter the theoretical aspects related to the grain refinement mechanism, the extrusion process and wear of aluminum and its microalloys will be dealt with.

5.1 Grain Refinement Mechanisms

Although the grain refinement of aluminum and its alloys by the binary Al-Ti and ternary Al-5Ti-1B master alloys is well established and currently in use in the aluminum industry, the mechanisms for grain refinement and the enhancement of grain refining efficiency by the presence of some elements and the deteriorating effect by the presence of others are still a controversial matter although many attempts have been made and reported in the literature. In this section review and a discussion of these mechanisms will be given.

I- The Peritectic Reaction Theory: researchers of this theory Abdel-Hamid et al. (1985) attribute the grain refinement to the nucleation of aluminum by the compound $TiAl_3$ particles, in the Al-Ti system, according to the following peritectic temperature reaction at 1340 ˚C

$$\text{Liquid} + TiAl ===== TiAl_3 \qquad (5.1)$$

The $TiAl_3$ compound has a tetragonal structure. The liquidus curve falls steeply from the peritectic temperature almost to the pure aluminum where there is reputed to be peritectic.

$$TiAl_3 + \text{liquid} ===== \text{Al at } 650\ ^\circ C \qquad (5.2)$$

The limit of the peritectic horizontal is placed at 0.14 % wt Ti. (Fink,1931)

The titanium aluminide $TiAl_3$ crystals are presented in all commercial Al-Ti master alloys used to grain refine Al and it alloys. It was suggested by many authors that $TiAl_3$ is an active substrate for the nucleation of α–Al. it was reported that the nucleation efficiency of these Al-Ti alloys is affected by the presence of other elements in the Al

melt. Some of these elements enhance the efficiency e.g. Si, Ci, B or Sr whereas other elements deteriorate their grain refining efficiency e.g. Zr, Cr, or Ta, when are present in the Al-melt. This due to the diffusion of these elements in the $TiAl_3$ replacing some Ti atoms in the crystal lattice forming a ternary $(AlMe)Al_3$ phases with inferior nucleation and grain refining efficiency.

The part of Ti atoms replaced by the Me atoms is directly proportional to the ratio of Me atoms to Ti atoms in the ternary melt particularly in Al-Ti-V and Al-Ti-Mo alloys. This is discussed in detail by (Abdel-Hamid, 1989), who also suggested that a continuous series of solid solution ($Ti_x,Me_{1-x})Al_3$ can be formed in all these ternary alloy system.

Davies et al (1970) investigated the grain refinement of aluminum by Al-Ti binary alloys. Their results confirmed the results obtained earlier by Eborall and Fink (1950), i.e. the grain size decrease with increase of Ti content from 0.01wt % Ti, despite the reported limit to the $TiAl_3$ liquidus at 0.14 % wt % Ti. From which it can be concluded that $TiAl_3$ compound is present even at very low titanium concentrations, as low as 0.01%wt.

The structure of B_2Al is hexagonal and it is isomophous with the binary TiB_2 compound. Until now, the phase diagram of the binary Al-B alloy system is raught with contradictory evidence which makes its evaluation difficult, (Abdel-Hamid,1992).

Although in the Ti-B system there are a number of inter metallic compounds but TiB_2 is reported as having the highest melting point and which is generally present in the Al-base ternary alloys. (Daives , 1970, Abdel-Hamid, 1989)

The enhancing effect of B was attributed to one of two broad groups of theories :

In one group, it is proposed that the role of TiB_2 particles is to provide a substrate which allows segregated layer of titanium to form on it, which in turn produces a

thermally stable layer of pseudo-alpha- aluminum. This ensures the presence of nuclei for Al solidification at all times after the addition of Al-Ti-B master alloy.

II- Jones and Pearson theory: it is suggested that $TiAl_3$ particles acts as nuclei for the solidifying Al, and the role of the TiB_2 particles is to stabilize a form of $TiAl_3$ and extend the time it takes to dissolve. Recently Johnson et al.(1994) reported that more than one mechanism is responsible for the grain refinement depending on the nucleant (master alloy) used, the chemical composition of the alloy cast and the processing conditions prevailing e.g. contact time, pouring temperature.

They also suggested that grain refining is a result of two processes: firstly, the nucleation of the α-Al crystals and secondly, the subsequent growth of new crystals up to a limited size. Both of these processes need a driving force. Thus, other criteria than the presence of nucleants must also be fulfilled, and hence, the potency of a nucleus may be of secondary importance. A driving force of growth which may be a local under cooling in the surrounding of the particle, is necessary to develop affine grained microstructure. If this force is too small the nucleated crystal may remelt again. As mentioned before Zr, Ta and Cr have a poisoning effect on the efficiency of the grain refining of Al-Ti and Al-Ti-B master alloys. Jone and Pearson (1976), attributed this effect to

$$Zr \text{ (in the melt)} + TiB_2 \text{ ====== } ZrB_2 + Ti \text{ (in Al melt)} \qquad (5.3)$$

Abdel-Hamid (2000) concluded that the above reaction is only possible when the mole fraction of Zr-content in the melt exceeds about four times that of excess Ti remaining in solution in the melt. Therefore, this condition does not apply except at a Zr-content of 0.2 wt % or more. Experimental observation showes that the poisoning effect of Zr occurs at 0.05 wt % and rises steeply with increasing Zr- content from 0.0 to 0.3 %. The coating of TiB_2 with a monolayer of Zr or ZrB_2 require very little amount of Zr to

isolate and prevent the good nucleant TiB_2 particles from being active nuclei for α-Al. This fact does not agree with the continuous and steep effect of Zr content on the grain coarsening shown in Fig.36. Also, the mechanism based on the formulation of ZrB_2 or Zr coating layer around TiB_2 does not agree with the slow action of Zr and its dependence on the contact time prior to casting. The mechanism proposed by Abdel-Hamid (1985), explains better the poisoning effect of Zr and further it can explain the effect of other elements like Ta and Cr.

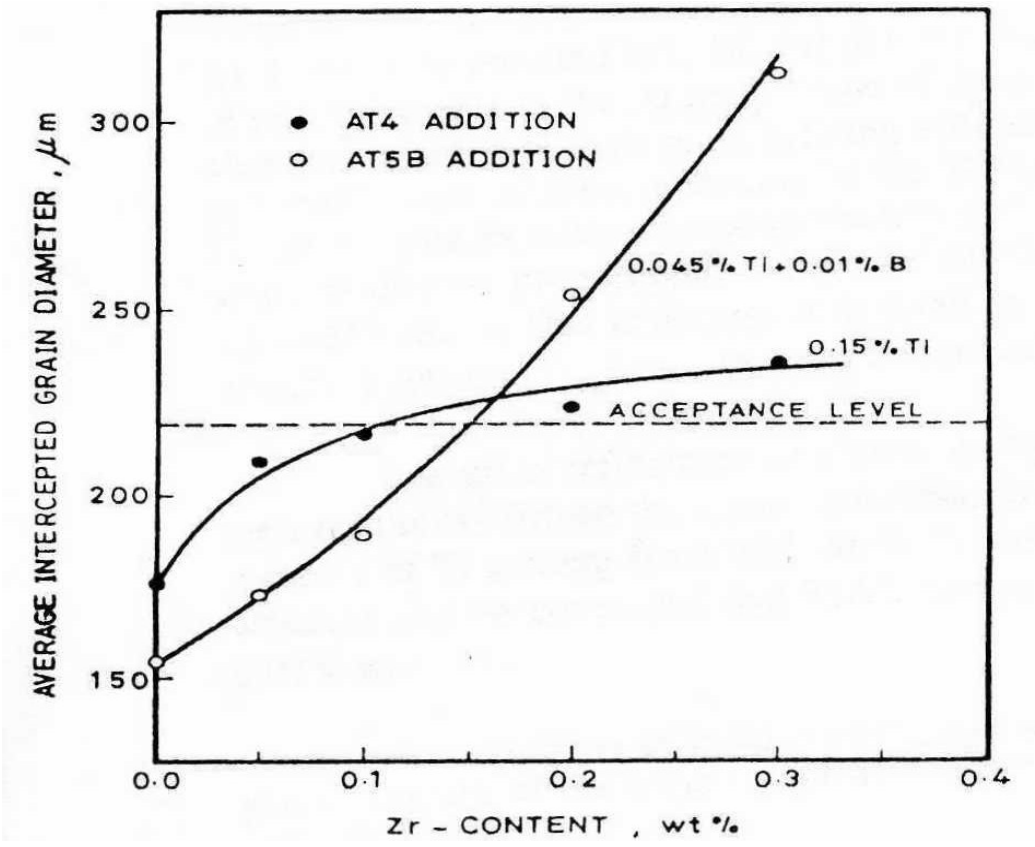

Fig. 36 : Poisoning effect of Zr on aluminum (Zaid, 2001)

According to this mechanism, the poisoning element (Zr, Ta, Cr) in the melt diffuses into the active nucleants $TiAl_3$ and TiB_2 present in grain refiner producing ternary components which are less effective nucleants for α-Al (probably due to unfavorable lattice parameters). Here, the free energies of formulation of the ternary phases are

lower than that of their corresponding binary aluminides or borides. The formation of the ternary compounds as well as their chemical formula can be represented by the following reactions into which Zr, Ta or Cr is replaced by Me

$$XMe\ (\text{in Al melt}) + TiAl_3 = = = = = = (Me_x, Ti_{1-x})Al_3 + XTi\ (\text{in Al melt}) \quad (5.4)$$

$$XMe\ (\text{in Al melt}) + TiB_2 = = = = = = (Me_x, Ti_{1-x})B_2 + XTi\ (\text{in Al melt}) \quad (5.5)$$

According to Abdel-Hamid's mechanism, increasing the poisoning element concentration in the melt and/or increasing the contact time before casting will increase the concentration of this element in the ternary aluminide or boride particles. This will increase the deviation of their lattice parameters and grain refining properties from that of the initial good nucleants for Al. Hence, it can be expected that the grain refining efficiency of the master alloy will deteriorate continuously with increasing the contact time and the poisoning effect will be greater at higher concentration of the poisoning element and at higher superheats in the Al melt. These facts are in good agreement with the experimental results and grain refining practice.

Furthermore, the difference in the effect of Zr on the grain refining efficiency of the Al-Ti and Al-Ti-B master alloys can be attributed to the large difference in grain refining properties of $TiAl_3$ and $ZrAl_3$ which is lower for the latter. This agrees also with the fact that addition of B to Al-Ti and Al-Zr alloys increase the difference in grain refining efficiency of the two alloys.

Recently, This mechanism was supported by experimental results, (1997, Arjona). They identified complex Ti aluminides containing Zr at the grain centers, Zr-aluminides containing Ti, Fe and Fe-aluminides containing Ti and Zr at the grain boundaries in the microstructure of Al-25 Zr alloy grain refined by Al-5Ti-1B master alloy at an addition rate of 0.01 %. They also assumed that Zr dissolved in the liquid Al reacts with the $TiAl_3$ particles of the grain refiner to form the complex Ti aluminide

containing Zr, making those impotent nucleants for Al. Finally, they concluded that $TiAl_3$ or TiB_2 particles (being nucleant sites) are poisoned by interaction with Zr dissolved in liquid Al and the extent of poisoning is decided by the amount of Zr present in the liquid.

Johnson (1994) argued that the poisoning effect of Zr is associated with the phase of $ZrAl_3$ in which some Ti dissolve to form complex ($Ti_{1-x},Zr_x)Al_3$ resulting in the loss of grain refining effect of Ti.

5.2 The Extrusion Process

The extrusion process may be considered equivalent to uniaxial compression process whose the billet of diameter d_o and length L_o is extruded to a part of smaller diameter d_f and larger length L_f. Hence the representative or effective strain $\bar{\varepsilon}$ is equal to

$$\bar{\varepsilon} = \text{Ln}\,(L_f/L_o) = \text{Ln}\,(A_o/A_f) \qquad (5.6)$$

In the extrusion (A_o/A_f) is the extrusion ratio, R. If the reduction in area percentage is r

then $r = (A_o - A_f)/A_o = 1 - (A_f/A_o)$ (5.7)

From which $R = 1/(1-r)$ (5.8)

Hence $\varepsilon = \text{Ln}\ 1/(1-r)$ (5.9)

5.2.1 Extrusion pressure

The first rational relationship between extrusion pressure, P,(defined as the ratio of the ram or plunger force over the cross-sectional area of the slug or billet) and the reduction in area appears to have been put forward by Siebel and Fanmeier, and it was based on the homogenous deformation, (Siebel and Fanmeier, 1931).

It was assumed that

$$P = \bar{K}\, Ln \frac{A\circ}{Af} = \bar{K}\, Ln \frac{1}{1-r} \qquad (5.10)$$

Where A_o and A_f are original and final cross sectional area and $\bar{K}$ is the resistance to deformation which depends on the temperature and speed of extrusion. The experimental values of extrusion pressure are always higher than the theoretical values obtained from the above formula because it neglects the friction between the total length of the billet and the container wall. Even when the above formula was modified to include a term to allow for friction it did not solve the problem because the formula did not take into consideration the work consumed in distortion or non homogenous deformation, i.e. the redundant work which is very high in the extrusion process and accounts for about 15 % of the plastic work.(Rowe, 1968)

Hill (1948), has calculated the plain strain extrusion pressure using theory of slip line field for reductions between 0.12 and 0.88 assuming dead metal zones to cover the whole of the die face and no friction between the billet and the container wall. Calculations of extrusion pressure were also made by (Johnson and kudo, 1962).

Johnson (1980), has suggested a useful empirical approach. for determining the value of extrusion pressure for pure aluminum and presented the following formula:

$$P = Y_{av} [a + b \text{ Ln } 1/(1-r)] = Y_{av} [a + b \text{ Ln } R] \qquad (5.11)$$

where P is the extrusion pressure for the pure aluminum and Y_{av} is the average flow stress and a = 0.8 and b = 1.5, from which the extrusion force F_{ext} can be obtained from

$$F_{ext} = P.(\pi d_o^2/4) \qquad (5.12)$$

5.2.2 The Energy Consumed in Extrusion

In general the energy consumed in any plastic deformation process is determined from the following relationship :

$$dWp = \bar{\sigma}\, d\bar{\varepsilon} \qquad (5.13)$$

Where dWp is the differential quantity of the plastic work per unit volume and $\bar{\sigma}, \bar{\varepsilon}$ are the representative stress and the representative strain respectively, Fig.37

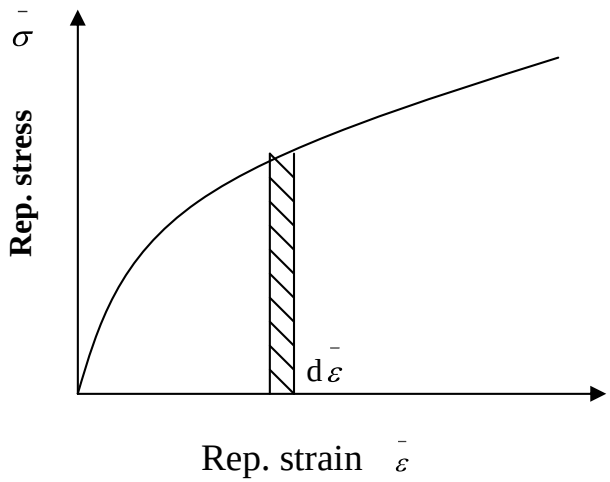

Fig. 37 : Typical representative stress-representative strain for an engineering material

For an engineering material the relationship between $\bar{\sigma}$ and $\bar{\varepsilon}$ at a particular temperature and strain rate may be given by

$$\bar{\sigma} = K\bar{\varepsilon}^{n} \tag{5.14}$$

Where K is a material constant and n is the strain hardening index. The total plastic work per unit volume can be determined by substituting for $\bar{\sigma}$ from equation (5.14) into equation (5.13) and carrying out the integration. The total plastic work is then determined by multiplying the results obtained from equation (5.13) after integration by the affected volume, which is the volume of the extruded part.

It is to be noted that this is the ideal value of the work where the deformations are assumed homogeneous and frictionless and the energy consumed is expended to overcome only the mechanical strength of the deformed part. Therefore to determine the actual consumed work, the work consumed to overcome friction between the billet and the container wall and which accounts to 35 % of the work consumed in the plastic deformation together with the redundant work to overcome the inhomogeneous

deformation which is maximum in the extrusion process and accounts for 15 % of the plastic deformation. Hence the total consumed work will be the total work consumed in plastic deformation as determined multiplied by a factor ranging from 1.25 to 1.5.

5.3 Determination of the Wear of Aluminum and its Microalloys

The basis of wear theories was attempted to explain the wear process on a microscopic scale and to relate the magnitude of the wear to the material properties, and to the number and nature of the local encounters. The first such theory was proposed which related the wear rate to the number of inter atomic encounters between the opposing surfaces,(Holm, 1946). However, the idea of material removal from solids by plucking of atoms has not been generally accepted.

More recently attempts have been made to establish a new wear theory based on atomic level of wear (Zharg, 1997), but the idea is still far from simplest and being applicable. The reason is that wear debris is generated more or less simultaneously with the onset of motion and in all cases the debris consists of aggregated particles of the material.

Holm's theory was followed by Archard who made the more realistic assumption that wear occurred as a result of interactions between surfaces asperities, (Archard,1953). Archard's theory for adhesive wear has become the most widely quoted in the literature.

As wear in aluminum and other soft material is of adhesive type, Archard's theory was repeatedly used to predict the mass loss of the worn material from the following equation:

$$V = \frac{KPL}{3H} \text{..... ....} (5.15)$$

Where V is the worn volume, P is the applied load, L is the sliding distance, H is the hardness and K is a constant which was interpreted as the probability that a particular

asperity contact could produce a wear particle, and may be considered as a wear coefficient.

Experimental testing of Archard's theory revealed that although it gives good indicator in some cases of adhesive wear, it fails in other cases particularly in determining the wear of aluminum and other soft materials where in addition to mass loss there exists some plastic deformation at the worn end. This phenomenon was reported by Zaid (2001), Zaid and Hussein (2001) and very recently by Zaid and Al-Banna (2007), where the plastic deformation is reported to be more predominant than the mass loss.

This led to develop a new theoretical model for assessing the wear of aluminum and other soft materials which accounts for both the mass loss and the plastic deformation at the worn end.

5.4 Suggested Model for Assessing Wear of Aluminum and its Microalloys

This model is based on the energy balance by considering the work from the applied load through the sliding distance between the two solids is mainly consumed in

1- Shearing the particles which represents the work consumed in mass loss or volume removal.

2- The plastic deformation at the worn end i.e. the mushrooming effect.

The work consumed in shearing the particles, *Ws*, may be calculated from the following relationship: $Ws = V\tau\gamma$ (5.16)

Where *Ws* is the work consumed in shearing the particles, *V* is the volume of the material removed=mass loss/density, τ is the shear stress, and γ is the shear strain.

The work consumed in the plastic deformation i.e. producing mushrooming, *Wp*, may be calculated from the following relationship:

$$Wp = Affected \quad volume \int_0^{\bar{\varepsilon}_{av}} \bar{\sigma}\, d\bar{\varepsilon} \ldots\ldots\ldots\ldots\ldots\ldots\ldots (5.17)$$

Where the affected volume is the volume of the mushrooming part at the worn end, which may be determined from the decrease in height Δh and the final diameter of the worn end. $\bar{\varepsilon}_{av}$, is the average representative strain, and $\bar{\sigma}$, is the representative stress of the pin material determined from the equation representing mechanical behavior, or from the representative stress-representative strain ($\bar{\sigma}$ - $\bar{\varepsilon}$) curve.

6. RESULTS AND DISCUSSION

In this chapter, the results obtained through this investigation will be presented and discussed. As aluminum is industrially grain refined by either titanium, Ti, or titanium and boron, Ti-B, the obtained results will be dealt with under the following headings:

Effect of zirconium addition at a weight percentage of 0.1 % (this percentage corresponds to the peretictic reaction limit on the phase diagram of Al-Zr on the grain size, microstructure, hardness, mechanical behavior illustrated by the representative stress, $\bar{\sigma}$,– representative strain, $\bar{\varepsilon}$, ultimate tensile strength,(UTS), and the ductility of commercially pure aluminum (Al), Al grain refined by Ti and Al grain refined by Ti+B**.** Finally, comparison is made between the effect of Zr addition at a rate of 0.1 % weight percentage to Al grain refined by Ti and Al grain refined by Ti+B.

6.1 Effect of Addition of Zirconium on the Metallurgical and Mechanical Characteristics of Aluminum Grain Refined by Ti

6.1.1 Effect of Zr addition on the metallurgical aspects of Al grain refined by Ti

The effect of addition of Ti or Zr alone or both together on the grain size is shown in the histogram of figure 38. It can be seen from the histogram that the addition of Ti alone at a rate of 0.15 % weight resulted in grain refinement of aluminum as the average grain size is decreased by 17 %, whereas addition of Zr alone at a rate of 0.1 % weight resulted in slight poisoning i.e. coarsening of the grains as the average grain size is increased by about 3.2 %.

This agrees with the finding of previous researchers, (Abdel-Hamid, 1985, Zaid and Abdel-Hamid, 2000, Zaid , 2003). On the other hand addition of Zr to Al in the presence of titanium resulted in enhancement of the grain refining efficiency of titanium as indicated in figure 38. This is in disagreement with the previous finding, (Abdel-

Hamid,1982) who reported that the addition of Zr to aluminum in the presence of Ti reduces the grain refining efficiency of Ti. This may be explained in terms of the chemical composition of the aluminum material used as it was found that the presence of small amount of impurities or elements can strongly affect the grain refining efficiency of Al-Ti master alloy. For example, it was found that the grain refining of pure aluminum by Ti was increased by 100 % when the Al purity was decreased from 99.999 % to 99.99, (Youdelis and Young, 1981).

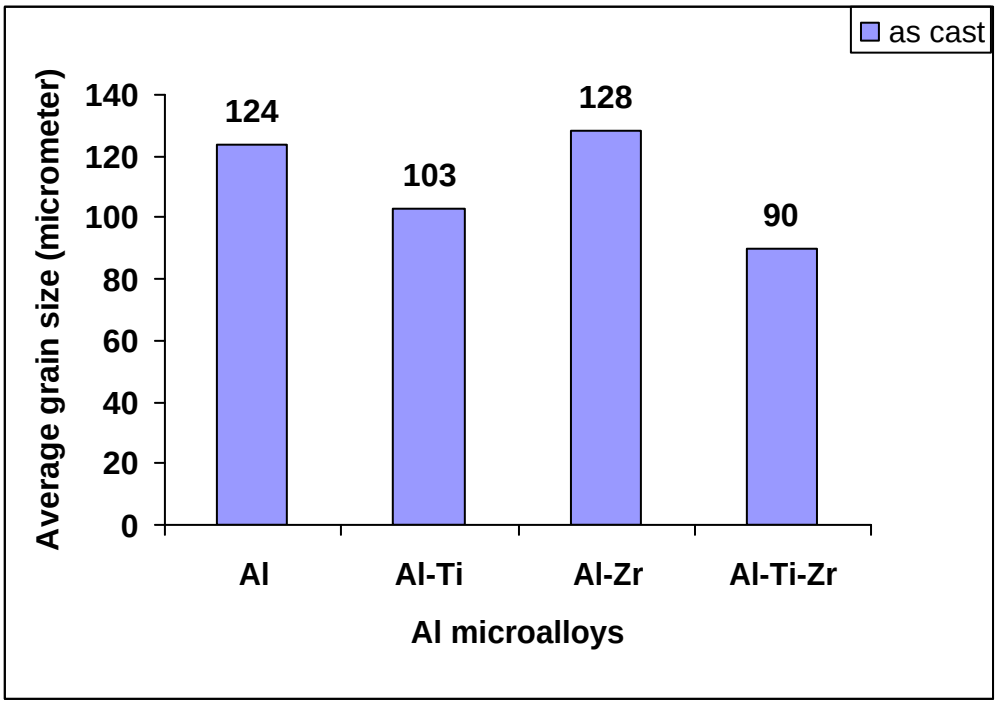

Fig.38: The effect of zirconium addition on the grain size of Al and Al grain refined by Ti in the as cast condition.

The effect of addition of Ti or Zr alone or together on the microstructure is explicitly shown in the photomicrographs of figures 39 (a),(b),(c)and (d) for Al, Al-Ti, Al-Zr and Al-Ti-Zr, respectively.

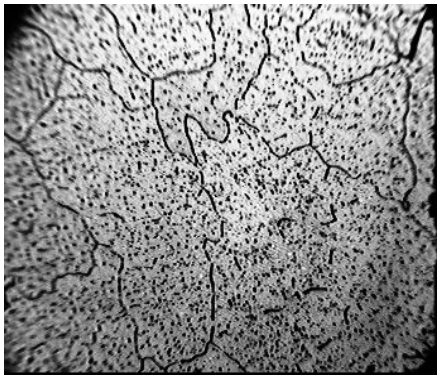

(a) Pure Al (124 μm)

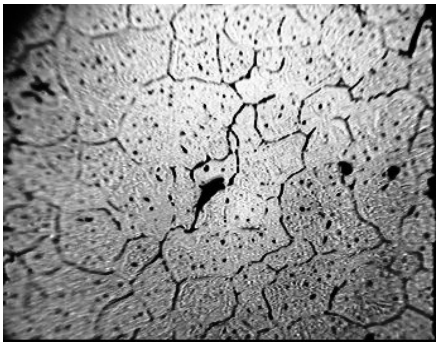

(b) Al -Ti (103 μm)

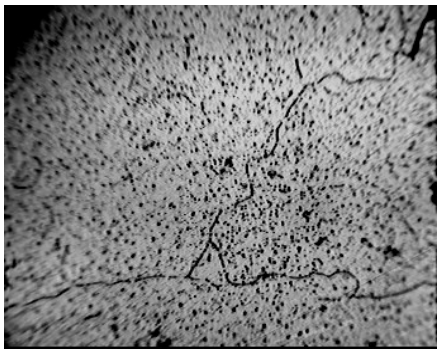

(c) Al-Zr (128 μm)

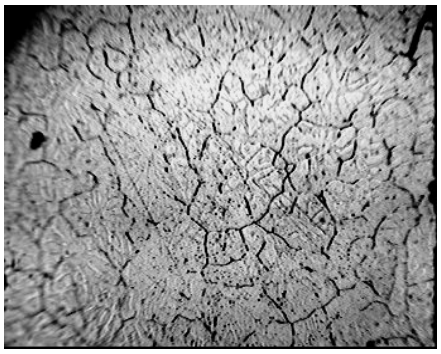

(d) Al-Ti-Zr (90 μm)

Fig. (39): Photomicrographs of Al and it's Micro Alloys: (a) Pure Al, (b) Al-Ti, (c) Al-Zr, (d) Al-Ti-Zr, in the as cast conditions, X 250

6.1.2 Effect of Zr Addition on the Mechanical Characteristics of Al and Al grain refined by Ti

It can be seen from the histogram of figure 40 that the addition of Ti resulted in enhancement of the hardness of aluminum, as an increase of 37.9 % was achieved, However, addition of Zr alone or in the presence of titanium resulted in slight decrease of it hardness, e.g. 10.3 % decrease in the case of Zr addition alone and 6.8 % decrease in the case of Ti+Zr addition.

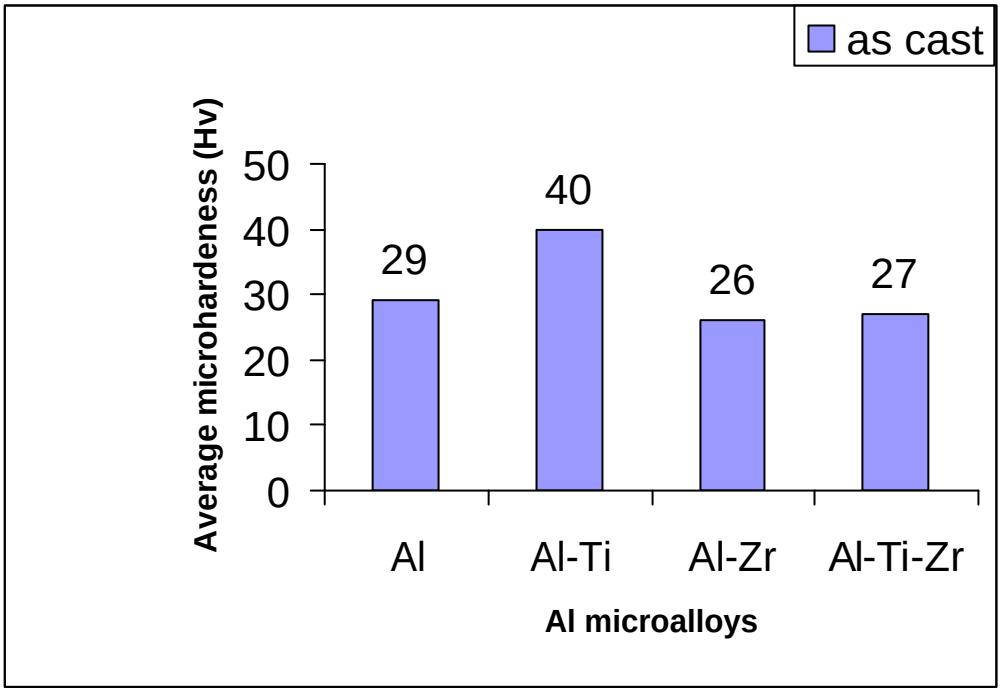

Fig 40: Effect of zirconium addition on the average Vicker's microhardness of Al and Al grain refined by Ti in the as cast condition

The effect of Zr addition on the general mechanical behavior of Al is shown in fig. 41.

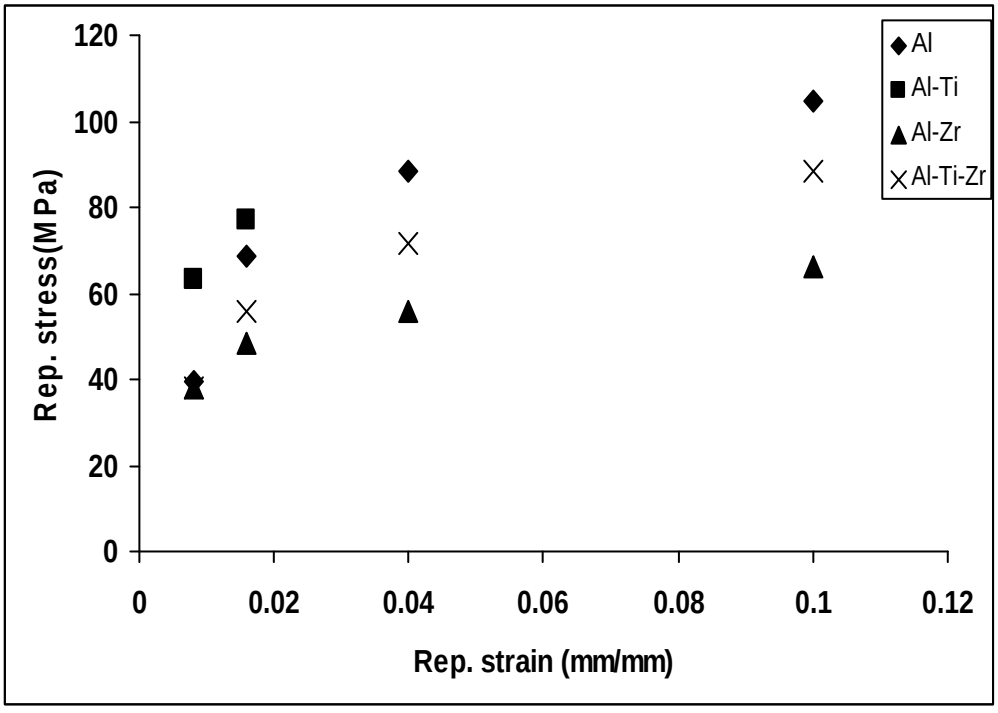

Fig. 41: Effect of zirconium addition on the Rep. Stress – Rep. Strain of Al and Al grain refined by Ti in the as cast condition

The mechanical properties are given in Table 8.

Table 8: Mechanical properties of Al and its different microalloys in the as cast.

Micro alloys	Flow stress (MPa)at strain= 20 %	Strain hardening index (n)	Strength coefficient (K) MPa	General equation of mechanical behavior
Al	93	0.04	102	$\bar{\sigma} = 102\ \bar{\varepsilon}^{0.04}$
Al-Ti	18	0.17	23	$\bar{\sigma} = 23\ \bar{\varepsilon}^{0.17}$
Al-Zr	71.2	0.172	94	$\bar{\sigma} = 94\ \bar{\varepsilon}^{0.17}$
Al-Ti-Zr	89	0.2	122	$\bar{\sigma} = 122\ \bar{\varepsilon}^{0.2}$

Similarly addition of either Ti or Zr alone or both together resulted in decrease of its flow stress at 20 % strain. The maximum decrease is at Ti addition being 80 % followed by Zr addition (23.6 %) and the least decrease is when both are added together, (4.3 %), figure 42, This is due to the existence of the intermetallic phases within the aluminum matrix which tends to reduce the mechanical strength. These are the alumide $TiAl_3$ in case of titanium and $ZrAl_3$ in case of Zr addition and both phases in case of Ti+Zr addition. The $TiAl_3$ phase particles are softer than $ZrAl_3$.This is why their existence causes more decrease than the $TiAl_3$.

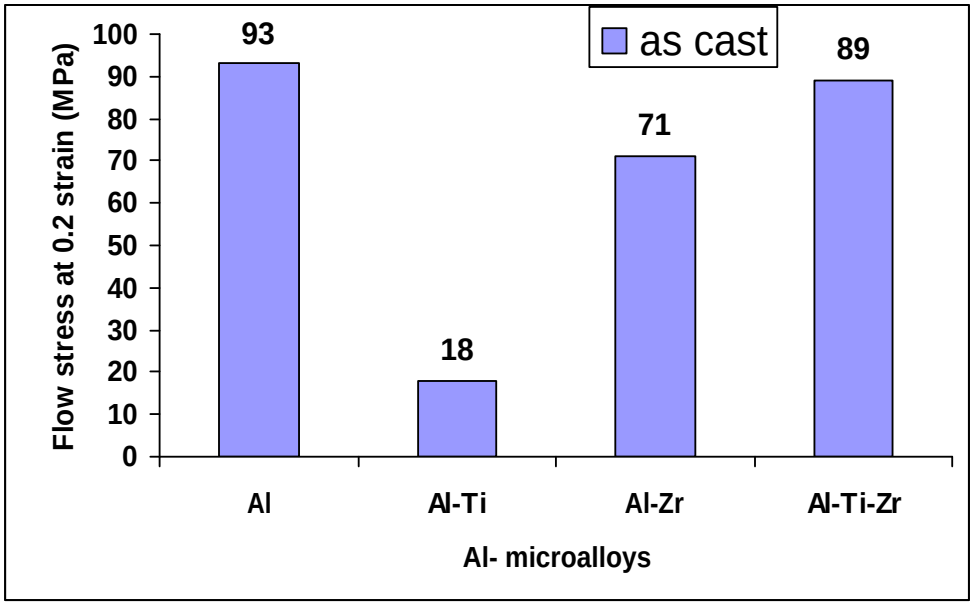

Fig. 42: Histogram of the flow stress at 0.2 strain of Al and Al grain refined by Ti in the as cast condition

Also the addition of either Ti or Zr alone or both together resulted in decrease of the ultimate tensile strength, UTS, maximum decrease is in the case of Zr addition alone whereas when both are added together they resulted only in slight decrease of its UTS being only 8.4 %, as illustrated by the histogram of figure 43. This means that the effect (Ti+Zr) is not additive when added together. This was also found by (Zaid, 2003) when tantalum Ta and Zr were added together.

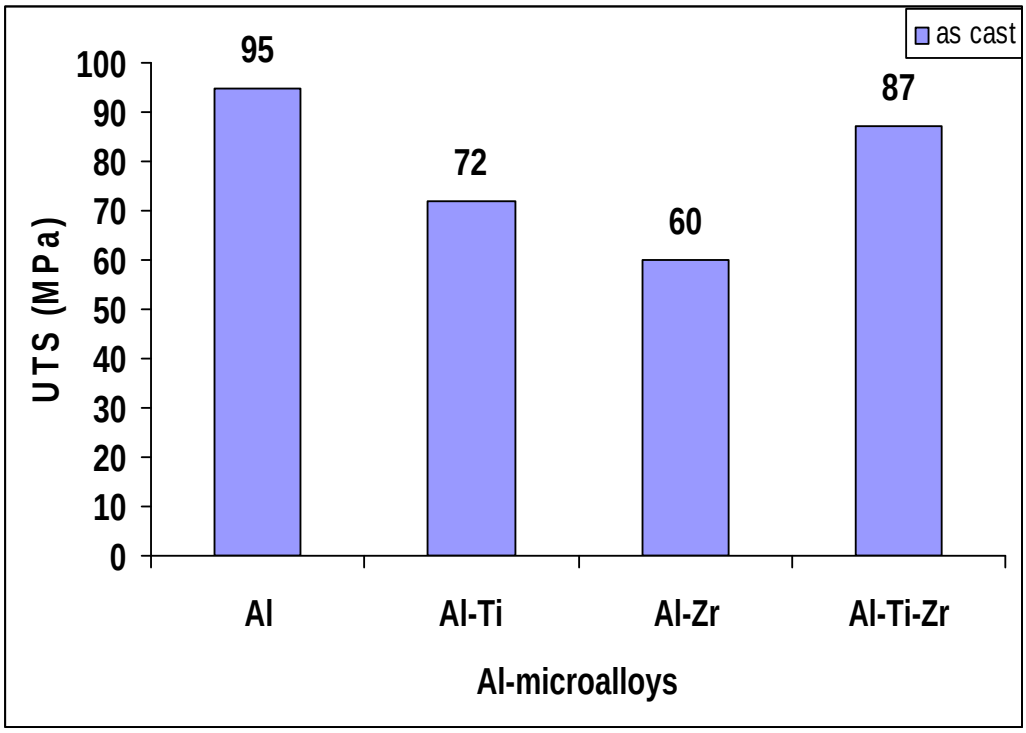

Fig. 43: Effect of zirconium addition on the UTS of Al and Al grain refined by Ti in the as cast condition

Finally, the effect of addition of Ti resulted in decrease of its ductility (represented by maximum elongation percentage and maximum reduction in cross sectional area in the tensile test), where a decrease of 30.8 % in elongation, and 57 % in maximum reduction in cross sectional area. However addition of either Zr or Ti+Zr resulted in improvement of its ductility by 107.7 % and 115.4 % in the elongation percent and 35.7 % 64.3 % in the cross sectional area as shown in figures 44 and 45, in the case of Zr and Ti+Zr additions respectively.

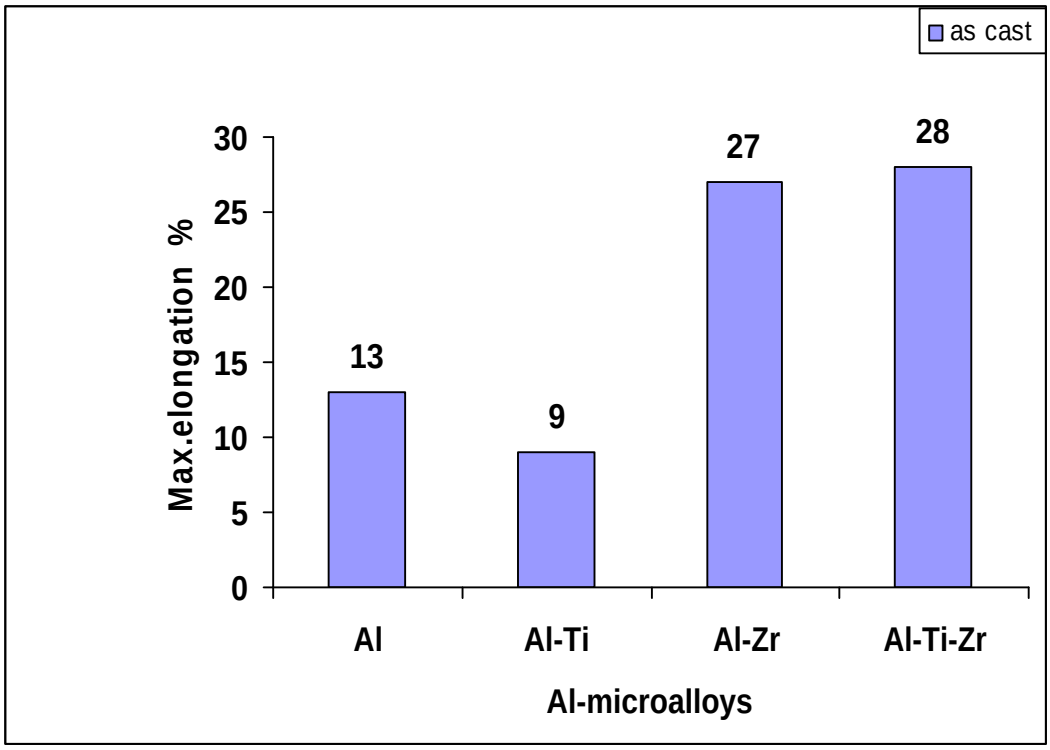

Fig.44: Effect of zirconium addition on the maximum elongation %, on Al and Al grain refined by Ti in the as cast condition

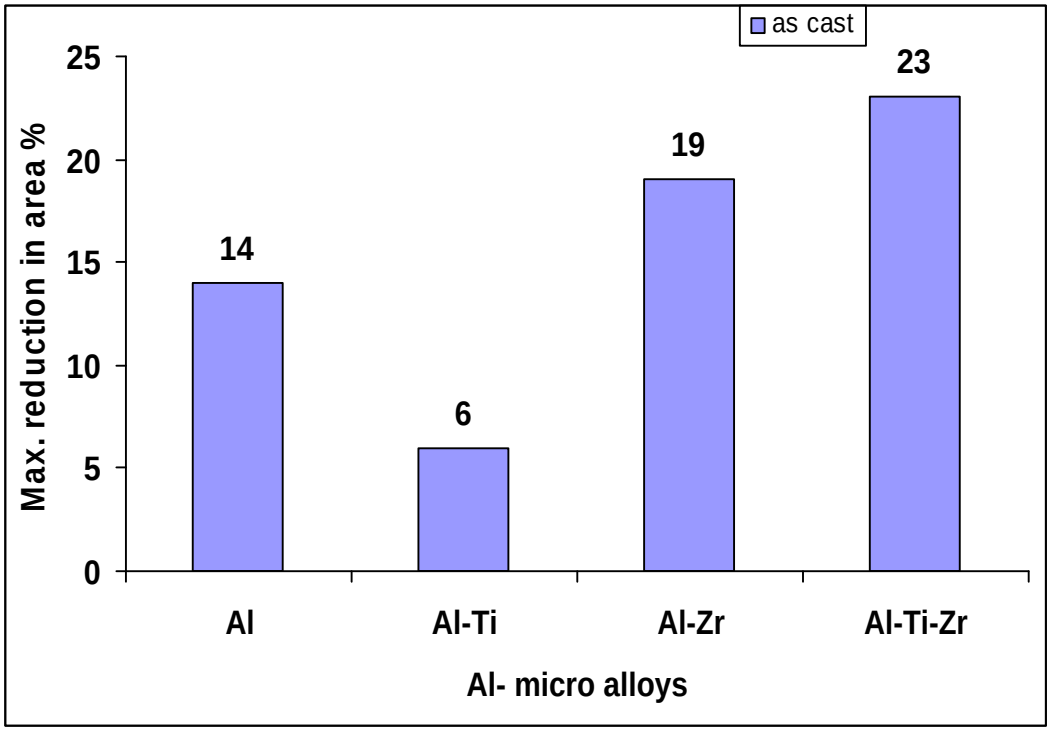

Fig 45: Effect of zirconium addition on the maximum reduction in area %, on Al and Al grain refined by Ti in the as cast condition

6.2 Effect of Addition of Zirconium on the Metallurgical and Mechanical Characteristics of Aluminum Grain Refined by Ti+B

6.2.1 Effect of Zr addition on the metallurgical aspects of Al and Al grain refined by Ti+B

Examination of the histogram of figure 46 reveals that the effect of Ti+B addition at a rate of (0.05 % Ti and 0.01 % B) weight percentage resulted in very pronounced grain refinement as a decrease of 33.33 % in the average grain size, whereas addition of zirconium alone at a rate of 0.1 % resulted in poisoning effect with slight decrease of the average grain size (3.2 %).

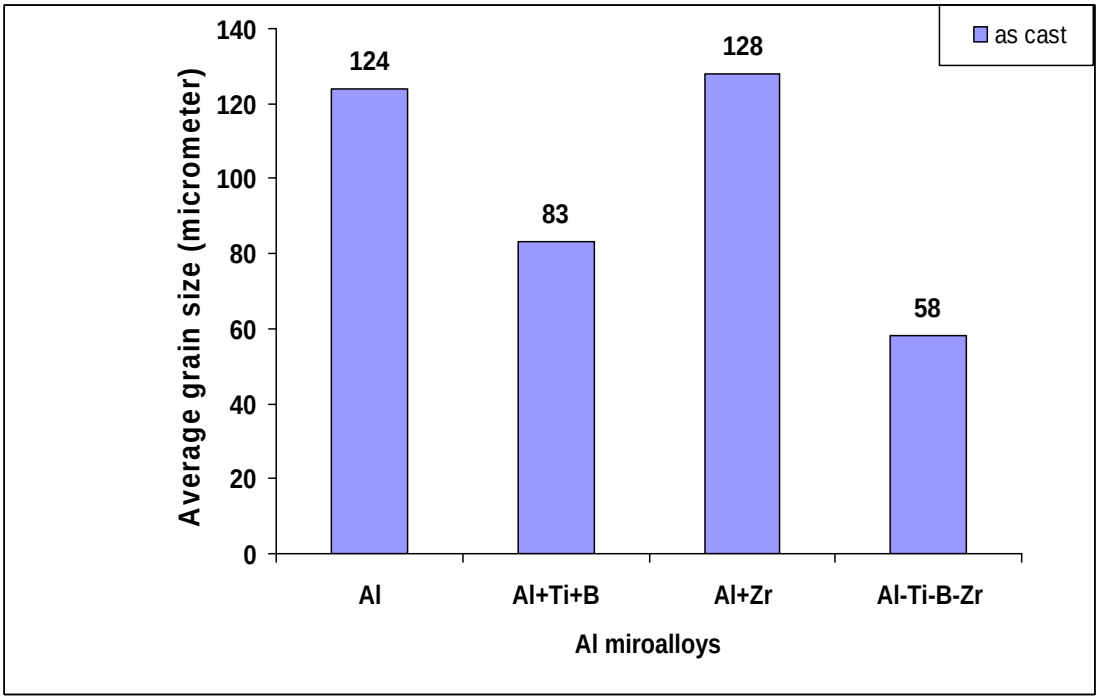

Fig. 46: Effect of zirconium addition on the grain size of Al and Al grain refined by Ti+B in the as cast condition

However, the addition of Zr to the Al grain refined by Ti+B (i.e. addition of Ti+B and Zr) resulted in better enhancement in grain refinement efficiency than when adding Ti+B alone, as a decrease in the average grain size of 53 % was achieved. This is shown by the photomicrographs of figure 47 (a), (b), (c) and (d), for Al, Al-Ti-B, Al-Zr and Al-

Ti-B-Zr respectively. Again this unexpected behavior of Zr addition can be explained in terms of the difference in the degree of aluminum purity as discussed.

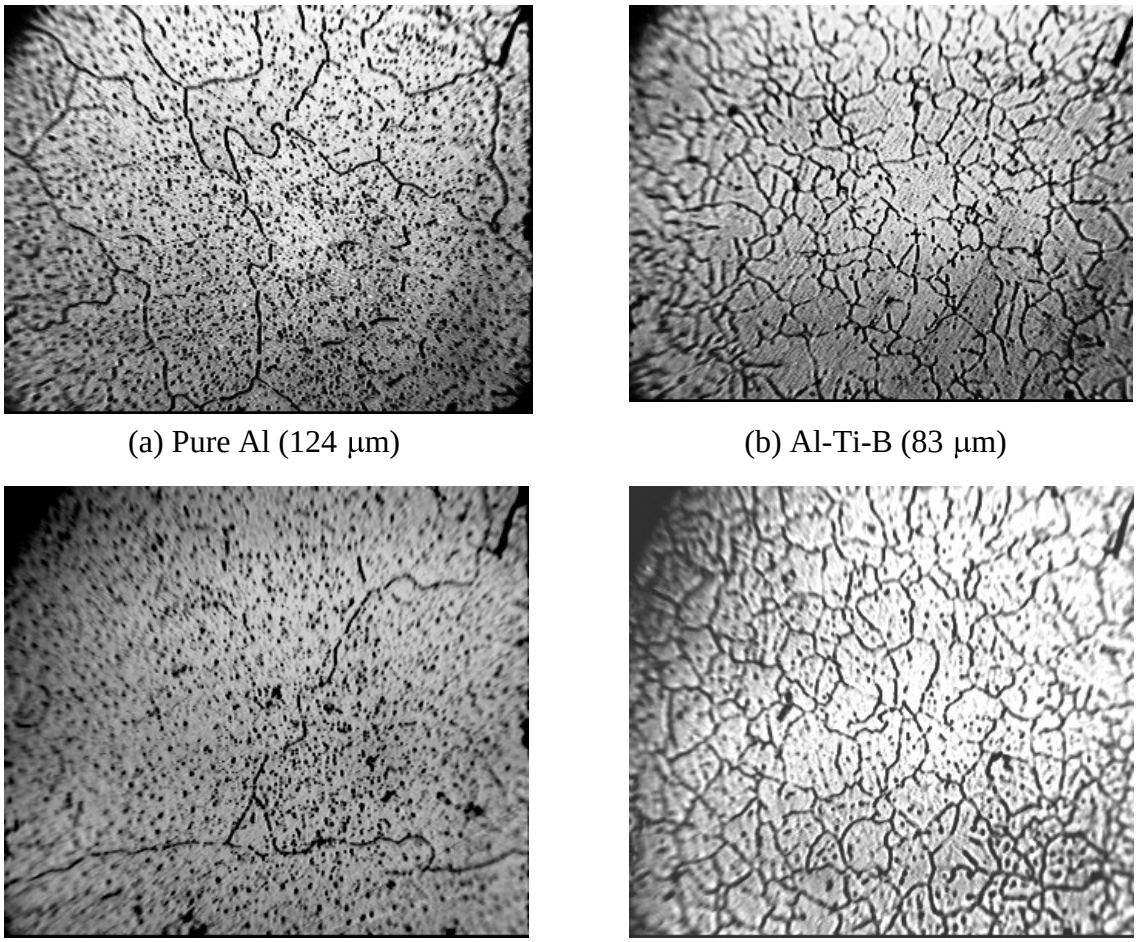

(a) Pure Al (124 μm) (b) Al-Ti-B (83 μm)

(c) Al-Zr (128 μm) (d) Al-Ti-B-Zr (58μm)

Fig. 47 : Photomicrographs of Al and it's Micro Alloys: (a) Pure Al, (b) Al-Ti-B (c) Al-Zr, (d) Al-Ti-B-Zr, in as cast condition, X 250

Regarding the effect of these additions on hardness it can be seen from the histogram of figure 48 that addition of Ti+B resulted in increase of 48.3 % in its hardness, Whereas, addition of Zr alone resulted in 10.3 % decrease in its hardness. However, addition of Ti+B and Zr together resulted in further increase of the hardness of aluminum. Again this emphasizes that addition of both of elements is not additive, which agrees with pervious finding, (Zaid, 2003).

6.2.2 Effect of Zr addition on the hardness and mechanical characteristics of Al Grain refined by Ti+B

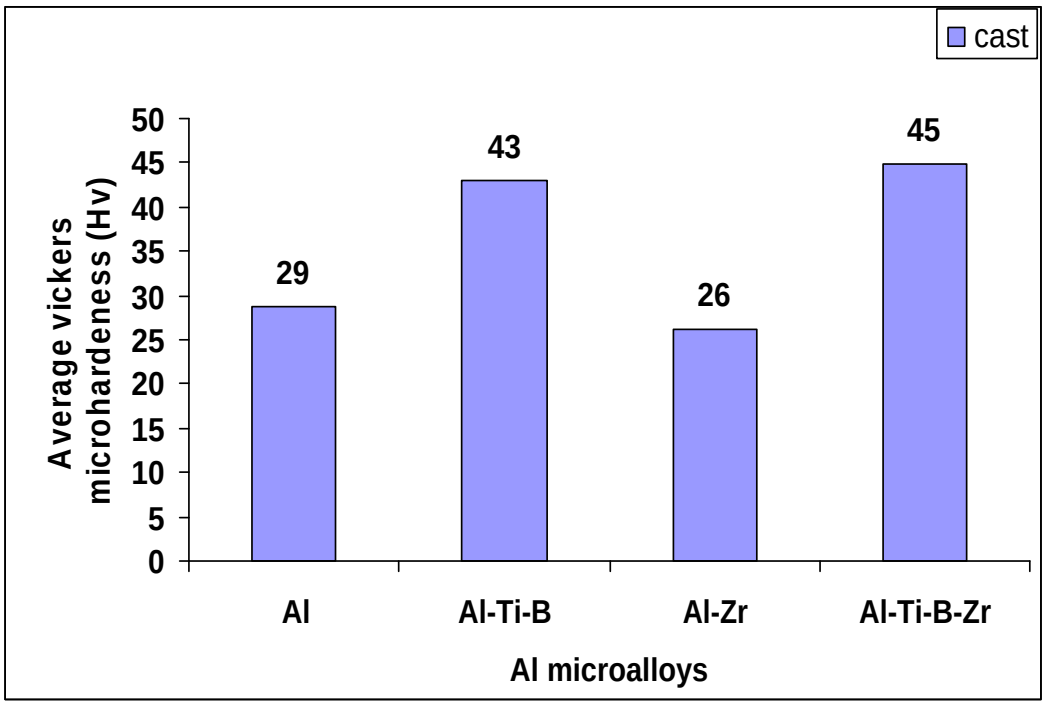

Fig. 48: Effect of zirconium addition on the average Vickers hardness of Al and Al grain refined by Ti+B in the as cast condition

The effect of Ti+B addition on the general mechanical behavior of Al is shown in figure 49. It can be seen from figure 49 that addition of Zr causes deterioration in the mechanical behavior of Al whereas addition of Ti+B or Ti+B+Zr resulted in enhancement of its mechanical behavior being better incase in case of Ti+B addition.

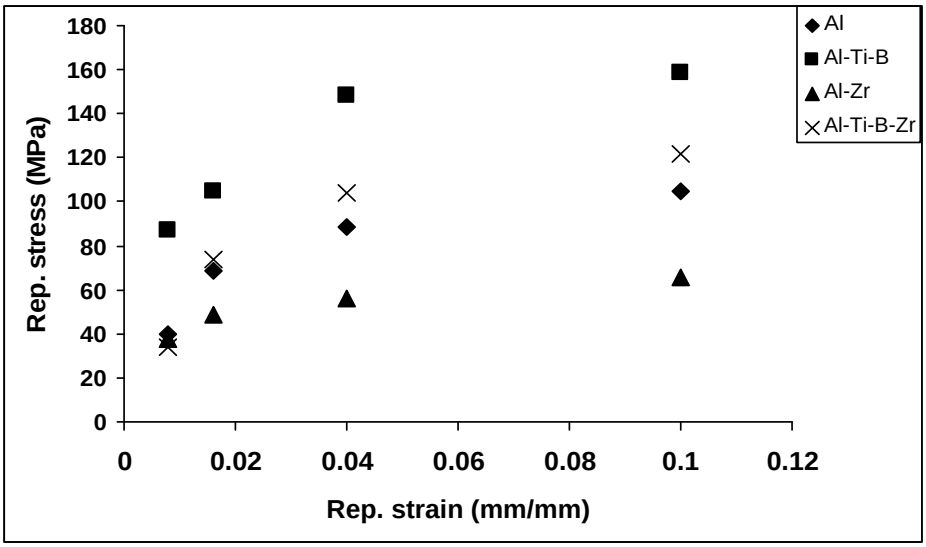

Fig. 49: Rep. Stress – Rep. Strain of Al and Al grain refined by Ti+B in the as cast condition

The main mechanical properties of Al, Al-Ti-B, Al-Zr and Al-Ti-B-Zr are shown in Table 9 which shows that the strength factor, K, increases in case of Ti+B or Ti+B+Zr addition. Regarding strain hardening index, n, it increased with addition of either Ti or Zr alone or together.

Table 9: Mechanical properties of Al and Al grain refined by Ti+B of different micro alloys of in the as cast condition.

Micro alloys	Flow stress (MPa)at strain= 20%	Strain hardening index (n)	Strength coefficient (K) MPa	General equation of mechanical behavior
Al	93	0.04	102	$\bar{\sigma} = 102\,\bar{\varepsilon}^{\,0.04}$
Al-Ti-B	250.5	0.34	433	$\bar{\sigma} = 433\,\bar{\varepsilon}^{\,0.34}$
Al-Zr	71.2	0.172	94	$\bar{\sigma} = 94\,\bar{\varepsilon}^{\,0.17}$
Al-Ti-B-Zr	174.8	0.34	302.2	$\bar{\sigma} = 302.2\,\bar{\varepsilon}^{\,0.34}$

Figure 50 gives comparison between addition of Ti+B, Zr and Ti+B-Zr on the flow stress at 0.2 strain which shows an increase of its value by 169 % incase of Ti+B addition and slight increase of about 110 % incase of Ti+B+Zr addition and a pronounced decrease of 23.6 % incase of Zr addition.

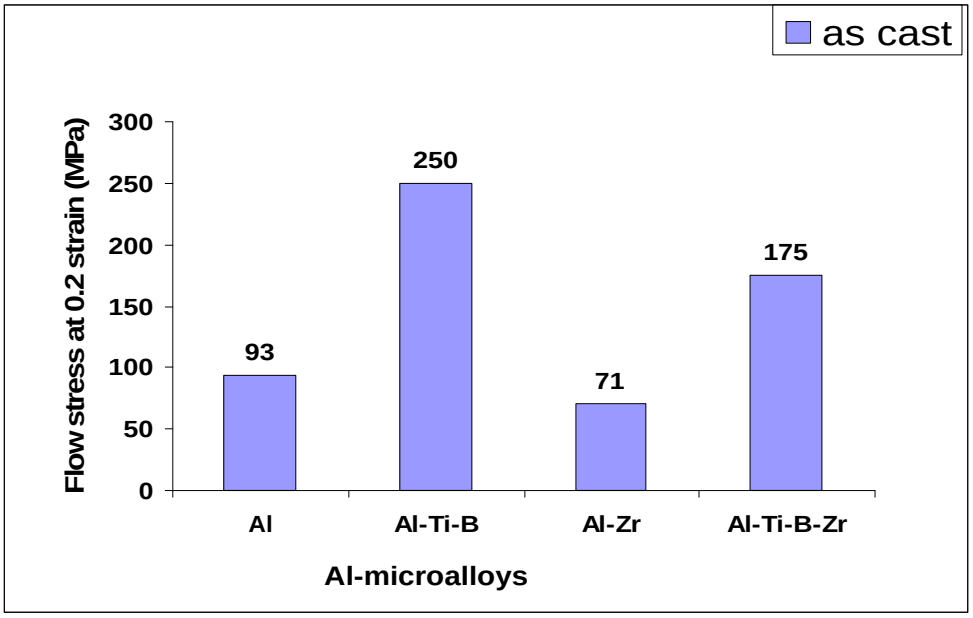

Fig.50: Effect of zirconium addition on the flow stress at 0.2 strain on Al and Al grain refined by Ti+B in the as cast condition

Similarly, the ultimate tensile strength is drastically reduced by addition of Zr about 36.8 % and slightly reduced by addition of Ti+B, 2 %.Whereas it enhanced by addition of Ti+B and Zr together (increase of 8.4 %), as illustrated by the histogram of figure 51.

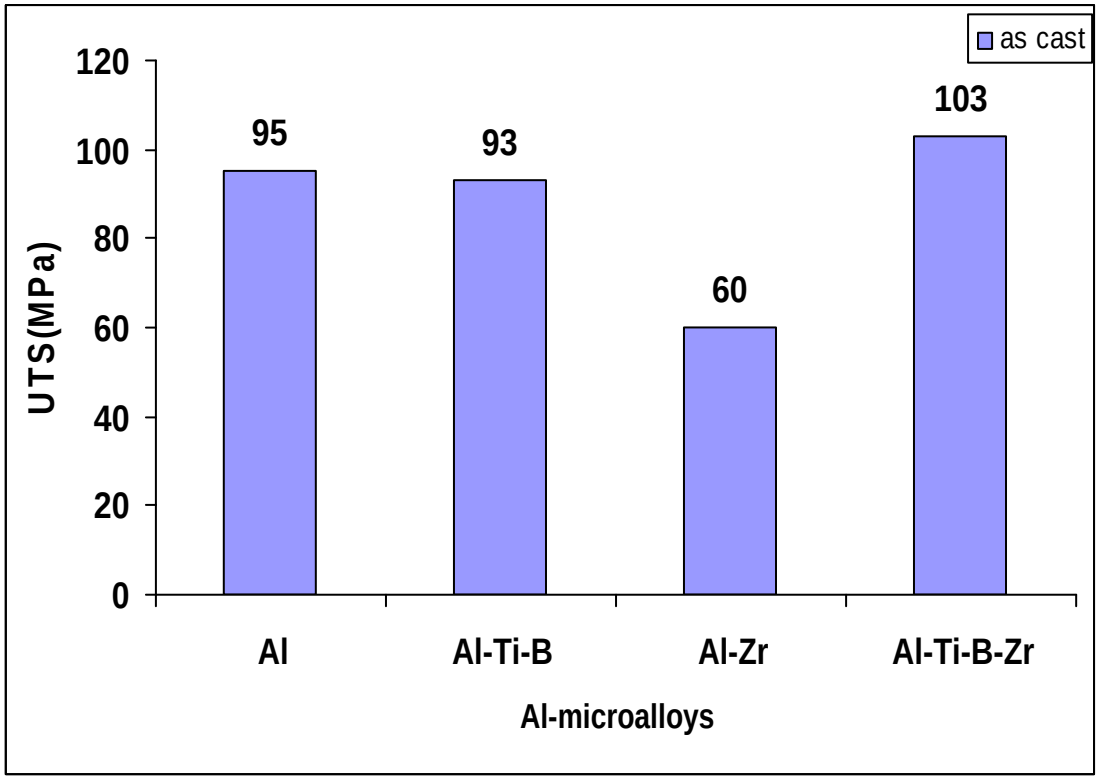

Fig. 51: Effect of zirconium addition on the UTS of Al and Al grain refined by Ti+B in the as cast condition

Regarding the effect of these elements on the ductility of aluminum it can be seen from the histograms of figures 52 and 53, which show the maximum elongation % and maximum reduction in area percentage respectively, that addition of Zr resulted in increase of ductility whereas addition of either Ti+B or Ti+B+Zr resulted in decrease of the ductility of aluminum.

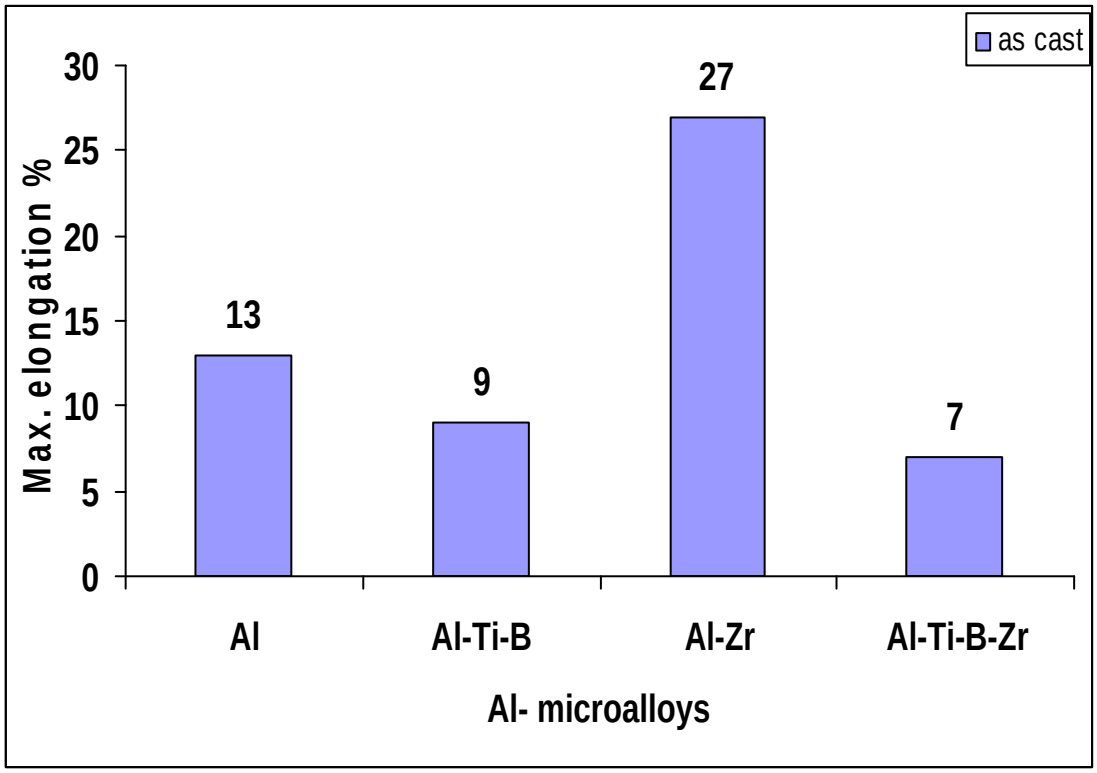

Fig.52: Effect of zirconium addition on the maximum elongation % of Al and Al grain refined by Ti+B in the as cast condition

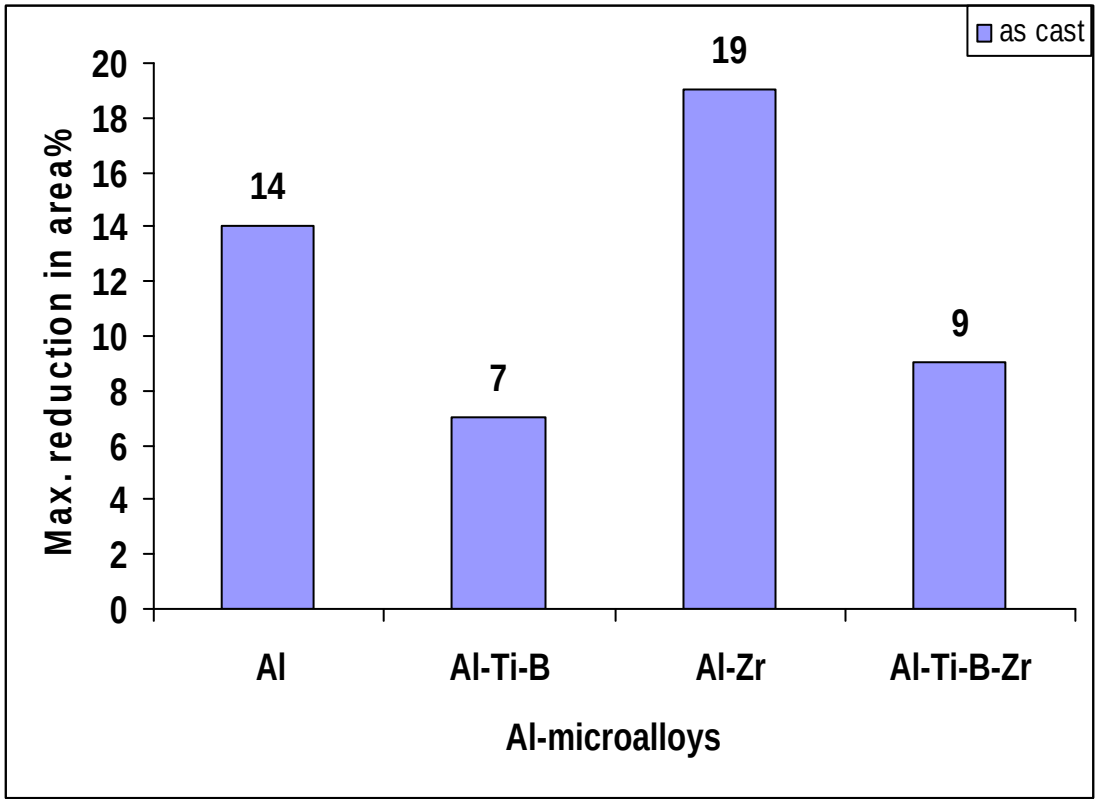

Fig.53: Effect of zirconium addition on the max. reduction in area % of Al and Al grain refined by Ti+B in the as cast condition

6.2.3 Comparison Between Zr Addition to Al Grain Refined by Ti and Al Grain Refined by Ti+B

Figures 54 to 61 inclusive are included for comparison purposes between addition of zirconium to Al grain refined by Ti and Al grain refined by Ti+B.

It can be seen from figure 54 that addition of Ti+B has better grain refining efficiency than Ti alone, although its value is three times its value when added with boron although boron itself is not a grain refiner when added alone.

Addition of Zr to Al in the presence of Ti+B resulted in improving the grain refining efficiency while addition of Zr alone resulted in poisoning. There is no explanation given by the metallurgists for these two phenomena.

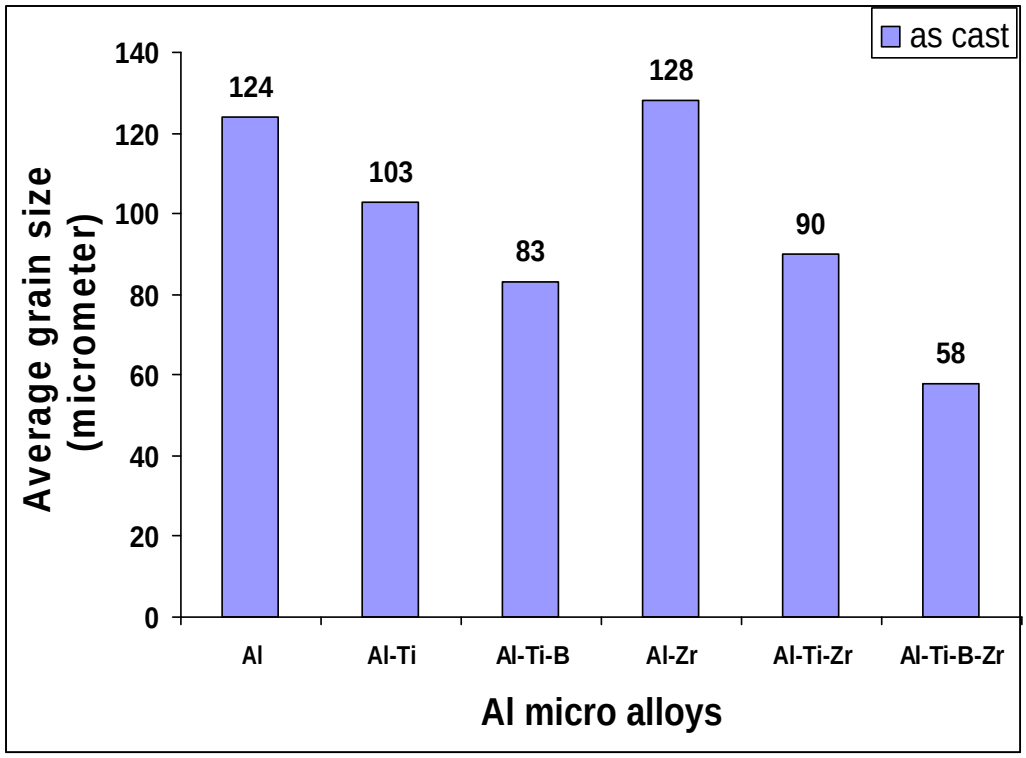

Fig.54: Effect of zirconium addition on the grain size of Al and Al grain refined by Ti and Ti+B in the as cast condition

In general, addition of Zr to Al grain refined by Ti or Ti+B resulted in grain refinement being better in the case of Al refined by Ti+B. Addition of Zr alone resulted in grain coarsening. This is clearly demonstrated by the photomicrographs of figure 55.

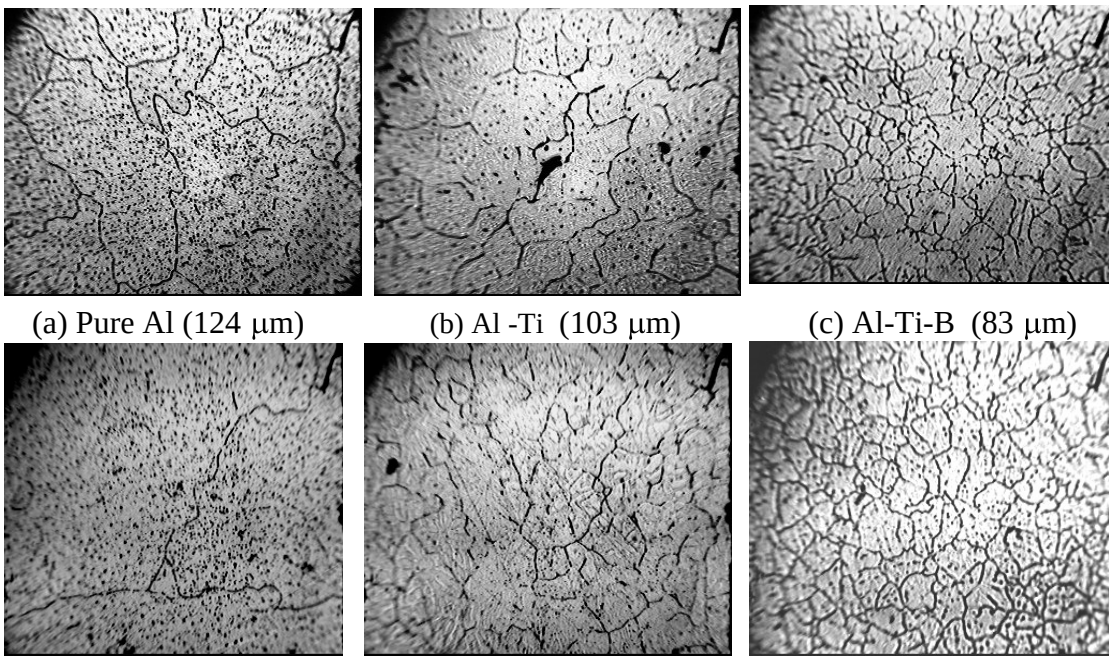

(a) Pure Al (124 μm) (b) Al -Ti (103 μm) (c) Al-Ti-B (83 μm)

(d) Al-Zr (128 μm) (e) Al-Ti-Zr (90 μm) (f) Al-Ti-B-Zr (58μm)

Fig.55: Photomicrographs of Al and it's Micro Alloys: (a) Pure Al, (b) Al-Ti, (c) Al-Ti-B, (d) Al-Zr, (e) Al-Ti-Zr, (f) Al-Ti-B-Zr, for as cast condition, X 250

Addition of Ti or Ti+B to aluminum resulted in enhancement of its hardness giving better enhancement in case of Ti+B. addition of Zr in presence of Ti resulted in reducing its hardness whereas the presence of Ti+B resulted in better enhancement than when Ti+B exists alone. Addition of Zr alone to Al resulted in slight decrease of its hardness, as shown in the histogram of figure 56.

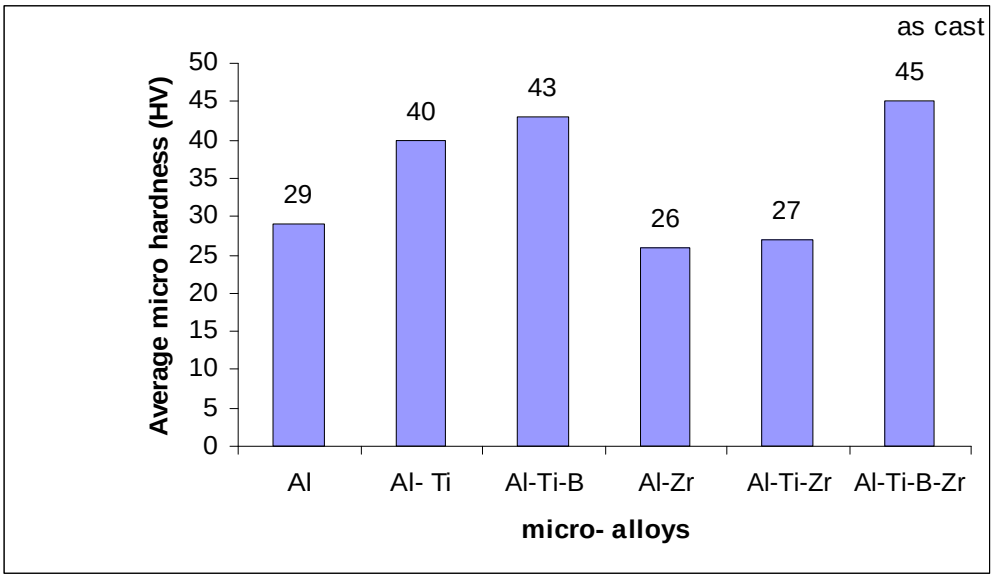

Fig.56: Effect of zirconium addition on the microhardness of Al and Al grain refined by Ti, Ti+B in the as cast condition

Regarding the effect addition of Zr on the mechanical behavior of Al, it can be seen that addition of Zr alone or in the presence of Ti resulted in deteriorating of its mechanical behavior, i.e. reduction of its flow stress and UTS . Similarly addition of Zr to Al grain refined by Ti+B resulted in deterioration of its mechanical behavior as indicated by figures 57, 58 and 59.

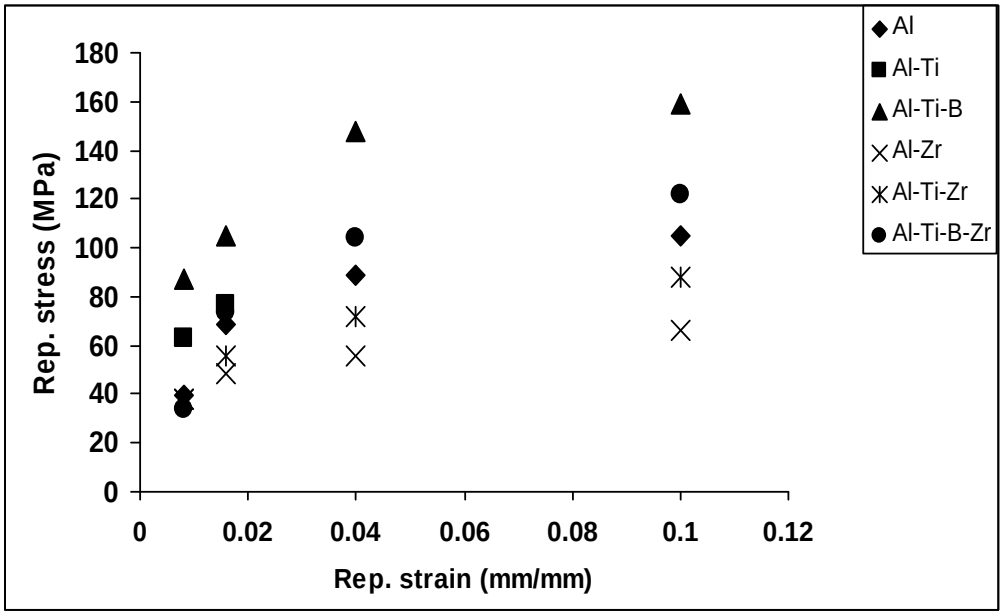

Fig. 57: Rep. Stress – Rep. Strain of Al and Al grain refined by Ti and Ti+B in the as cast condition

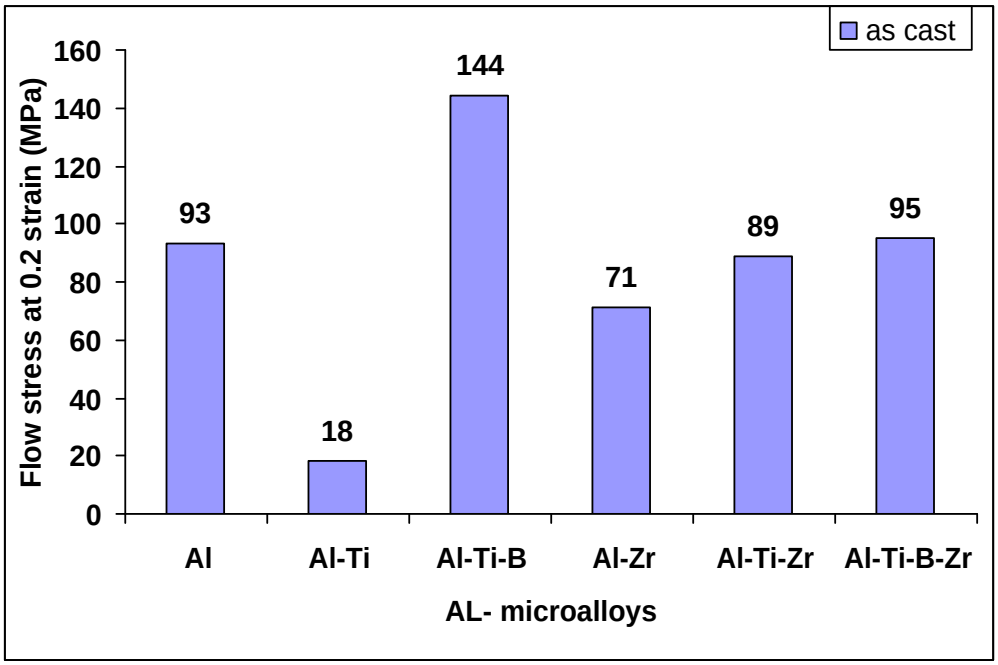

Fig.58: Effect of zirconium addition on the flow stress at 20 % strain of Al and Al grain refined by Ti and Ti+B in the as cast condition

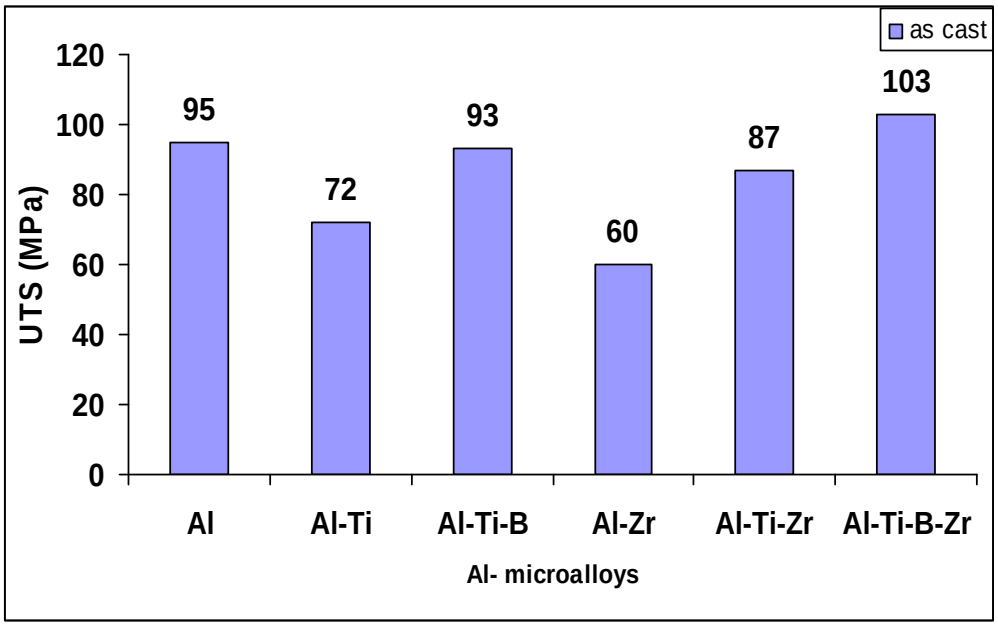

Fig.59: Effect of zirconium addition on the UTS of Al and Al grain refined by Ti and Ti+B in the as cast condition

Regarding of these elements on the ductility, figures 60 and 61 indicate that addition of Ti or Ti+B to Al resulted in decrease of ductility and addition of Zr alone to Al and Al grain refined by Ti resulted in improvement of its ductility whereas addition of Zr to Al grain refined by Ti+B resulted in decrease of its ductility.

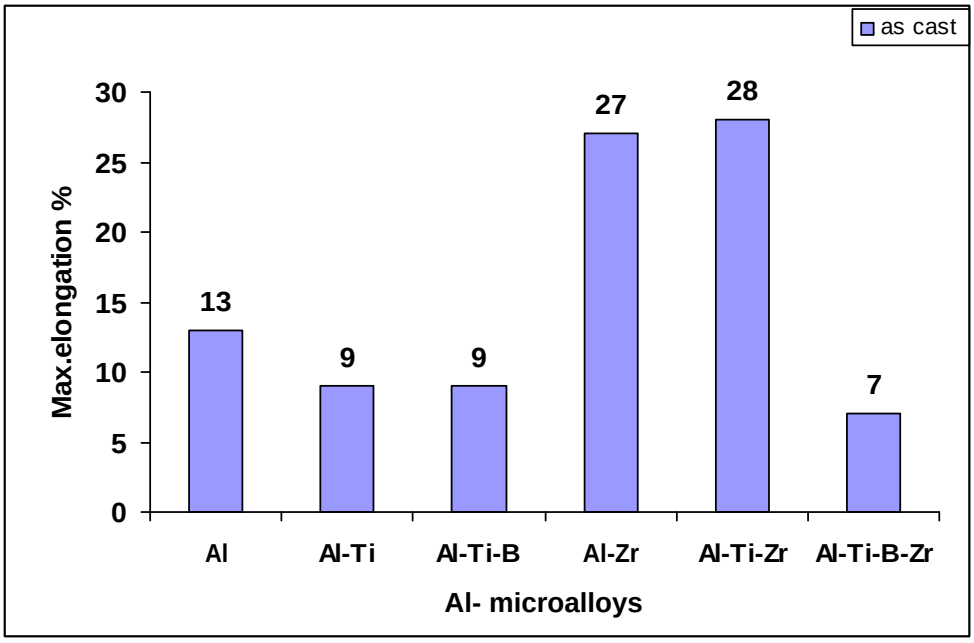

Fig. 60: Effect of zirconium addition on the maximum elongation %, of Al and Al grain refined by Ti and Ti+B in the as cast condition

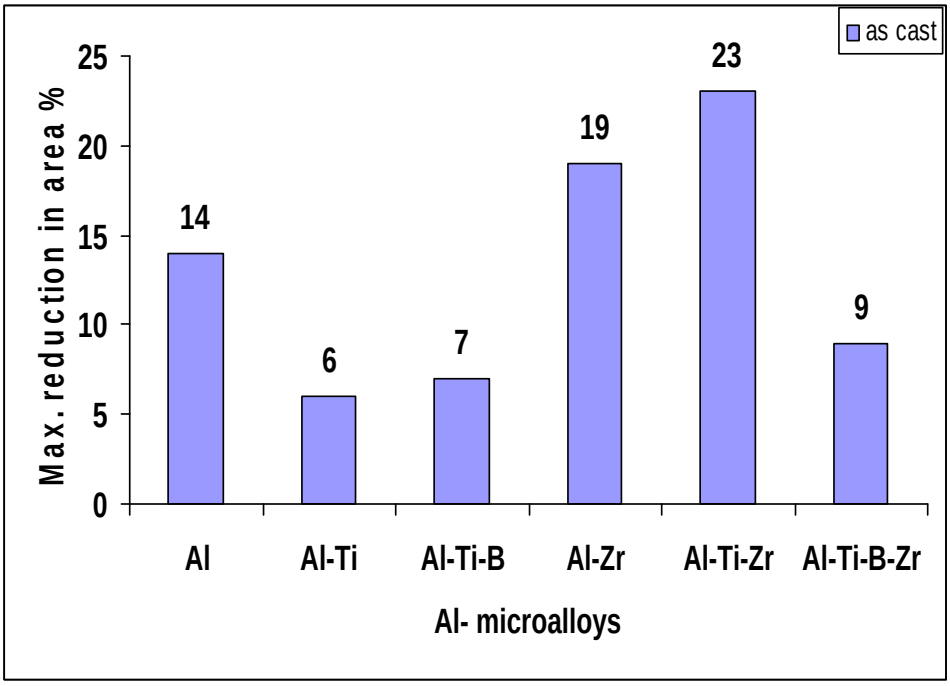

Fig. 61: Effect of zirconium addition on the maximum reduction in area %, of Al and Al grain refined by Ti and Ti+B in the as cast condition

6.3 The Effect of Zirconium Addition at a rate of 0.1 Weight Percentage on the Formability of Aluminum, Al Grain Refined by Ti and Al grain Refined by Ti+B

Formability was investigated from: 1) Extrusion test, 2) free upsetting test i.e. compression test. Also, comparison is made between the effect of Zr addition on Al grain refined by Ti and Al grain refined by Ti+B.

6.3.1 Extrusion

Assessment of the effect of the addition of different grain refiners on the extrusion process is investigated through the autographic record of each microalloy i.e. (punch load-punch displacement) from which the maximum extrusion force and energy are obtained. Atypical autographic record for the forward extrusion process on the Al-Ti-B microalloy is shown in fig. 62 The autographic records of Al and the other microalloys, namely Al-Ti, Al-Zr, Al-Ti-Zr and Al-Ti-B-Zr are shown in appendix B.

Furthermore, the extruded parts were investigated from the metallurgical aspects and mechanical characteristics and compared with those in the as cast before extrusion.

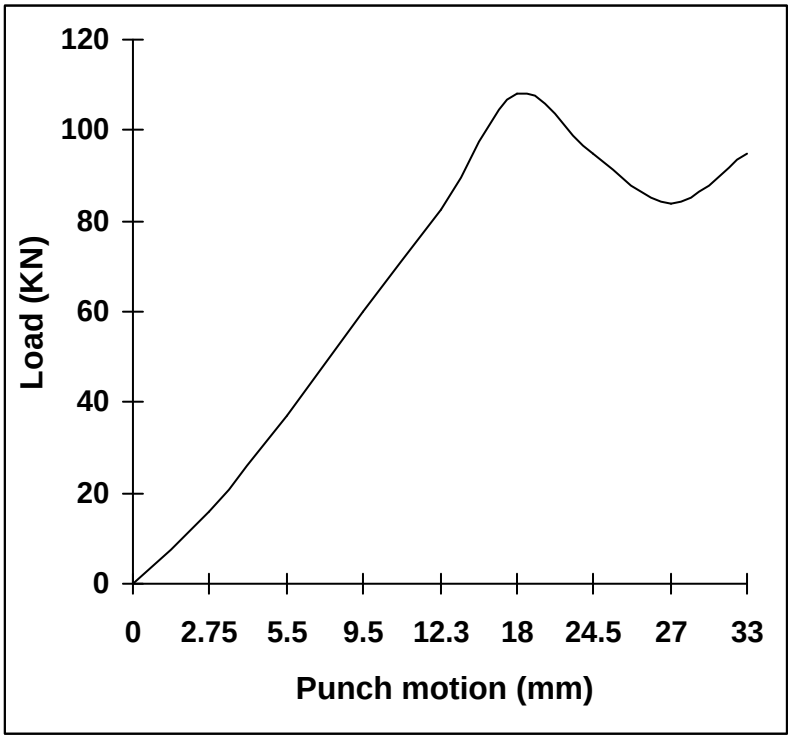

Fig. 62: Autographic Record (Extrusion) for Al-Ti-Zr microalloy

Tables 10 and 11 give comparison between the experimentally determined values of the extrusion force for Al and its different microalloys, and the theoretical values calculated from Johnson's formula which was given and discussed in the previous chapter, using the average flow stress Y_{av} from the mechanical behavior obtained by two methods : one from the tensile test, Table 10, and the second from compression test , Table 11.

Table 10: Theoretical and experimental extrusion force (Tensile test)

Micro Alloy	Actual Extrusion Force (KN)	Y_{av} MPa	Extrusion Pressure (MPa) Y_{av} (a + b Ln R)	Extrusion Force (KN)
pure Al	133.6	74.2	134.5	20.753
Al-Ti	112.8	110.7	200.8	30.983
Al-Ti-B	170.6	175.1	317.6	49.005
Al-Ti-Zr	108.13	83	150.56	23.231
Al-Zr	105.3	113	204.98	31.328
Al-Ti-B-Zr	173.5	208.7	378.6	58.417

Table 11: Theoretical and experimental extrusion force (compression test)

Micro Alloy	Actual Extrusion Force (KN)	Y_{av} MPa	Extrusion Pressure (MPa) Y_{av} (a + b Ln R)	Extrusion Force (KN)
pure Al	133.6	110	199.54	31.225
Al-Ti	112.8	116.7	211.7	32.665
Al-Ti-B	170.6	239.12	433.76	66.882
Al-Ti-Zr	108.13	89.7	162.72	25.108
Al-Zr	105.3	119.6	216.95	33.475
Al-Ti-B-Zr	173.5	188.5	341.9	52.755

Table 12: The actual extrusion energy and energy from mechanical behavior

Micro Alloy	Actual Extrusion Energy (1) J	Actual Extrusion Energy (2) J	Aver. Actual Extrusion Energy J	Energy from mechanical behavior (comp) J	% Difference In Energy
pure Al	2475	2231.8	2353.4	1339	43.1
Al-Ti	1546	1617.6	1581.8	1399	11.5
Al-Zr	1719	1501.5	1610	1063	34
Al-Ti-B	2173.1	2351.3	2262.2	3784	-67
Al-Ti-B-Zr	2454	2010.9	2232.5	2392	-7.1
Al-Ti-Zr	1441.6	1460	1451	1443	1.5

It can be seen from the results in these Tables that there is a large discrepancy between the experimentally determined values and those obtained from Johnson's formula. The discrepancy may be attributed to the following :

i) Neglecting friction between the billet and the container wall over the whole length of the billet.

ii) Neglecting friction between the billet and the die during the extrusion process.

iii) The redundant energy due to the non- homogenous deformation.

The great variation between the theoretical and experimental values was also reported previously, (Rowe, 1968).

6.3.1.1 metallurgical aspects of the extrusion process

It can be seen from figure 63 the extrusion process resulted in great refinement of all the as cast microalloys. This is clearly demonstrated in the histogram of figure 63 as the percentage decrease in grain size for the different microalloys is 60 %, 78.6 %, 64.9 %, 57.78 %, 68.7 %, 70 % in case of Al, Al-Ti, Al-Zr, Al-Ti-Zr, Al-Ti-B and Al-Ti-B-Zr respectively. The following conclusions may be obtained that the extrusion process resulted in grain refinement of Al and its five microalloys, the maximum refinement is in Al-Ti microalloy.

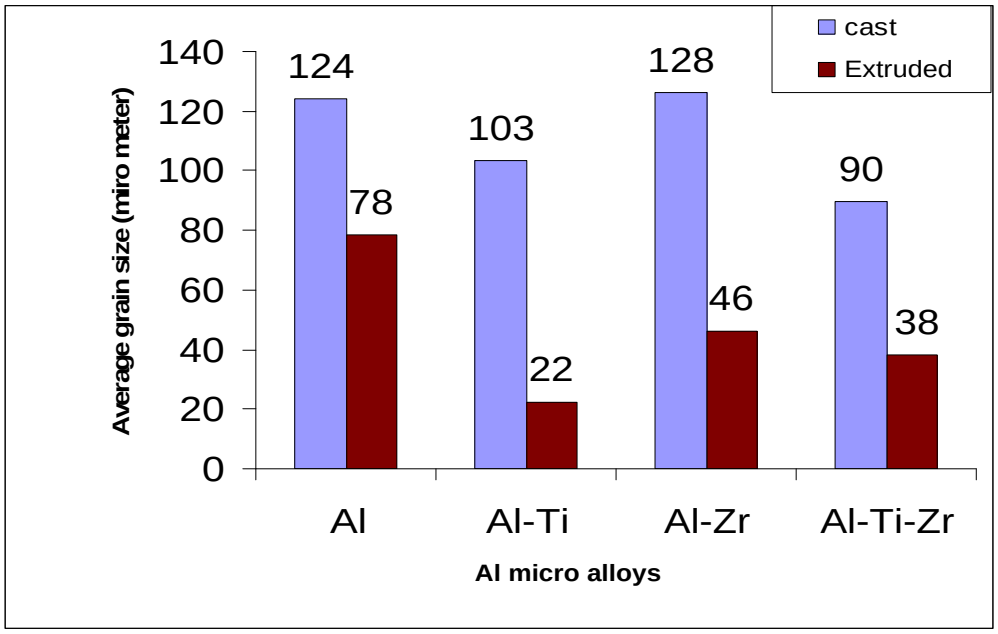

Fig. 63: Effect of zirconium addition on the grain size of Al and Al grain refined by Ti in the as cast condition and after extrusion

Also it can be seen that addition of Zr to Al grain refined by Ti resulted in decrease of its refining efficiency whereas it improved the refining efficiency when added to Al grain refined by Ti+B. The effect of the extrusion process on the general microstructure of Al and its five microalloys is shown in figures 64 (a'), (b'), (c'), (d'), (e') and (f') respectively. For comparison purposes with the as cast condition figures 64 (a), (b),(c),(d),(e) and (f) are included, where the grain refinement is clearly demonstrated in the figures 64 (a'),(b'), (c'), (d'),(e') and (f').

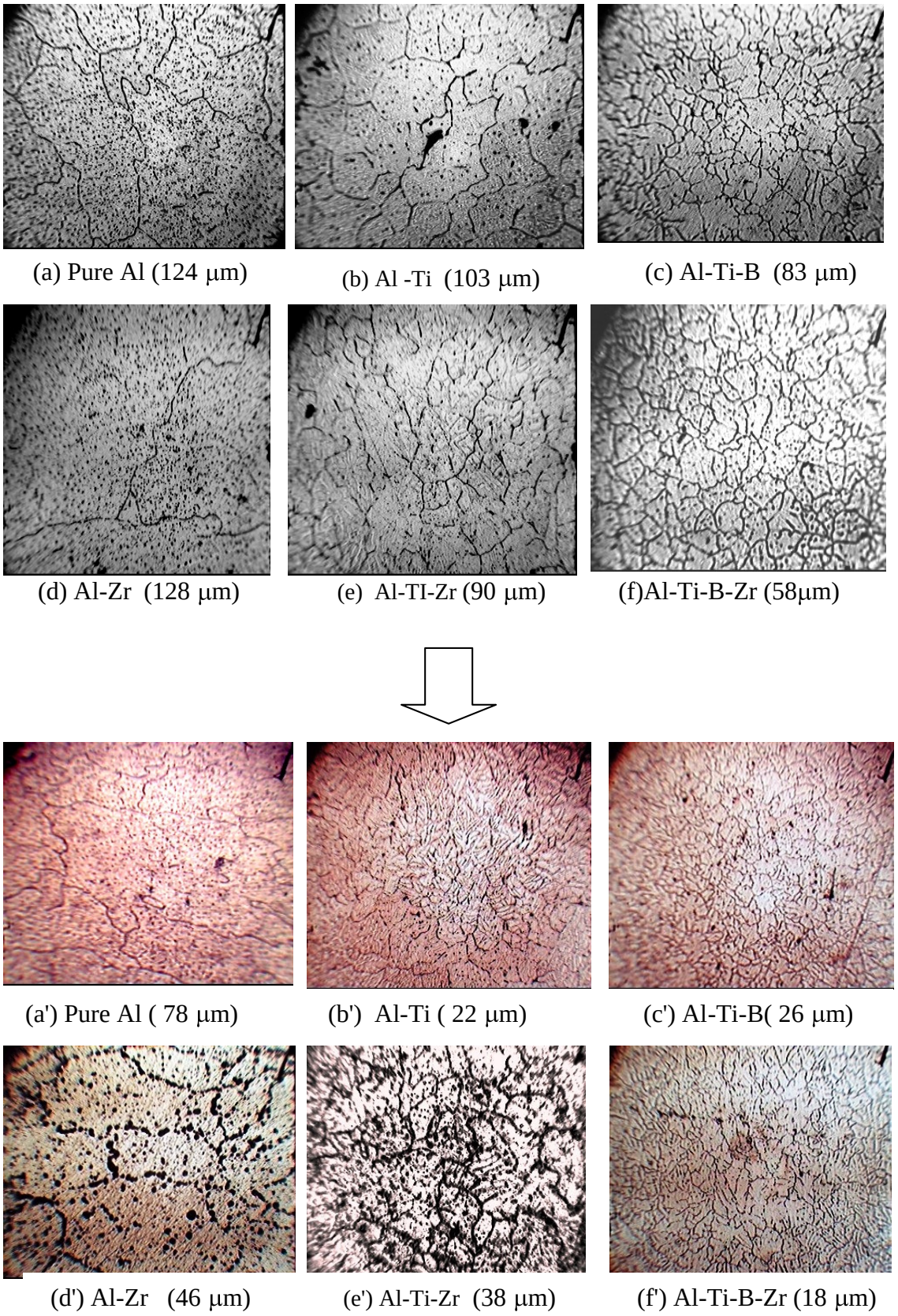

Fig. 64: Photomicrographs showing the general microstructure of Al and Al grain refined by Ti and Ti+B in the as cast condition (a),(b), (c), (d), (e) and (f) and after extrusion (a'),(b'), (c'), (d'), (e') and (f').

6.3.2 The effect of the extrusion process on the hardness and mechanical characteristics of Al and its microalloys

It can be seen from the histogram of figure 65 that the extrusion process resulted in enhancement of the hardness of Al and its five microalloys. This is expected as a result of the work hardening due to plastic deformation as Al and its microalloys are strain hardening or work hardening materials.

The maximum increase in the hardness is in the addition of Zr to Al grain refined by Ti being 96.3 % increase due to the existence of $TiAl_3$ and $ZrAl_3$ both of which are hard phases followed by Al-Zr (73.1 % in increase), then Al-Ti microalloy (62.5 %), and 60 % in case of Al-Ti-B-Zr microalloys because boride phase is softer than $TiAl_3$ and $ZrAl_3$, and the least in case of aluminum as there is no metallic interphases in the aluminum matrix in case of Al.

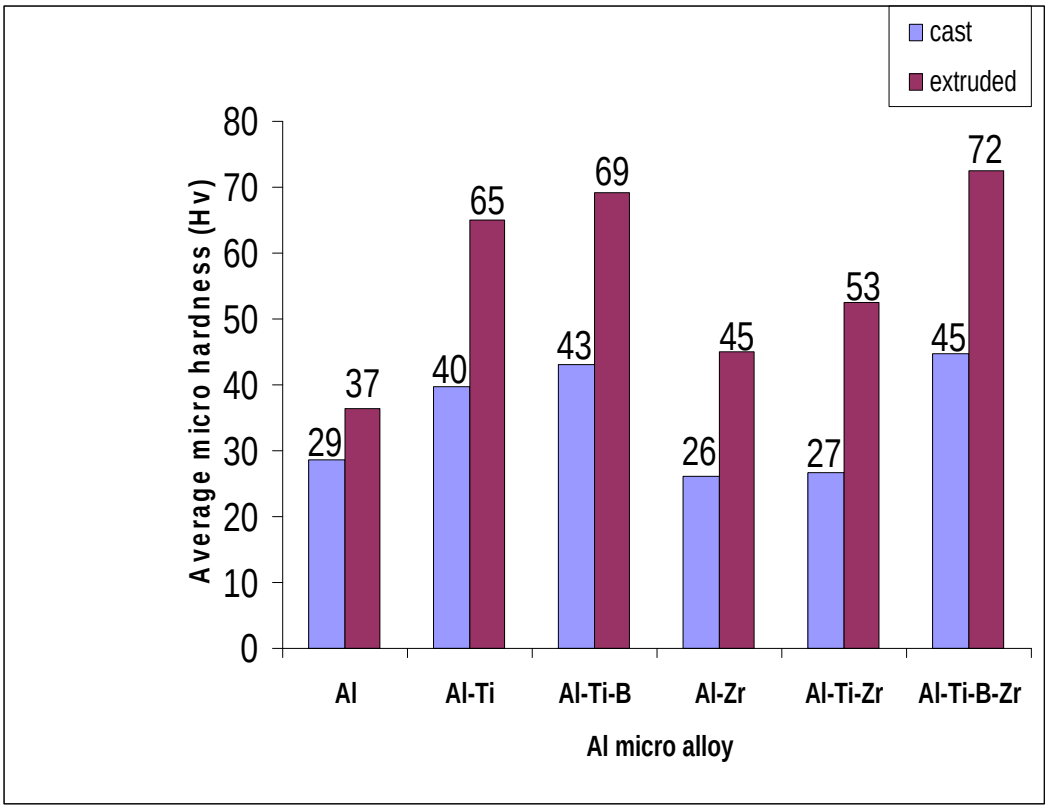

Fig. 65: Effect of zirconium addition on the average microhardness of Al, Al grain refined by Ti and Ti+B in the as cast condition and after the extrusion

Figure 66 gives comparison between the mechanical behavior of Al and its five microalloys namely Al-Ti, Al-Zr, Al-Ti-B, Al-Ti-Zr and Al-Ti-B-Zr for the as cast and after extrusion conditions. It can be seen be seen that the mechanical behavior of Al, Al-Zr, Al-Ti-B and Al-Ti-Zr is improved by the casting process whereas the mechanical behavior was deteriorated for Al-Ti and Al-Ti-B-Zr microalloys. Furthermore, it can be seen from figure 66 that addition of Zr alone to Al has resulted in pronounced improvement of its mechanical behavior after extrusion although it caused deterioration of its mechanical behavior when added in the as cast condition.

On the other hand, addition of Zr to Al-Ti-B microalloy in the as cast condition resulted in improvement of its mechanical behavior while it resulted in deterioration of its mechanical behavior after extrusion.

Comparison of the flow stress at 20 % strain of Al and its different microalloys is shown in figure 67, from which it can be concluded that the extrusion process has resulted in increase of its flow stress at 20 % strain. The maximum increase was obtained in the Al-Ti microalloy where 650 % increase was achieved followed by Al-Ti-B-Zr microalloy (180 %).

Similarly, the extrusion process resulted in increase of the ultimate tensile strength, UTS, of the Al and its microalloys except for Al-Ti microalloy which has not been affected, figure 68. The old mechanical behavior of the Al-Ti microalloy may be attributed to its microstructure which is a nodular type as compared to the equiaxed structure of the other Al microalloys.

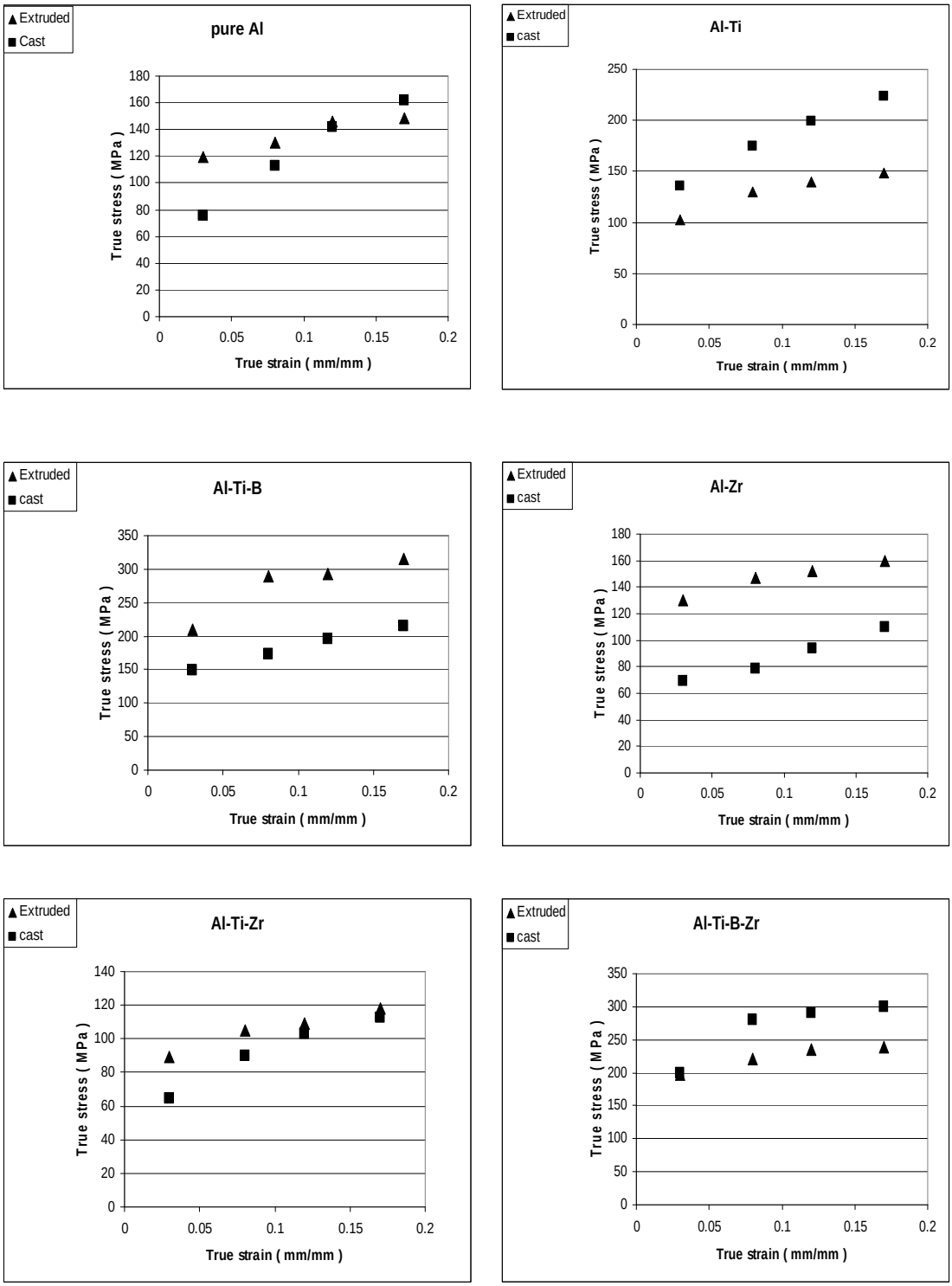

Fig. 66: True stress- True strain curves of Al and its five microalloys in the as cast, (symbol ■) and after extrusion, (symbol ▲).

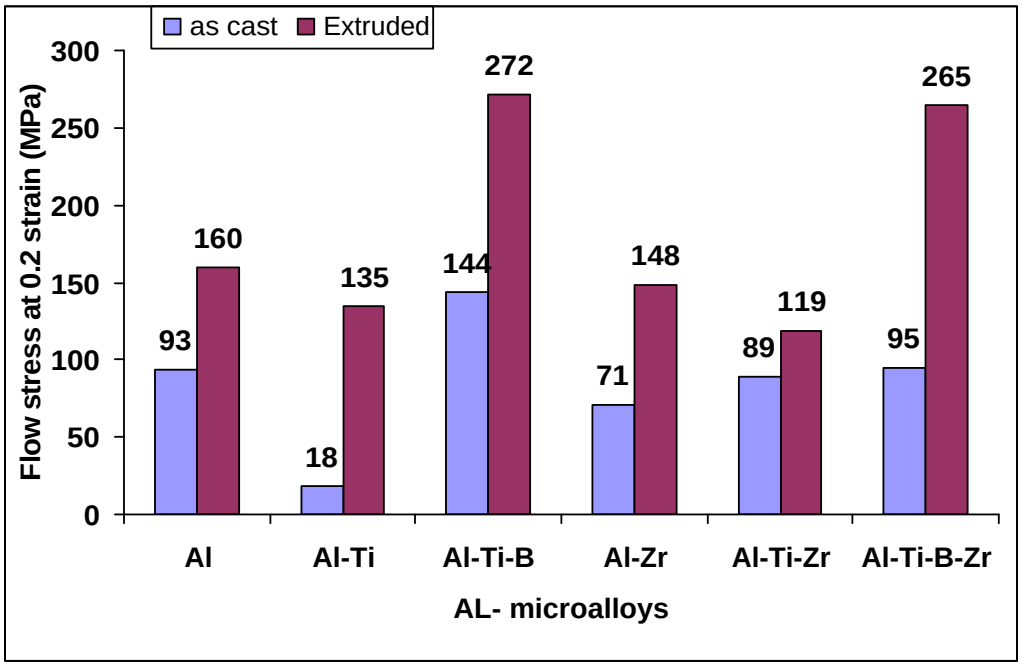

Fig .67: Effect of zirconium addition on the flow stress at 20 % strain of Al and Al grain refined by Ti and Ti+B in the as cast condition and after extrusion

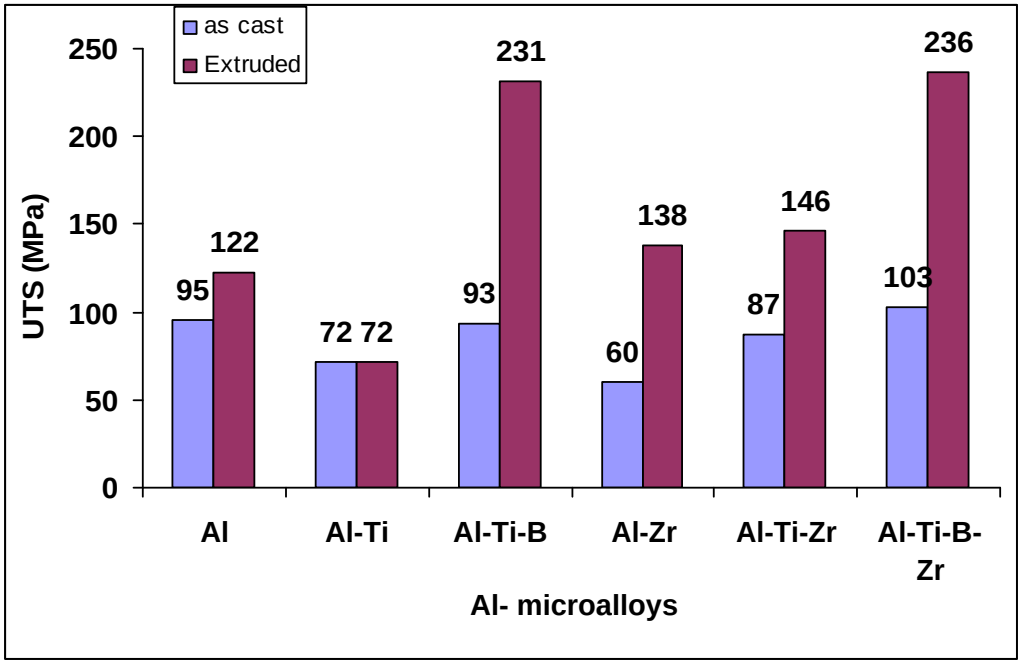

Fig .68: Effect of zirconium addition on the UTS of Al and Al grain refined by Ti and Ti+B in the as cast condition and after extrusion

The effect of the extrusion process on the ductility of Al and its microalloys is shown in figures 69 and 70, from which it can be seen that, except for Al, Al-Zr and Al-Ti-Zr (Al grain refined by Ti), the extrusion process resulted in deterioration of its ductility represented by decrease of the maximum elongation %, figure 69, and the maximum

reduction in area % figure 70, whereas the extrusion process resulted in improvement of ductility of Al-Ti, Al-Ti-B, Al-Ti-B-Zr microalloys, i.e. increase in the maximum elongation %, figure 69 and an increase in the maximum reduction in area %, figure 70. The best enhancement in ductility is in the Al-Ti microalloy, which again may explained in terms of the nodular type microstructure.

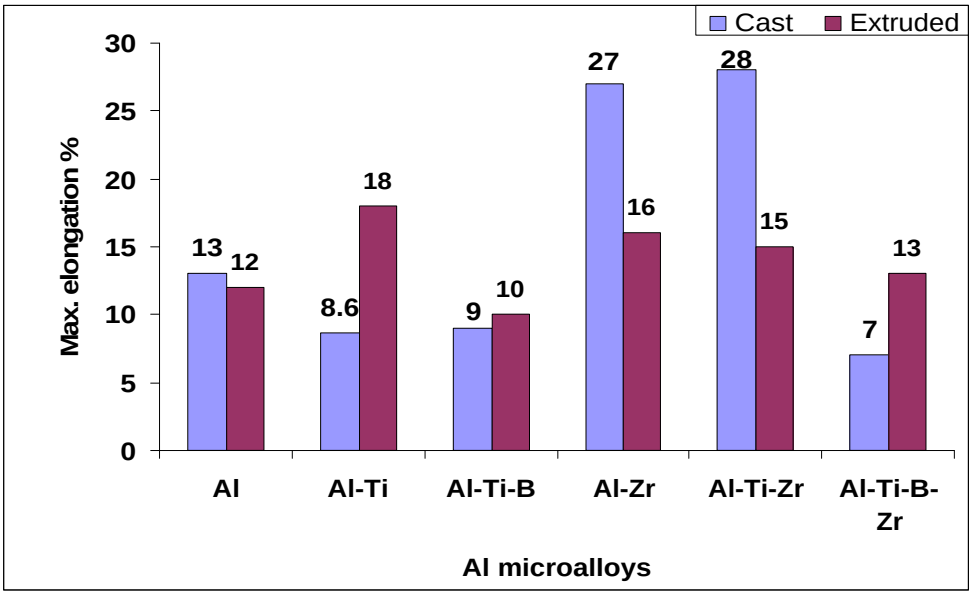

Fig. 69: Effect of zirconium addition on the maximum elongation % for Al, Al grain refined by Ti and Al grain refined by Ti+B in the as cast condition and after extrusion.

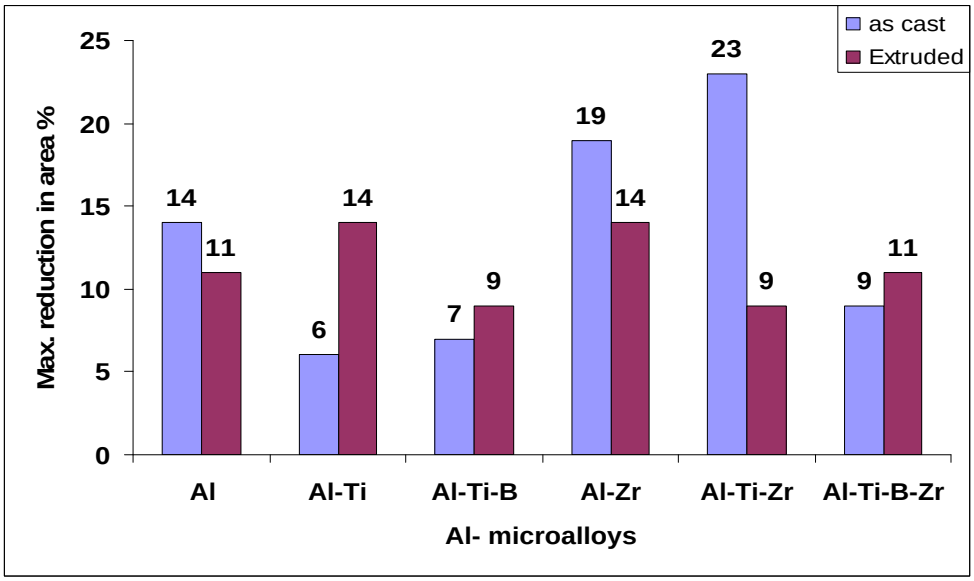

Fig.70: Effect of zirconium addition on the maximum reduction in area % for Al , Al grain refined by Ti and Al grain refined by Ti+B in the as cast condition and after extrusion.

The effect of the different grain refiners on the mechanical characteristics of Al and its five microalloys namely Al-Ti, Al-Zr, Al-Ti-B, Al-Ti-Zr and Al-Ti-B-Z are explicitly shown in Table 13 and the effect of the extrusion process on these characteristics is shown in Table 14. From these tables it can be seen that the extrusion process resulted in increase of the strength coefficient, K, for Al and its five microalloys and similarly resulted in increase of the strain hardening index, n, for all of them expect for Al-Ti-Zr.

Table 13:Mechanical properties of Al and its different micro alloys of in the as cast

Micro alloys	Flow stress (MPa)at strain=20%	Strain hardening index (n)	Strength coefficient (K) MPa	General equation of mechanical behavior
Al	93	0.04	102	$\bar{\sigma} = 102\ \bar{\varepsilon}^{0.04}$
Al-Zr	71.2	0.172	94	$\bar{\sigma} = 94\ \bar{\varepsilon}^{0.17}$
Al-Ti-B	250.5	0.34	433	$\bar{\sigma} = 433\ \bar{\varepsilon}^{0.34}$
Al-Ti-B-Zr	174.8	0.34	302.2	$\bar{\sigma} = 302.2\ \bar{\varepsilon}^{0.34}$
Al-Ti	18	0.17	23	$\bar{\sigma} = 23\ \bar{\varepsilon}^{0.17}$
Al-Ti-Zr	89	0.2	122	$\bar{\sigma} = 122\ \varepsilon^{0.2}$

Table 14: Mechanical properties of Al and its different microalloys after extrusion

Micro alloys	Flow stress (MPa)at strain=20%	Strain hardening index (n)	Strength coefficient (K) MPa	General equation of mechanical behavior
Al	99	0.11	118.6	$\bar{\sigma} = 118.6\ \bar{\varepsilon}^{0.11}$
Al-Zr	133.4	0.28	209.3	$\bar{\sigma} = 209.3\ \bar{\varepsilon}^{0.28}$
Al-Ti-B	321.8	0.43.	643	$\bar{\sigma} = 643\ \bar{\varepsilon}^{0.43}$
Al-Ti-B-Zr	276.7	0.38	510	$\bar{\sigma} = 510\ \bar{\varepsilon}^{0.38}$
Al-Ti	133	0.28	209	$\bar{\sigma} = 209\ \bar{\varepsilon}^{0.28}$
Al-Ti-Zr	106.3	0.18	142	$\bar{\sigma} = 142\ \bar{\varepsilon}^{0.18}$

6.3.2 Forging : Free upsetting

Assessment of the effect of different grain refiners on the forgability of aluminum is investigated from the autographic record of each microalloy obtained at the same punch force of 80 KN, from which the maximum true strain for each microalloy is obtained. The microalloy which suffers more strain at the same load is of lower strength. A typical autographic record of free upsetting for Al-Ti-Zr microalloy is shown in Fig. 71.

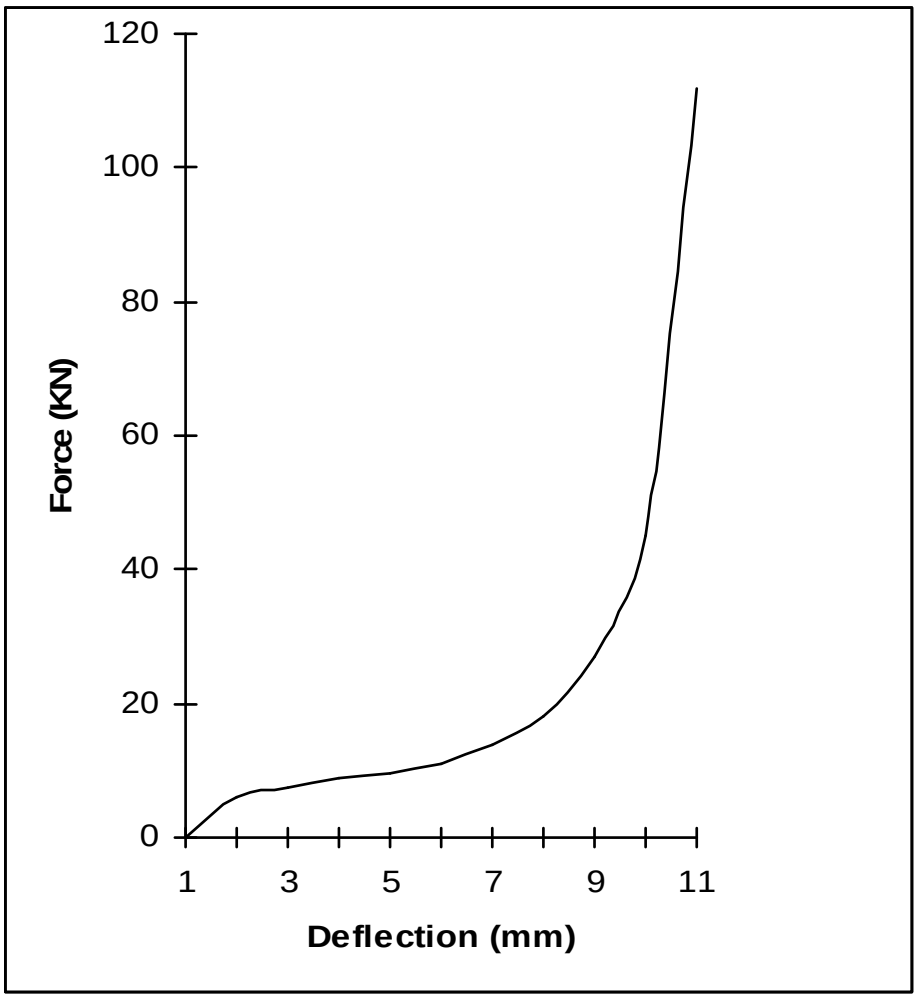

Fig. 71: A typical autographic record from the free upsetting test on the specimen Al-Ti-Zr microalloy

Tables 15 and 16 give the details of the free upsetting tests for Al and its different microalloys, in the as cast condition and after prestraining by extrusion

Table 15: Effect of grain refiners on forgability of Al (free upsetting) at 80 KN

Alloy	A_o ($mm^{2)}$	L_o (mm)	Lc (mm)	e	ε
Pure Al	82.79	10.49	5.376	0.488	0.669
Al-Ti	139.14	11.8	7.525	0.362	0.450
Al-Ti-B	81.56	10.05	4.520	0.550	0.799
Al-Zr	141.58	14.37	7.498	0.478	0.651
Al-Ti-Zr	77.97	9.46	5.69	0.601	0.920
Al-Ti-B-Zr	135.47	9.72	3.32	0.342	0.294

Table 16: Effect of prestraining on Forgability of Al (free upsetting) at 80 KN

Alloy	A_o($mm^{2)}$	L_o (mm)	Lc (mm)	e	ε
Al (Extruded)	79.012	9.61	4.586	0.5229	0.740
Al-Ti (Extruded)	79.17	9.3	4.314	0.536	0.768
Al-Ti-B (Extruded)	79.12	8.96	4.684	0.477	0.648
Al-Zr (Extruded)	78.07	10.38	5.630	0.457	0.611
Al-Ti-Zr (Extruded)	79.6	17.49	8.330	0.524	0.741
Al-Ti-B-Zr (Extruded)	78.53	17.20	8.738	0.492	0.677

6.4 Effect of Zirconium Addition on Wear Resistance of Aluminum and Aluminum Grain Refined by Titanium and Titanium + Boron

In this sectoin the results obtained on the effect of adition of titanium, Ti, titanium + boron , Ti+B, on the wear resistance of commercially pure aluminum under different conditions of loads and speeds are presented and disscussed.

Furthermore, the results obtained on the effect of zirconium , Zr, addition on the wear resistance of aluminum grain refined by Ti or Ti+B are also presented and disscussed, from which comparison between both Ti and Ti+B is achieved.

All the data for different cases are in the as cast condition.

6.4.1 Effect of Zirconium Addition on the Wear Resistance of Aluminum and Aluminum Grain Refined by Titnium

It can be seen from figure 72 that the relationship between the accumulated mass loss and time for Al and its microalloys Al-Ti, Al-Zr and Al-Ti-Zr at low speed and small load (0.276 m/sec, 5 N) is almost linear. The commercially pure aluminum indicated less wear rate i.e. better resistance than Al-Ti-Zr, Al-Zr, and Al-Ti. Hence, addition of Ti or Zr or both together Ti+Zr to Al resulted in deteioration of its wear resistance.

However, increasing the load to four times its value (20 N) at the same speed (0.276 m/sec), revealed that the addition of these refiners Ti, Zr or Ti+Zr became more effective and gave better wear resistance than Al, as illustrated by figure 72.

These results are explictly indicated by the wear coeffecient, K, in th last column of Tables 17 and 18. The wear coeffecient shown in these tables is calculated from equation 5.15 in chapter 5.

$$V= (KPL)/3H$$

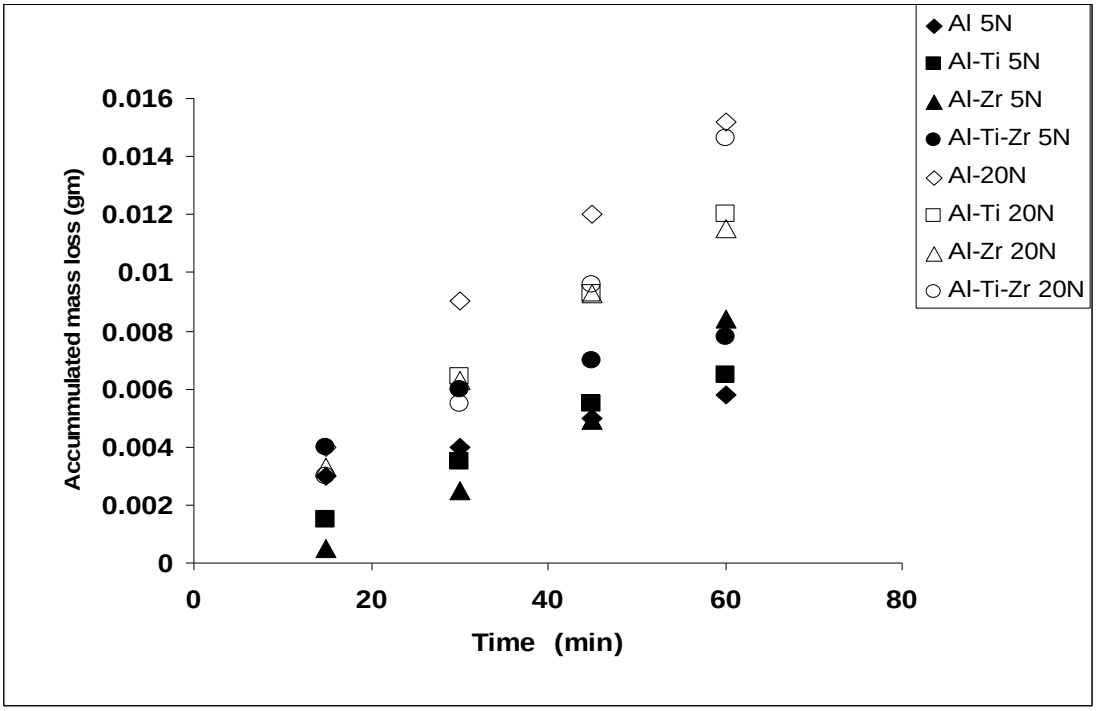

Fig.72: Effect of Zr addition on the wear of Al and Al grain refined by Ti at S = 0.276 m /sec, loads = 5, 20 N

Table 17: Mass loss and dimensional changes after one hr. wear for Zr addition to Al and Al grain refined by Ti in the as cast condition. (Load = 5 N, S = 0.276 m /sec, A_o = 38.48 mm^2)

Name	Mass loss (g)	D_f (mm)	Δ h (mm)	A_f (mm^2)	K Wear rate
Al	0.0058	7.1	0.1	39.59	0.075
Al-Ti	0.0065	7.1	0.2	39.59	0.12
Al-Zr	0.0084	7.2	0.19	40.72	0.098
Al-Ti-Zr	0.0078	7.6	0.24	45.36	0.094

Table 18: Mass loss and dimensional changes after one hr. wear for Zr addition to Al and Al grain refined by Ti as in the cast condition.(load = 20 N,S = 0.276 m /sec, A_o = 38.48 mm^2)

Name	Mass loss (g)	D_f (mm)	Δ h (mm)	A_f (mm^2)	K Wear rate
Al	0.0152	8.3	0.17	54.1	0.05
Al-Ti	0.0049	7.4	0.14	43.0	0.022
Al-Zr	0.0115	8.0	0.18	50.27	0.033
Al-Ti-Zr	0.0146	7.3	0.26	41.85	0.044

Increasing the speed to 0.801 m/sec or 3.01 m/sec at loads 5 and 20 N followed the same previous trend of wear resistance in the following sequence starting with the

highest wear resistance: Al, Al-Zr, Al-Ti-Zr and finally Al-Ti, as illustrated by figures 73 and 74 and explicitly in Tables 19, 20, 21 and 22.

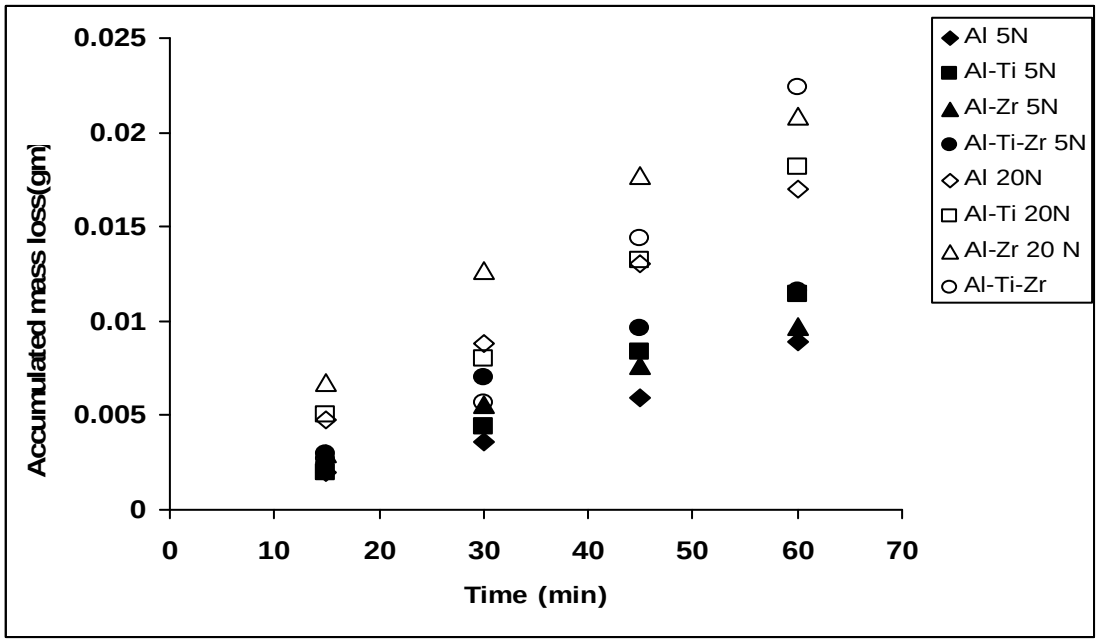

Fig.73: Effect of Zr addition on the wear of Al and Al grain refined by Ti at S = 0.801 m/sec, loads = 5, 20 N

Table 19: Mass loss and dimensional changes after one hr. wear for Zr addition to Al and Al grain refined by Ti in the as cast condition. (Load = 5 N, S = 0.801 m/sec, A_o = 38.48 $mm^{2)}$

Name	Mass loss (g)	D_f (mm)	Δ h (mm)	A_f (mm^2)	K Wear rate
Al	0.0089	7.1	0.24	39.59	0.0382
Al-Ti	0.0114	7.6	0.26	45.36	0.0856
Al-Zr	0.0097	8	0.18	50.27	0.0375
Al-Ti-Zr	0.0116	8	0.26	50.27	0.0465

Table 20: Mass loss and dimensional changes after one hr. wear for Zr addition to Al and Al grain refined by Ti in the as cast condition.(load = 20 N,S = 0.801 m/sec, A_o = 38.48 $mm^{2)}$

Name	Mass loss (g)	D (mm)	Δ h (mm)	A_f (mm^2)	K Wear rate
Al	0.017	7.5	0.19	44.18	0.0183
Al-Ti	0.0182	8.5	0.35	56.75	0.0270
Al-Zr	0.0209	9	0.44	63.62	0.0202
Al-Ti-Zr	0.0224	8.8	0.33	60.82	0.0225

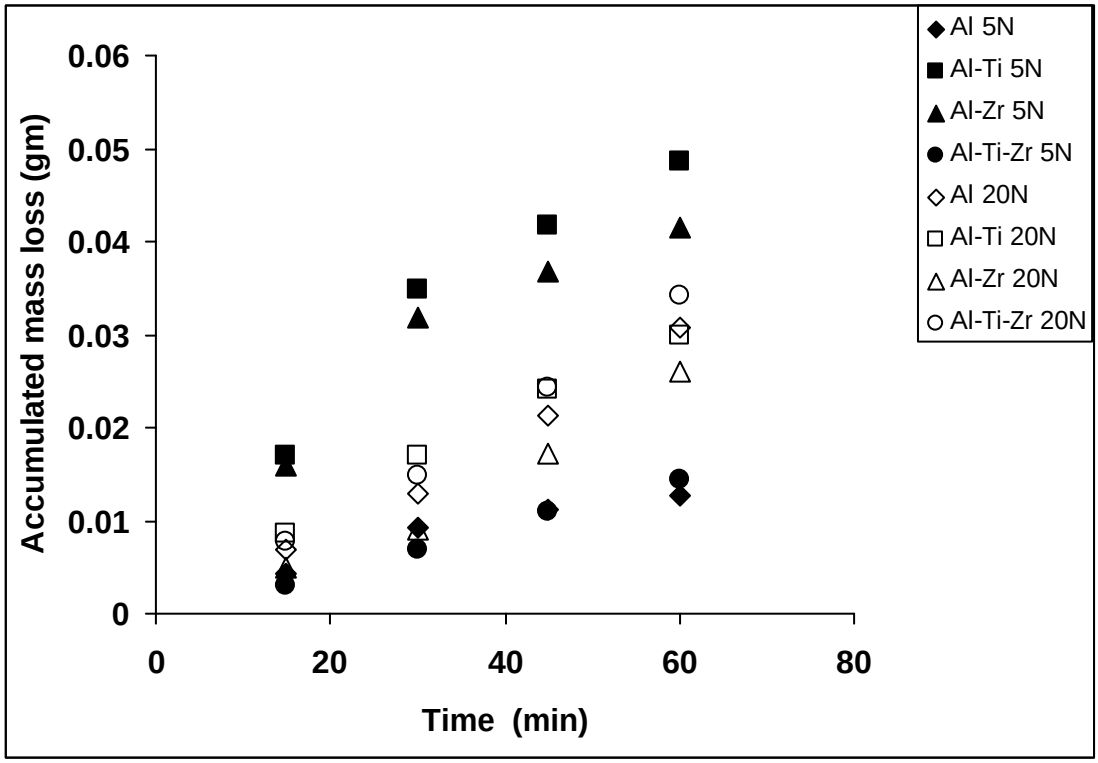

Fig.74: Effect of zirconium addition of Al and Al grain refined by Ti at S = 3.01 m/sec, loads = 5, 20 N

Table 21: Mass loss and dimensional changes after one hr. wear for Zr addition to Al and Al grain refined by Ti in the as cast condition. (Load = 5 N, S =3.01 m/sec, A_o = 38.48 mm^2)

Name	Mass loss (g)	D_f (mm)	Δ h (mm)	A_f (mm^2)	K
Al	0.0126	7.9	0.23	49.02	0.0144
Al-Ti	0.0485	8.7	0.55	59.45	0.0766
Al-Zr	0.0415	8.5	0.52	56.75	0.0426
Al-Ti-Zr	0.0144	8.4	0.34	55.42	0.0153

Table 22: Mass loss and dimensional changes after one hr. wear for Zr addition to Al and Al grain refined by Ti in the as cast condition.(load =20 N, S = 3.01 m/sec, A_o = 38.48 mm^2)

Name	Mass loss (g)	D_f (mm)	Δ h (mm)	A_f (mm^2)	K Wear rate
Al	0.0308	8.6	0.37	58.88	0.009
Al-Ti	0.03	10.2	0.43	81.71	0.0118
Al-Zr	0.0261	8.7	0.52	59.45	0.0070
Al-Ti-Zr	0.0343	8.4	0.5	55.42	0.0091

This is attributed to the precipitated secondary phases in the aluminum matrix which also resulted in heavier shear zone as indicated by the photomacrographs of figure 75.

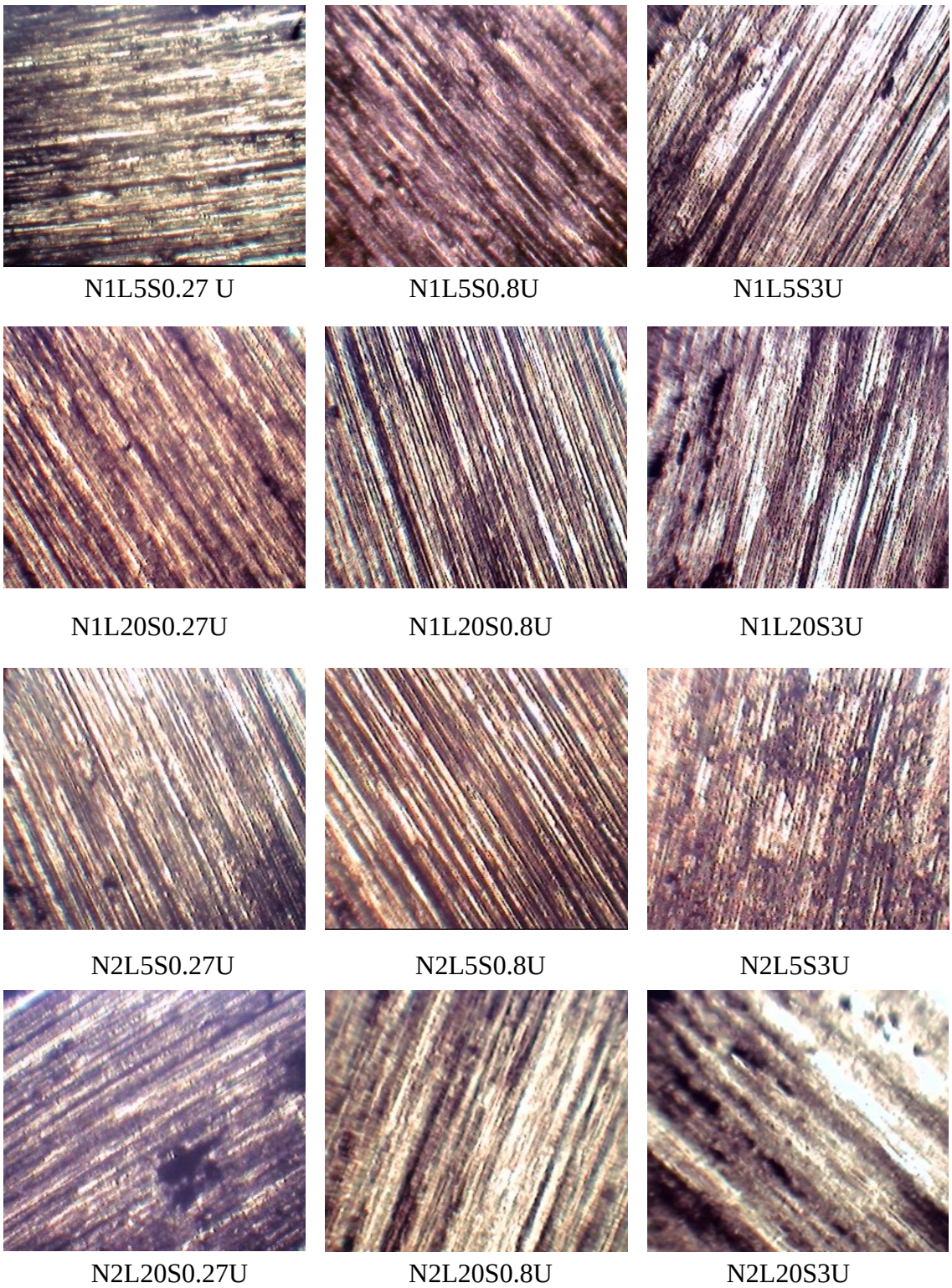

Fig. 75: Photomacrographs showing the shear lines at the worn ends after one hour runing . (N1: Al, N2: Al-Ti at Speeds = (0.27, 0.8, 3) m/sec and loads 5, 20 N)

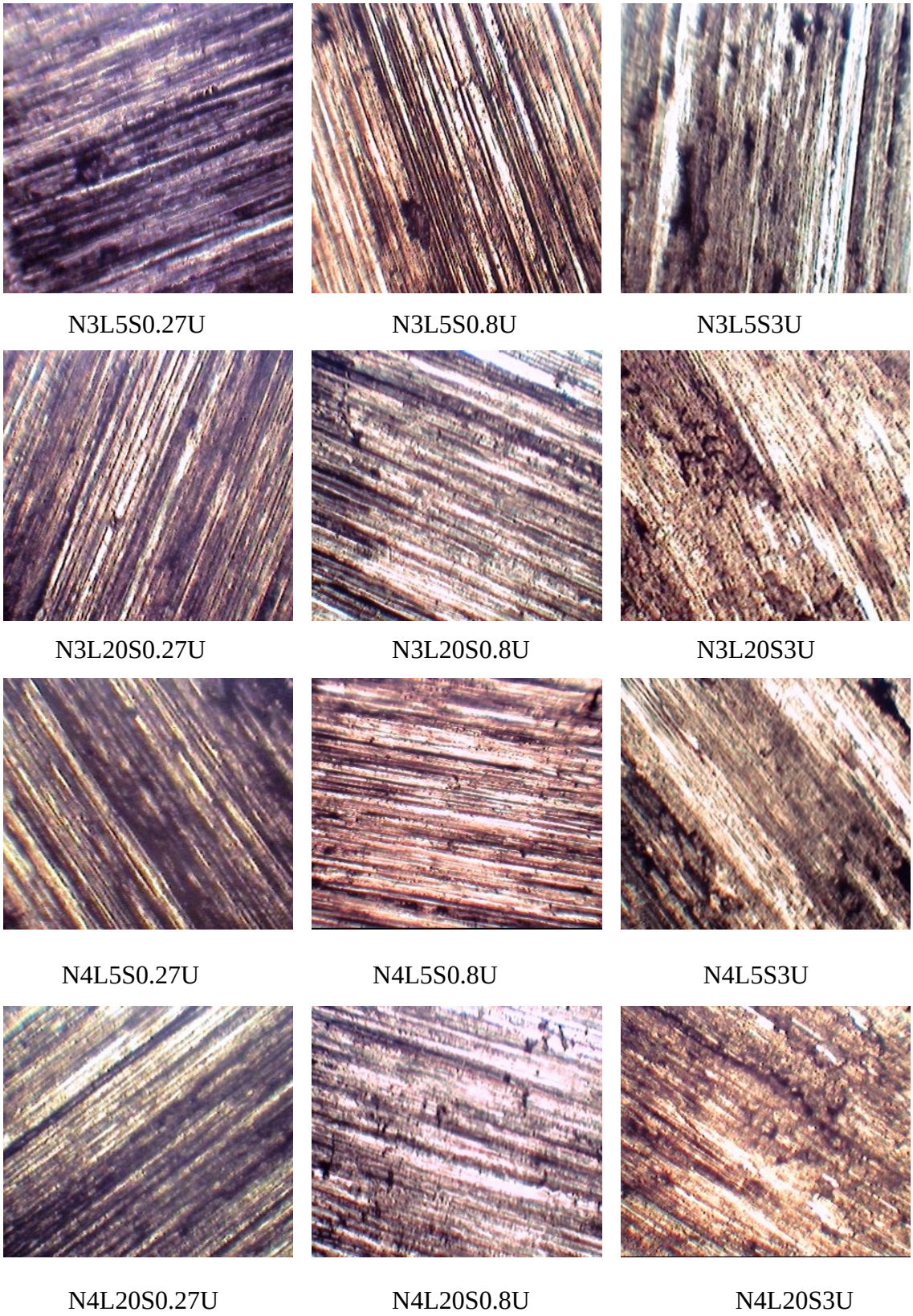

Fig. 76: Photomacrographs showing the shear lines at the worn ends after one hour runing . (N3: Al-Zr, N4: Al-Ti-B at Speeds = (0.27, 0.8, 3) m/sec and loads 5, 20 N)

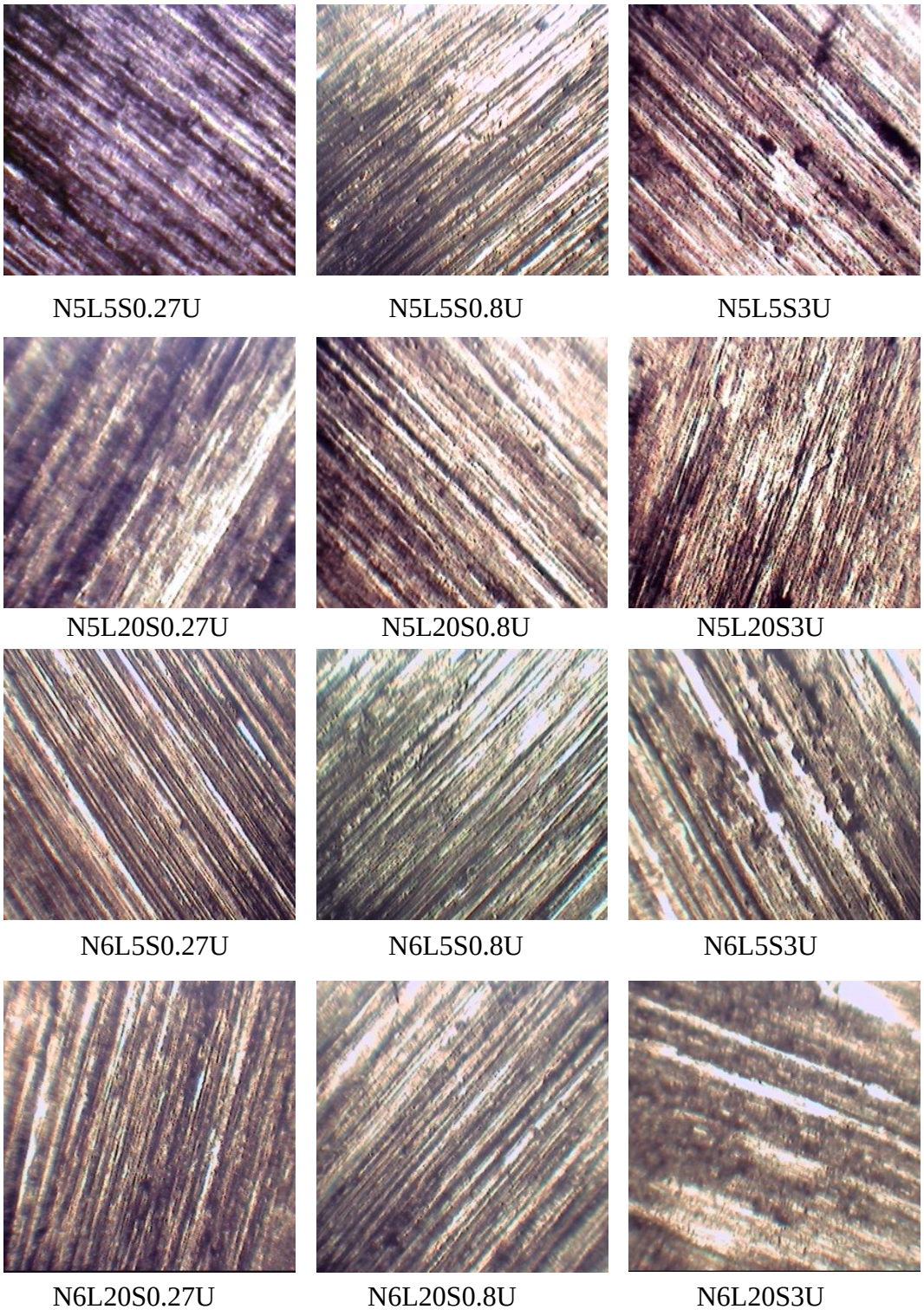

Fig. 77: Photomacrographs showing the shear lines at the worn ends after one hour runing . (N5: Al-Ti-B-Zr, N6: Al-Ti-Zr at Speeds = (0.27, 0.8, 3) m/sec and loads 5, 20 N)

The wear data are presented three diemntionally accumulated mass loss, speed and decrease in height as shown in figures 78 to 89 inclusive.

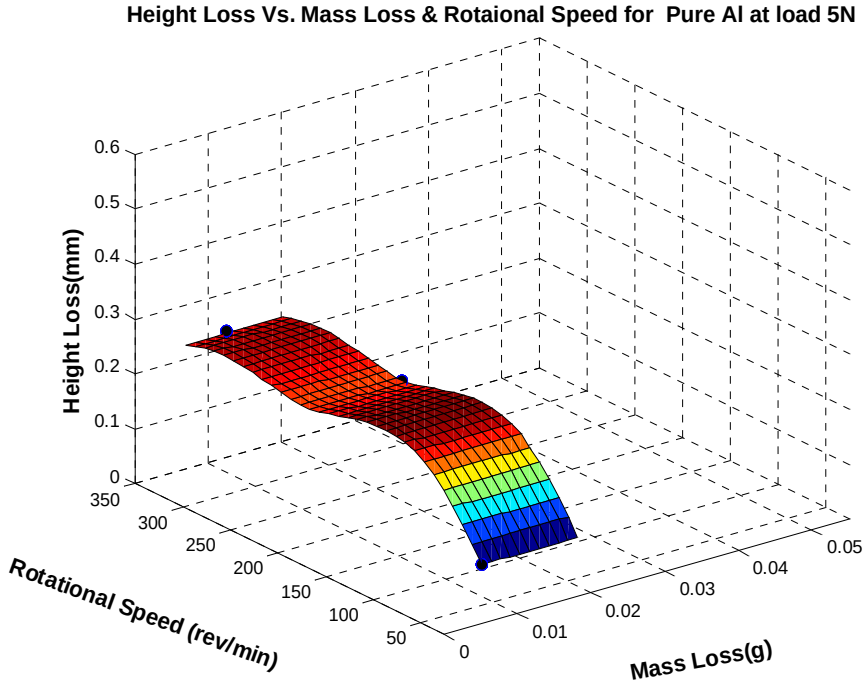

Fig. 78: Decrease in height Vs. accumulated mass loss and rotational speed for pure Al at load = 5 N

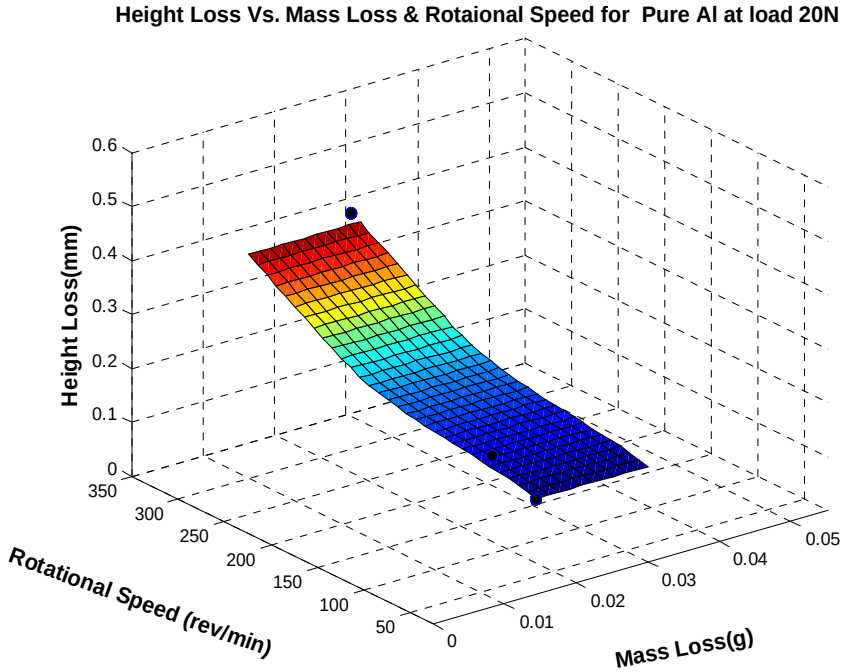

Fig. 79: Decrease in height Vs. accumulated mass loss and rotational speed for pure Al at load = 20 N

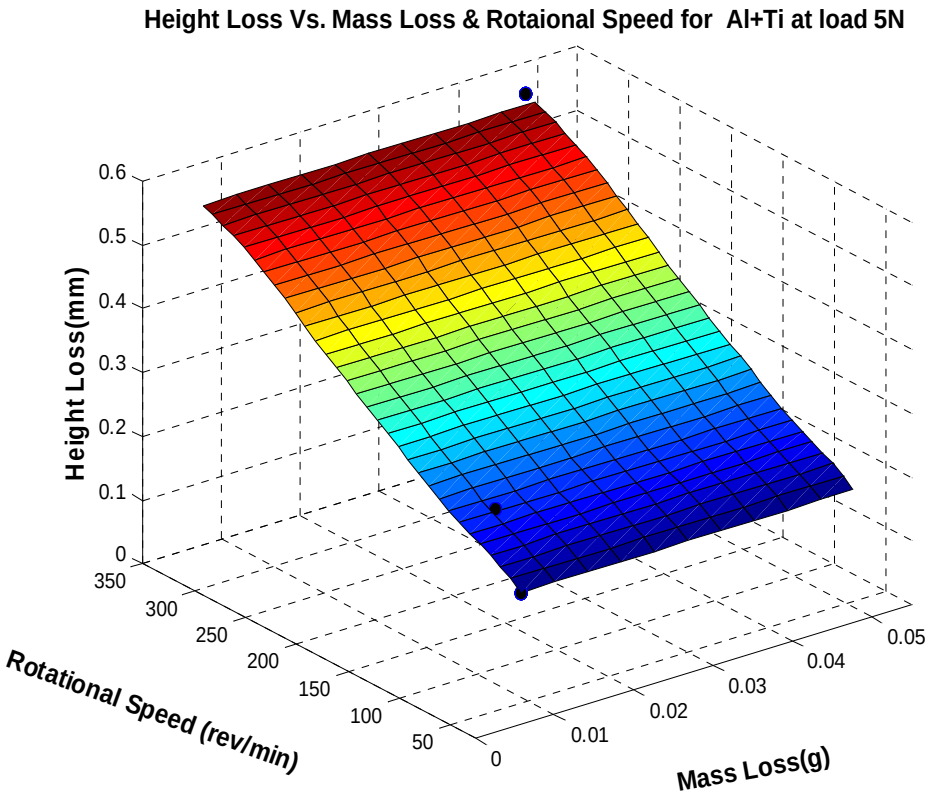

Fig. 80: Decrease in height Vs. accumulated mass loss and rotational speed for Al-Ti at Load = 5 N

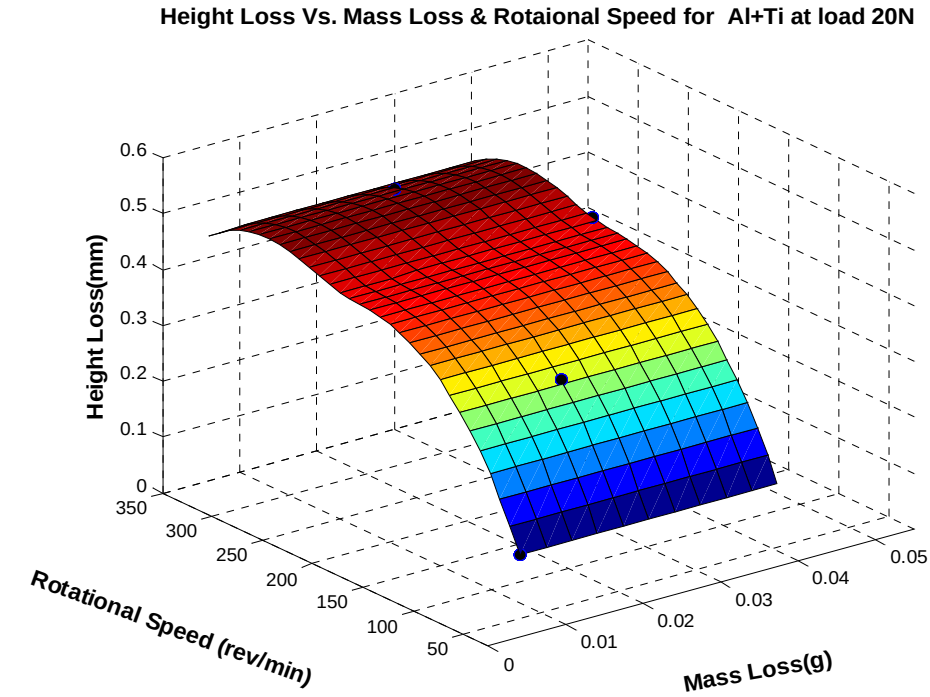

Fig. 81: Decrease in height Vs. accumulated mass loss and rotational speed for Al-Ti at Load = 20 N

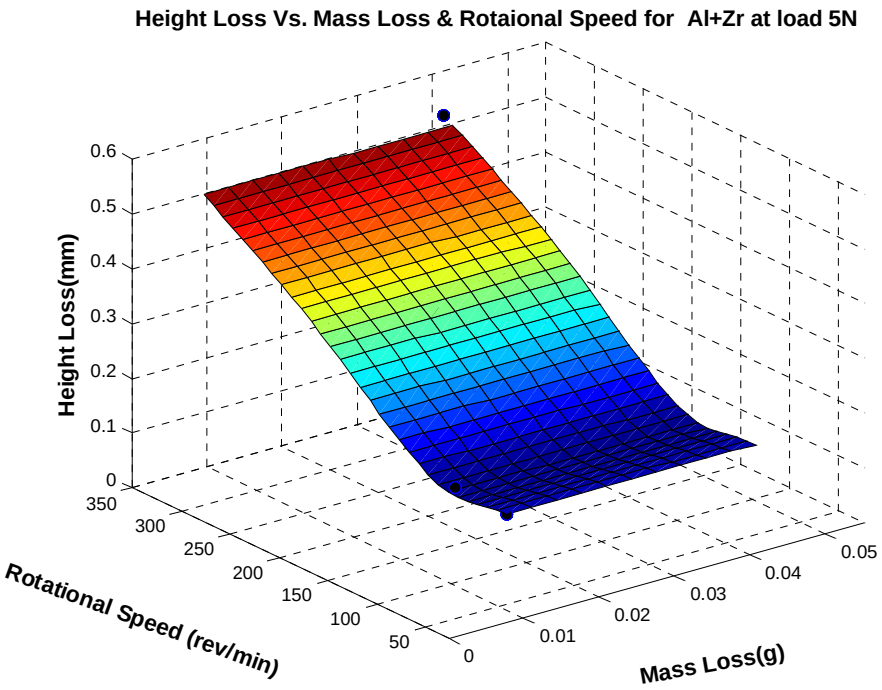

Fig. 82: Decrease in height Vs. accumulated mass loss and rotational speed for Al-Zr at Load = 5 N

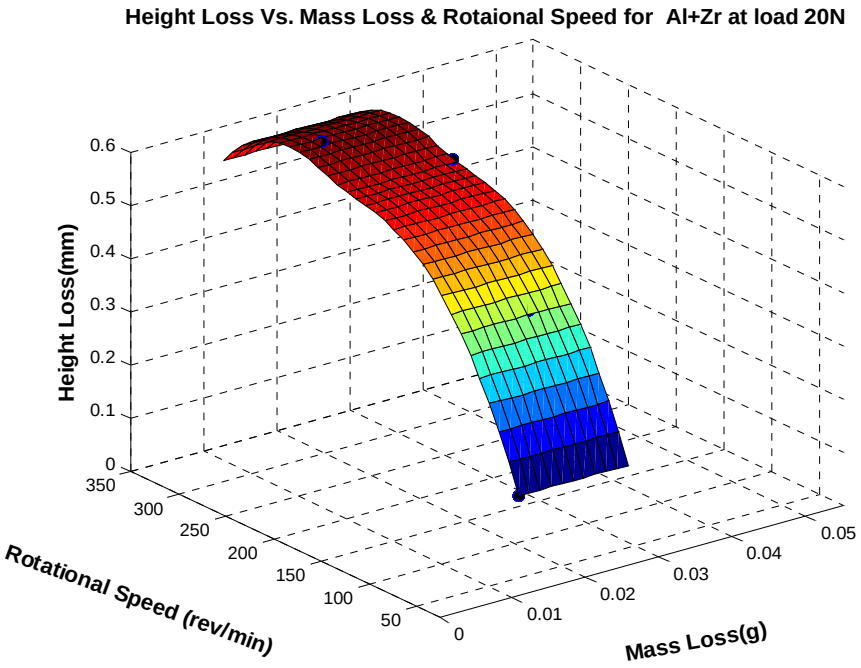

Fig.83: Decrease in height Vs. accumulated mass loss and rotational speed for Al-Ti at Load = 20 N

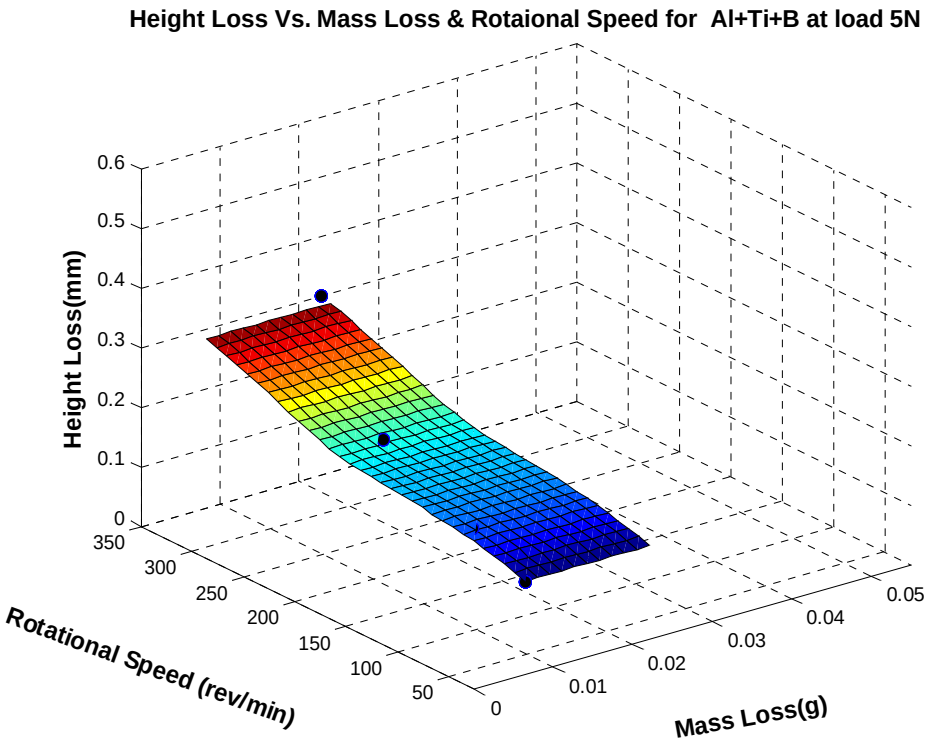

Fig. 84: Decrease in height Vs. accumulated mass loss and rotational speed for Al-Ti-B at Load = 5 N

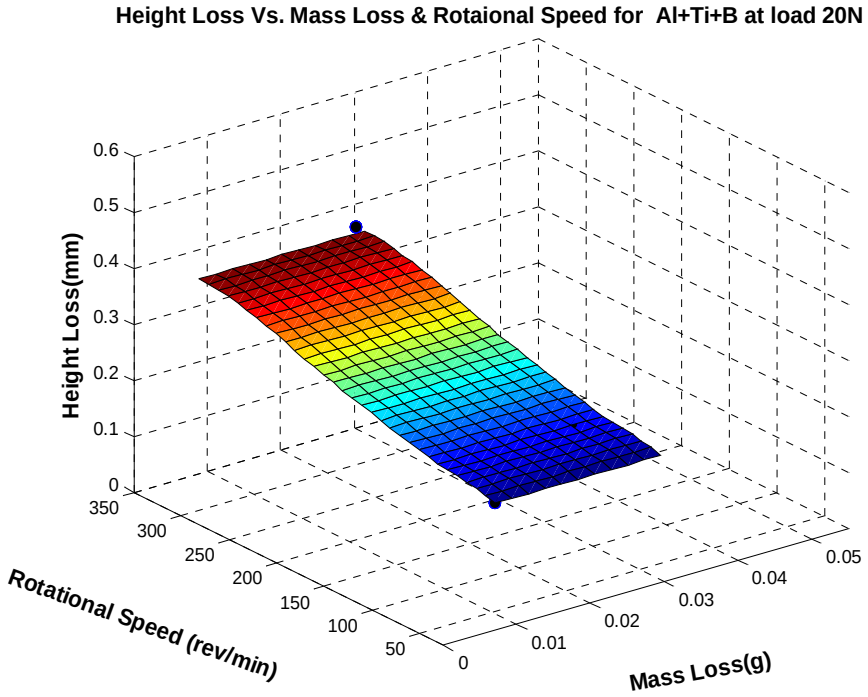

Fig. 85: Decrease in height Vs. accumulated mass loss and rotational speed for Al-Ti-B at Load = 20 N

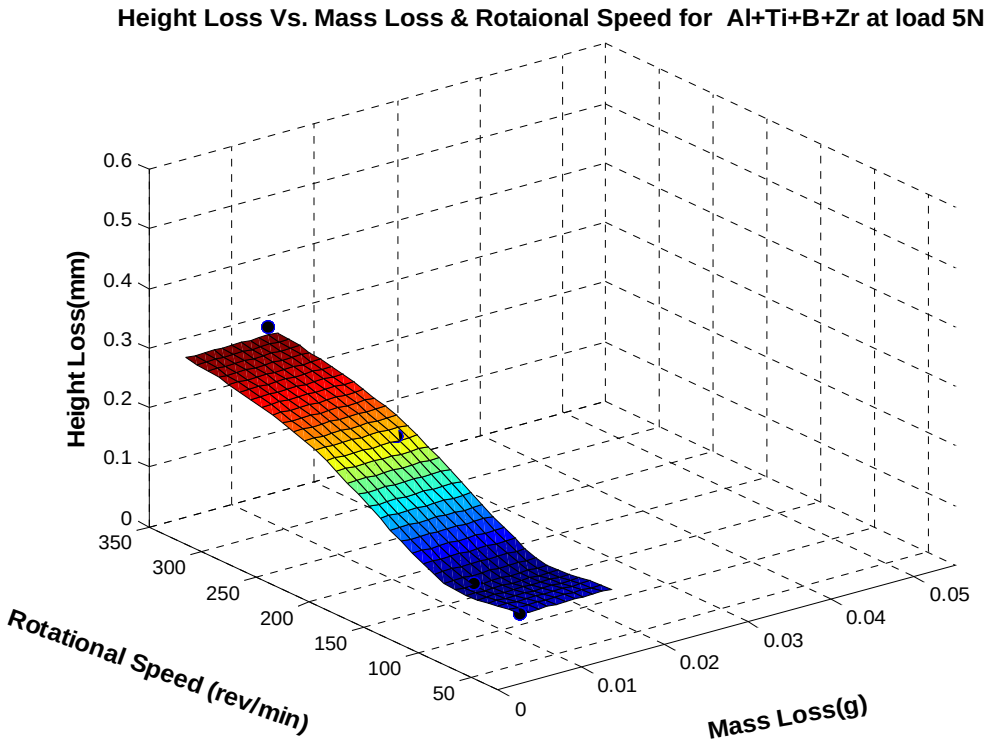

Fig. 86: Decrease in height Vs. accumulated mass loss and rotational speed for Al-Ti-B-Zr at Load = 5 N

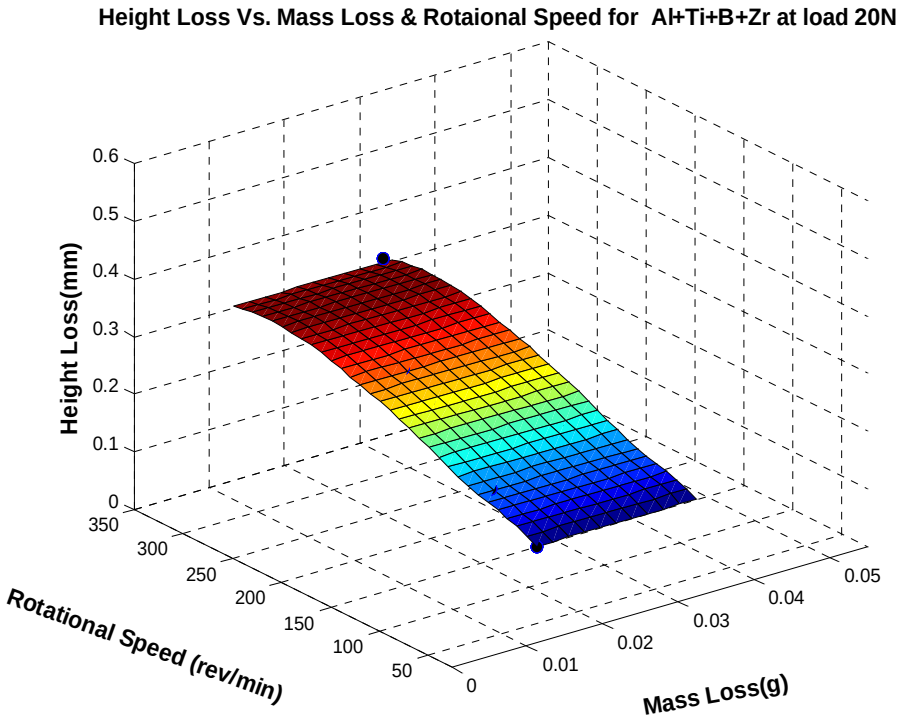

Fig. 87: Decrease in height Vs. accumulated mass loss and rotational speed for Al-Ti-B-Zr at Load = 20 N

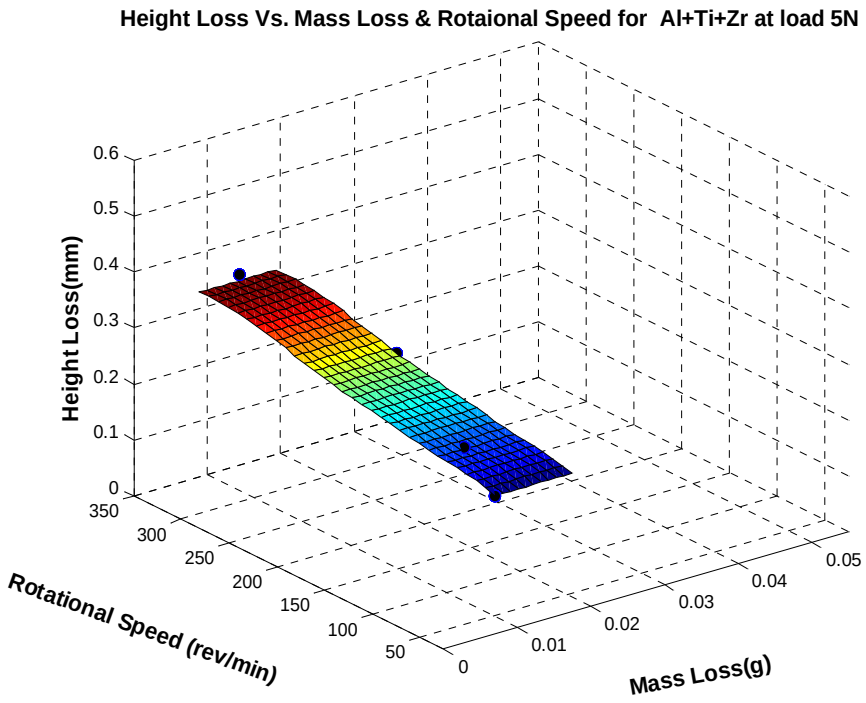

Fig. 88: Decrease in height Vs. accumulated mass loss and rotational speed for Al-Ti-Zr at Load = 5 N

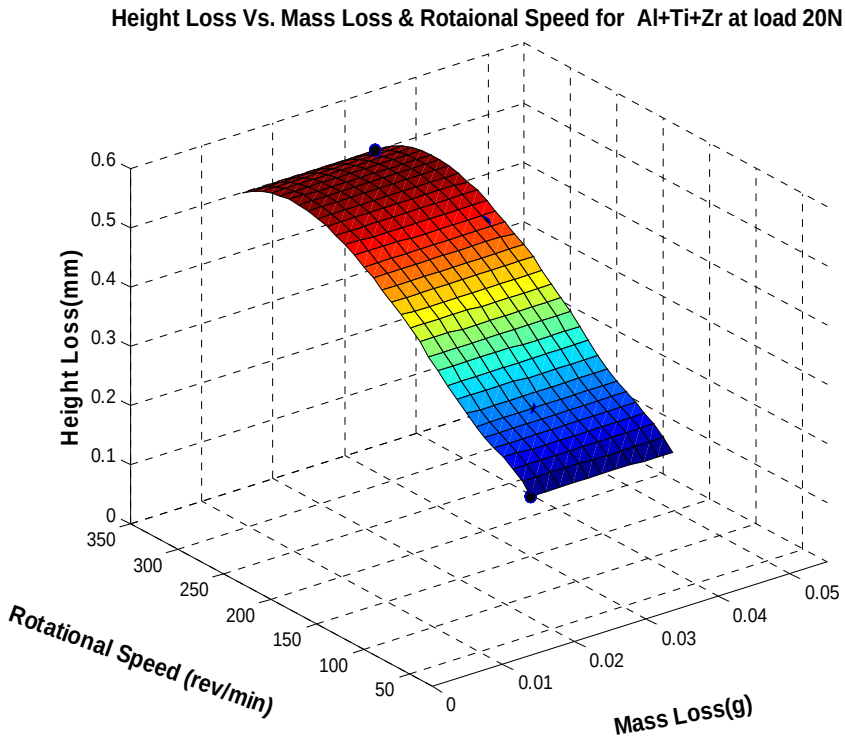

Fig. 89: Decrease in height Vs. accumulated mass loss and rotational speed for Al-Ti-Zr at Load = 20N

6.4.2 Effect of Zirconium Addition on the Wear Resistance of Aluminum and Aluminum Grain Refined by Ti+B

Figure 90 shows the effect of Zr addition on the wear resistance of Al grain refined by Ti+B as accumulated mass loss versus time , at speed of 0.27 m / sec and loads 5 and 20 N, from which it can be seen that aluminum showed the least accumulated mass loss at 5 N load. This indicates that the effect of addition of grain refiners Ti+B, Zr either alone or together deteroriates the wear resistance of Al. However increasing the load to 20 N the trend has changed and the addition of Zr to the Al or Al grain refined by Ti or Ti +B resulted in enhancement of its wear resistance.

Increasing the speed at low loads (0.8 m / sec, 5N) dose not seen to change this trend as shown in figures 91 and 92, whereas increasing the speed at higher loads e.g. at (0.8 m/sec, 20 N) or (3 m / sec, 20N) the trend somewhat changed.

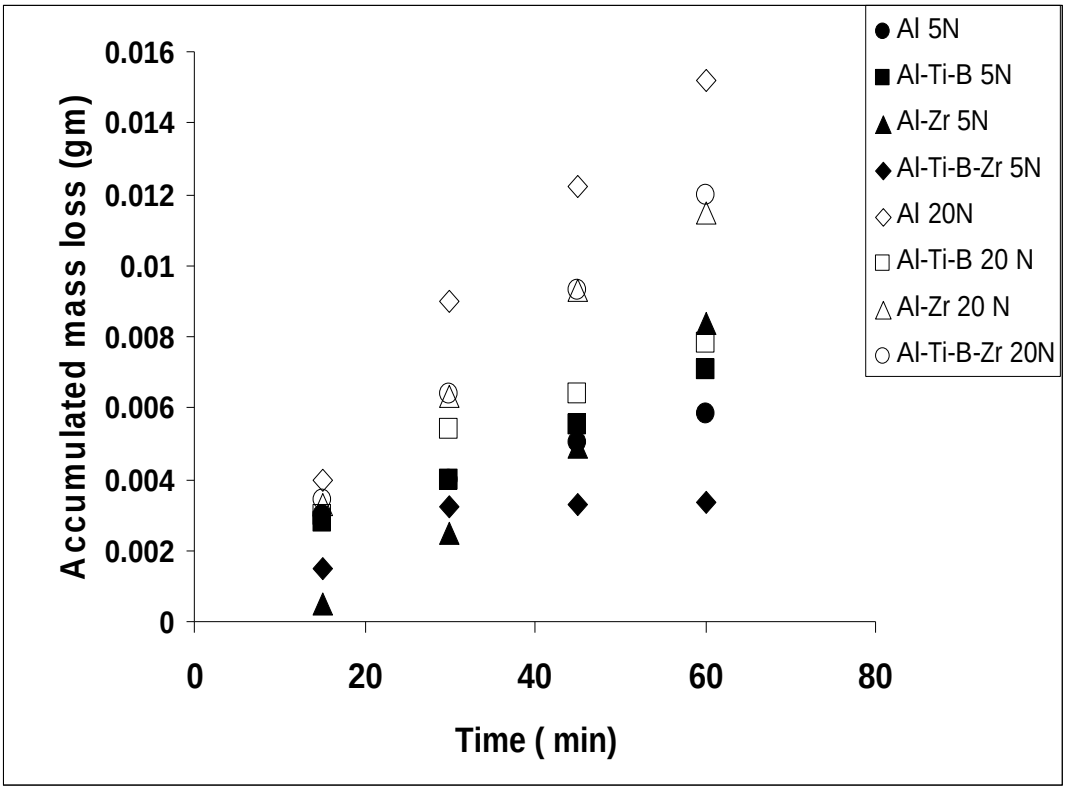

Fig. 90: Effect of zirconium addition of Al and Al grain refined by Ti+B at (S = 0.27 m/sec, loads = 5, 20 N)

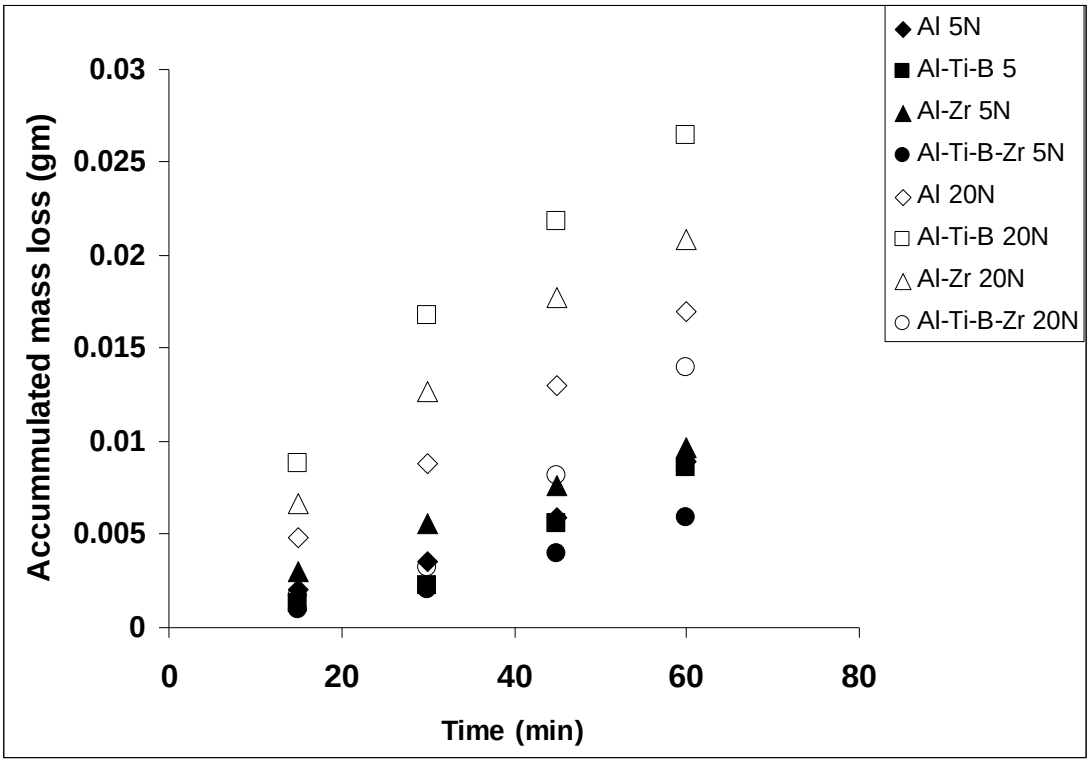

Fig. 91: Effect of zirconium addition of Al and Al grain refined by Ti+B at (S = 0.8 m/sec, loads = 5, 20 N)

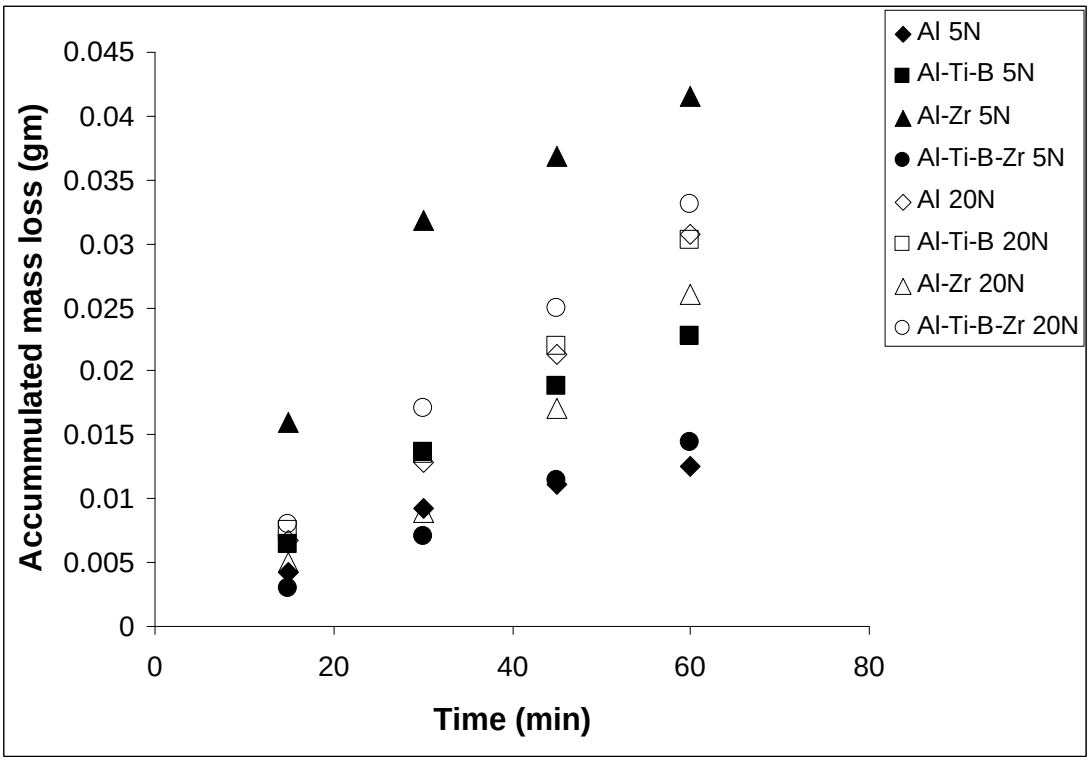

Fig. 92: Effect of zirconium addition of Al and Al grain refined by Ti+B at (S = 3 m / sec, loads = 5, 20 N)

If the criteion of wear based on accumulated mass loss or the criterion based on the wear coeffecient K are used to correlate the previous wear results. However, if the dimentional changes are included in addition to mass loss for asseeing the wear resistance of Al or Al grain refined by either Ti or Ti+B in the absence or prsence of Zr gives better assessment of wear. It can be concluded from the results of the wear tests, that the addition of Zr to Al or to Al grain refined by Ti at the same loads and speed resulted in more plastic deformation at the worn end (more mushrooming) than in the case of Zr addition to Al grain refined by Ti+B. This may attributed to the increase of ductility of Al when Zr is added alone to Al or to Al grian refined by Ti; figures 44, 45 whereas addition of Ti+B alone or in the presence of Zr resulted in less plastic deformation at the worn end as addition of either of them alone or together resulted in decrease of ductility of commercially pure aluminum as shown in figures 59 and 60, the worst is in the case of Zr addition to Al grain refined by Ti+B.

In general, it can be concluded from the results of the wear tests for alumnium and its different microalloys that increasing either load or speed will results in more wear, Furthermore, it is misleading to assess the effect of wear resistance of Al and its microalloys based on the traditional methods i.e. using mass loss or the wear coefecient as both of these methods does not take into consideration the effect of plastic deformation at the worn end which is more pronounced than mass loss and may be crucial in assessing wear. The suggested model based on both mass loss and plastic deformation as suggested in chapter five will be more representative and realistic for assessing wear resistance of aluminum and other soft materials and their alloys. This may be assessed experimentally by the mass loss (which represents the shearing effect) and the ductility of the material as indicated by the decrease in height of the pen (which represent the plastic deformation effect at the worn end i.e. mushrooming).

This is verified by the results reported in Tables 17 to 28 inclusive. For example, consider Tables 18 to 23 (at speed 0.27 m /sec and load 20 N) and (speed 3 m /sec and 20 N) for addition to Al and Al grain refined by Ti respectivily. The material which has higher ductility (Al-Zr), figures 44, 45, should suffer more reduction in height Δ h and less mass loss as compared to Al-Ti which should have higher mass loss and less reduction in height, which indeed is the case.

Similarly, for the case of Zr addition to Al and Al grain refined by Ti+B (the results reported in Tables 24 to 28 inclusive). The same concept applies.

Table 23: Mass loss and dimensional changes after one hr. wear for Zr addition to Al and Al grain refined by Ti+B in the as cast condition.(load = 5 N, S = 0.27 m/sec, A_o = 38.48 mm^2)

Name	Mass loss (g)	D_f (mm)	Δ h (mm)	A_f (mm^2)	K Wear rate
Al	0.0058	7.1	0.1	39.59	0.0751
Al-Ti-B	0.0071	7.1	0.15	39.59	0.1362
Al-Zr	0.0084	7.2	0.19	40.72	0.0974
Al-Ti-B-Zr	0.00336	7.1	0.11	39.59	0.0675

Table 24: Mass loss and dimensional changes after one hr. wear for Zr addition to Al and Al grain refined by Ti+B in the as cast condition.(load = 20 N, S = 0.27 m/sec, A_o = 38.48 mm^2)

Name	Mass loss (g)	D_f (mm)	Δ h (mm)	A_f (mm^2)	K Wear rate
Al	0.0152	8.3	0.17	54.1	0.0492
Al-Ti-B	0.0078	7.5	0.22	44.18	0.0374
Al-Zr	0.0152	8	0.18	50.27	0.0441
Al-Ti-B-Zr	0.012	7.4	0.160	43.00	0.0602

Table 25 : Mass loss and dimensional changes after one hr. wear for Al and Al grain refined by Ti+B in the as cast condition.(load = 5 N, S = 0.8 m/sec, A_o= 38.48 mm^2)

Name	Mass loss (g)	D_f (mm)	Δ h (mm)	A_f (mm^2)	K
Al	0.0089	7.1	0.24	39.59	0.0384
Al-Ti-B	0.0086	7.3	0.18	41.53	0.0575
Al-Zr	0.0097	8	0.18	50.27	0.0375
Al-Ti-B-Zr	0.0059	7.4	0.1	43.00	0.0395

Table 26: Mass loss and dimensional changes after one hr. wear for Al and Al grain refined by Ti+B in the as cast condition.(load = 20 N, S = 0.8 m/sec, = 38.48 mm^2)

Name	Mass loss (g)	D_f (mm)	Δ h (mm)	A_f (mm^2)	K Wear rate
Al	0.017	7.5	0.19	44.18	0.0183
Al-Ti-B	0.0264	7.6	0.24	45.36	0.0422
Al-Zr	0.0209	9	0.44	63.62	0.0202
Al-Ti-B-Zr	0.014	7.5	0.20	44.18	0.0234

Table 27: Mass loss and dimensional changes after one hr. wear for Al and Al grain refined by Ti in the as cast condition.(load = 5 N, S = 3 m/sec, A_o = 38.48 mm^2)

Name	Mass loss (g)	D_f (mm)	Δ h (mm)	A_f (mm^2)	K Wear rate
Al	0.0126	7.9	0.23	49.0	0.0144
Al-Ti-B	0.0228	8	0.3	50.27	0.0387
Al-Zr	0.0415	8.5	0.52	56.75	0.0426
Al-Ti-B-Zr	0.0144	7.6	0.28	45.36	0.0256

Table 28 : Mass loss and dimensional changes after one hr. wear for Al and Al grain refined by Ti in the as cast condition.(load = 20 N, S = 3 m/sec, A_o = 38.48 mm^2)

Name	Mass loss (g)	D_f (mm)	Δ h (mm)	A_f (mm^2)	K Wear rate
Al	0.0308	8.6	0.37	58.08	0.0088
Al-Ti-B	0.0303	8.6	0.36	58.08	0.0129
Al-Zr	0.0261	8.7	0.52	59.45	0.0070
Al-Ti-B-Zr	0.0331	8	0.31	50.27	0.0147

7. CONCLUSIONS AND SUGGESTIONS FOR FUTURE WORK

7.1 CONCLUSIONS

From the results obtained through this investigation the following points are concluded:

i) Addition of zirconium, Zr, to the commercially pure aluminum, Al, resulted in poisoning of its grains i.e. coarsening them, whereas addition of Zr to Al grain refined by Ti or Ti+B resulted in further refining of its grains, which means their addition is not additive.

ii) Addition of Zr to Al or Al grain refined by Ti resulted in decrease of its microhardness whereas addition of Zr to Al grain refined by Ti+B resulted in further increase of its hardness.

iii) Addition of Zr to Al or to Al grain refined by Ti resulted in deterioration of its mechanical behavior i.e. its true stress-true strain ($\sigma-\varepsilon$) curve, flow stress, ultimate tensile strength, whereas it improved its work hardening index, n, and its ductility, i.e. improved formability and hence reduces the number of stages required for forming at large process strains in excess of the plastic instability strain.

iv) Addition of Zr to Al grain refined by Ti+B resulted in improvement of its mechanical behavior i.e. its true stress-true strain ($\sigma - \varepsilon$) curve, increase of flow stress, increase of ultimate tensile strength, (U.T.S), increase of work hardening index but resulted in decrease of its ductility.

v) Addition of Zr to Al or Al grain refined by Ti resulted in decrease of extrusion force and energy whereas it resulted in high increase of the extrusion force and energy required for Zr addition to Al grain refined by Ti+B at the same extrusion ratio. This is attributed to the decrease in the

mechanical strength in case of Zr addition to Al or Al grain refined by Ti and increase of the mechanical strength when added to Al grain refined by Ti+B.

vi) The extrusion process resulted in grain refining of Al and Al grain refined by Ti or Ti+B in the absence or presences of Zr. In all cases the refining was more than that caused by the addition of the refiners themselves.

vii) The extrusion process resulted in increase of hardness of Al and all its investigated microalloys. Similarly it resulted in increase of their flow stress, ultimate tensile strength, whereas, the extrusion process resulted in decrease of these mechanical characteristics for commercially pure aluminum and the Al-Zr and Al-Ti-Zr, microalloys. Also it resulted in decrease of their work hardening index, n, i.e. decrease of their formability. The same conclusion is obtained from the free upsetting results.

viii) The wear results revealed that it is difficult or not possible to conclude from them as there is no correlation exists among the obtained results at different loads and speeds due to the presence of the mushrooming (plastic deformation) at the worn end which complicated the process. This led to the conclusion that the normally used relation, (Archard theory) when tested for the obtained results did not fit them because it does not take into consideration the plastic deformation (mushrooming) at the worn end, which in most cases it is more damaging than the mass loss.

ix) The suggested model which takes into consideration the effect of the plastic deformation at the worn end is more realistic and gives better correlation of the results than the mass loss or Archard theory.

7.2 SUGGESTIONS FOR FUTURE WORK

The following points are suggested for future work which may be investigated.

1- The effect of addition of other grain refiners such as molybdenum (Mo), vanadium (V), hafnium (Hf), lithium (Li), tantalum (Ta) and chromium (Cr) to commercially pure aluminum or Al grain refined by Ti or Ti+B following the same procedure in this thesis may be investigated

2- Effect of Zr addition on other characteristics of commercially pure aluminum and aluminum grain refined by Ti or Ti+B e.g. Creep resistance, impact strength and corrosion resistance may be investigated.

3- Effect of other rare earth elements additions like Hf, Mo, V, Li, and Cr on the creep resistance, impact strength, machinability and corrosion resistance may be investigated.

4- The suggested model for assessing wear resistance of Al should be further investigated and tested for other soft materials and their alloys e.g. copper to ensure its validity.

5- Effect of the investigated grain refiners namely Ti, Ti+B and Zr in addition to others e.g. Hf, Mo, V, Li and Cr on other forming processes like closed forging, shallow and deep drawing, blanking may be investigated.

REFERENCES

Abdel Hamid, A. A., (1989). **Effect of other elements on the grain refinement of Al by Ti or Ti and B**, part II Effect of Refractory Metals V, Mo, Zr and Ta. Z. Metallkd, 80, pp. 643-646

Abdel Hamid, A. A., (1985). **On the mechanism of the grain refinement of aluminum by small addition of Ti and B**", The Second Arab Aluminum Conference ARBAL ,85, Egypt, Oct.

Abdel Hamid, A. A., and Zaid, A.I.O.,(2000). **Poisoning .of grain refinements some aluminum alloys**, Current Advances in Mechanical Design and Production, MDP-6, PP 323-331.

Archard, J. F., (1953). **Contact and rubbing of flat surfaces**, Journal of Applied Physics 24, 981-988.

Arjuna A. Rao, Murty B.S., and Chakraborty M., (1996). **Influence of chromium and impurities on the grain-refining behavior of aluminum**, Metallurgical and Materials Transactions A, 27(A): pp.791-800.

Arjuna A. Rao, Murty B.S., and Chakraborty M, (1997). **Role of zirconium and impurities in the grain refinement of aluminum with Al-Ti-B**, Material Science and Technology, 13, pp.769-777.

ASM. Handbook, (1990). **Non ferrous materials**, V2.

ASM. Handbook, (1998). **Formability of materials**, V14.

Cibula A. : J. Institute of Metals, 76,(1949-1950), pp. 321-360

Cibula A. : J. Institute of Metals, 80, (1951-1952), pp.1-15

Daives I. G., Dennis J. M. and Hellawell A., (1970). **The nucleation of aluminum grains in alloys of aluminum with Ti and B**, Metallurgical Translation, 1, pp.275-279

Dieter, S.P.,(1989). **Mechanical metallurgy**,3rd edition, McGraw-hill, Singapore.

Eboral.M.D.,(1950). J.Institute of metals,76,, pp. 295-303.

Johnson M., (1994). **Influence of Zr on the grain refinement of Al**, .Z. Metallkd, 85, pp. 786-789

Johnson.W, Mellor.P.B, (1980). **Engineering plasticity**,1st edition, vannostarnd.

Johnson.W, Kudo.H,(1962). **The mechanics of the metal extrusion**,1st Edition, Manchester uni.press.

Johnson.W., (1955). **Extrusion through square dies of large reduction**,1st edition, J.Mech.Phys.Solids.191.

Johnson.W., (1957). **The pressure of cold extrusion of lubricated rod through square dies of moderate reduction of slow speed**, 1st edition, J.inst.Metal. PP. 403.

Jones G.P., Pearson J., (1976). **Factors affecting the grain refinement of aluminum using titanium and boron additives**, met. Trans. B, pp. 223-234

Hill, R.,(1948). **A theoretical analysis of the stresses and strains and extrusion and piercing**, 1st edition, J.Iron steel inst. 158,177.

Kalpakjian,S., Schmid,S.r., (2003). **Manufacturing processes for engineering materials**, 4th edition, prentice Hall.

Mondolfo L. F., (1976). **Aluminum alloys structure and properties**, Butterworth and Co., London.

Rollasaon, R., (1973). **Metallurgy for engineers**, 4th edition, Edward Arnold, Great Britain.

Rowe.G.W.,(1968). **Principles of industrial metal working process**, 1st edition, Edward Arnold.

Siebel.E, Fangmeier.E, (1931). **Research on power consumption in extrusion and punching of metals**, 1st edition, Mitt.K-wilhehm-inst.Eisenfosch.

Youdelis. W.V., yang.C.S.,(1981).**Aluminum**, pp.159-161.

Zaid A. I. O., Al-Alami A. A., (2001). **Effect of vanadium on the fatigue life of aluminum**, ICPR-16, Proc. Int. Conf. on Production Research, Prague, Chzech.

Zaid, A.I.O., Al-Banna M.A., (2002). **Effect of zirconium on the fatigue life of aluminum**, PEDD-6, Proc. International Conference on Production Engineering Design and Development, Egypt.

Zaid, A.I.O.,(2001). **Grain refinement of aluminum and its alloys**, 7th, international symposium on advanced materials, Pakistan.

Zaid, A.I.O., Abdel- Hamid.A.A.,(2000). **Effect of zirconium addition on Mechanical behavior and machinability of aluminum**, 15th international conference on production research ICRP-15, Bangkok, Thailand.

Zaid, A. I. O., Hussein, M. J. (2006).**Effect of Zr addition on the wear resistance of zinc-aluminum alloy 5, zamak 5, grain refined by Ti,** Proceedings of the 12th international conference on machine design and production, Kusadasi, Turkey

Zaid A. I. O., Al-Afsha, M. (2001*).***Effect of tantalum on the mechanical behaviour and machinability of aluminum,** Proceedings of the 16th international conference on production research, ICPR-16, Prague, Chzech, August

APPENDICES

Appendix (A): Tables

Table (29): Height reduction of Al and its microalloys at 5N.

SPEED (rpm)	TIME (min)	Al mm	Al-Zr mm	Al-Ti-B mm	Al-Ti mm	Al-Ti-B-Zr mm	Al-Ti-Zr mm
31	15	0.03	0.05	0.01	0.06	0.03	0.02
31	30	0.09	0.09	0.03	0.2	0.06	0.05
31	45	0.12	0.15	0.05	0.25	0.08	0.09
31	60	0.15	0.3	0.08	0.3	0.09	0.13
93	15	0.06	0.06	0.04	0.06	0.06	0.06
93	30	0.15	0.13	0.09	0.13	0.09	0.12
93	45	0.24	0.2	0.13	0.18	0.11	0.18
93	60	0.32	0.26	0.17	0.3	0.14	0.24
215	15	0.09	0.12	0.07	0.07	0.04	0.08
215	30	0.2	0.21	0.13	0.16	0.09	0.13
215	45	0.29	0.29	0.21	0.24	0.13	0.19
215	60	0.39	0.39	0.3	0.31	0.19	0.28
350	15	0.1	0.1	0.11	0.18	0.08	0.21
350	30	0.22	0.25	0.25	0.3	0.17	0.25
350	45	0.33	0.37	0.34	0.4	0.25	0.28
350	60	0.43	0.5	0.42	0.5	0.32	0.32

Table (30): Accumulated mass loss of Al and it's micro alloys at 10N

SPEED (rpm)	TIME (min)	Al gm	Al-Zr gm	Al-Ti-B gm	Al-Ti gm	Al-Ti-B-Zr gm	Al-Ti-Zr gm
31	15	0.001	0.0019	0.0009	0.0017	0.001	0.002
31	30	0.0019	0.0034	0.0019	0.0032	0.0018	0.0035
31	45	0.0034	0.0054	0.0027	0.0047	0.0033	0.0041
93	15	0.0027	0.0028	0.0025	0.0042	0.0023	0.0029
31	60	0.0044	0.0069	0.0036	0.0062	0.0043	0.0065
93	30	0.0047	0.0048	0.0048	0.008	0.0044	0.0055
215	15	0.0075	0.005	0.004	0.004	0.0022	0.0082
93	45	0.0067	0.0084	0.0068	0.011	0.0073	0.0105
350	15	0.004	0.005	0.005	0.0086	0.006	0.0082
93	60	0.0083	0.0114	0.0086	0.0139	0.01	0.0149
215	30	0.0135	0.0095	0.0078	0.0084	0.0052	0.0162
215	45	0.0179	0.0175	0.0098	0.0164	0.0084	0.0244
350	30	0.0079	0.0099	0.0091	0.0156	0.0116	0.0162
215	60	0.0219	0.025	0.0118	0.0238	0.0114	0.0319
350	45	0.0104	0.0152	0.0132	0.0206	0.0136	0.0244
350	60	0.0108	0.0202	0.0172	0.0237	0.0153	0.0319

Table (31): True stress- true strain for (Al-Ti-Zr) based on compression test.

No	Load (N)	L_O mm	A_O mm^2	L_c mm	A_c mm^2	σ=Pc/Ac MPa	ε mm/mm	Ln σ	Ln ε
1	5902	10.07	79.6	9.97	80.39	73.41	0.01	4.296	-4.61
2	7291	10.07	79.6	9.77	82.02	88.89	0.03	4.487	-3.51
3	9027.2	10.07	79.6	9.26	86.75	104.7	0.08	4.651	-2.53
4	9722	10.07	79.6	8.93	89.75	109	0.12	4.691	-2.12
5	11110	10.07	79.6	8.49	94.4	118	0.17	4.770	-1.77
6	11800	10.07	79.6	8.08	99.2	119	0.22	4.779	-1.51

Table (32): Representative (Stress-Strain) for Al-Ti-B based on tensile test. (Extruded)

No	Load (N)	L_O mm	A_O mm^2	L_c mm	A_c mm^2	σ=Pc/Ac MPa	ε mm/mm	Ln σ	Ln ε
1	1000	25	20	25.1	19.92	50.2	.004	3.92	-5.52
2	3000	25	20	25.4	19.64	152.36	0.016	5.026	-4.13
3	5000	25	20	26.4	18.94	263.4	0.054	5.58	-2.92
4	4200	25	20	27.5	18.18	231	0.1	5.44	-2.35
5	3000	25	20	27.5	18.18	165	0.1	5.105	-2.35
6									

Table (33) : Calibration the velocity of wear tester. (rpm)

Apparatus rpm	Tachometer(up) reading rpm	Tachometer (down) reading rpm	Average (rpm)
50	31	31	31
100	35	37	36
150	60	62	61
200	92	94	93
250	126	125	126
300	164	165	165
350	214	216	215
400	290	293	292
450	352	348	350
500	375	366	370

APPENDIX (B): FIGURES AND AUTOGRAPHIC RECORDS

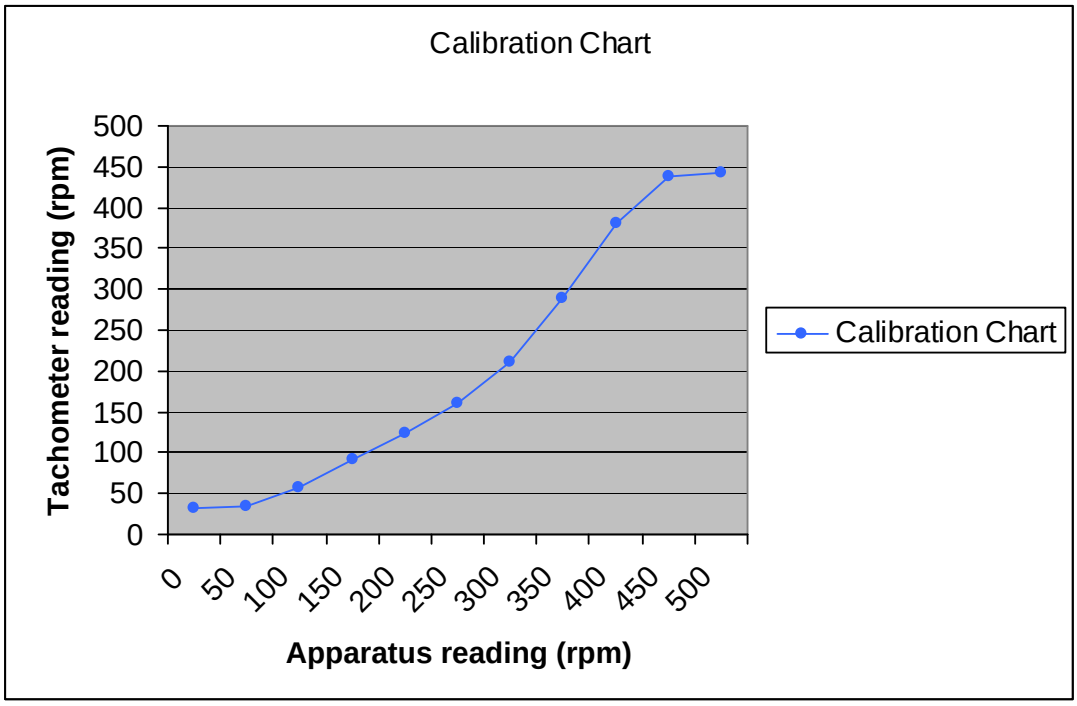

Fig..93 : The calibration chart for the rotational speed of the pin-rotating apparatus

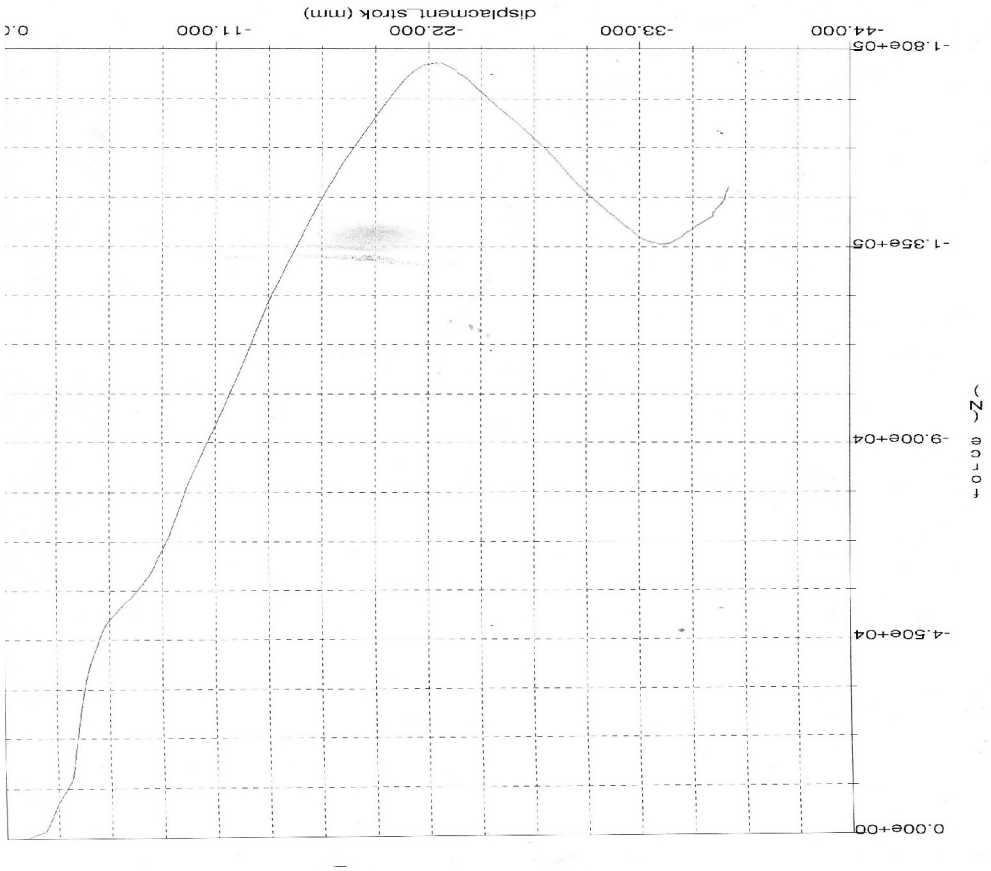

Fig.94 : Autographic record of Extrusion test(Al-Ti-B)

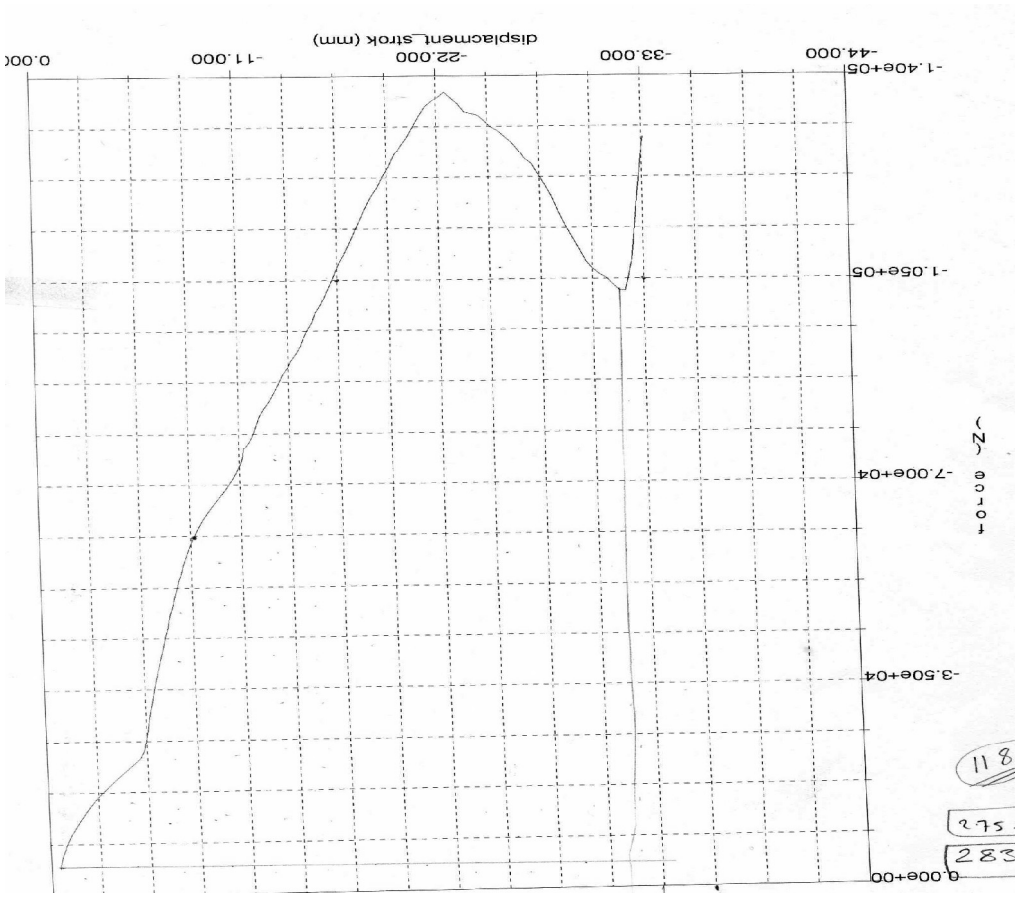

Fig 95 : Autographic record of Extrusion test(Al)

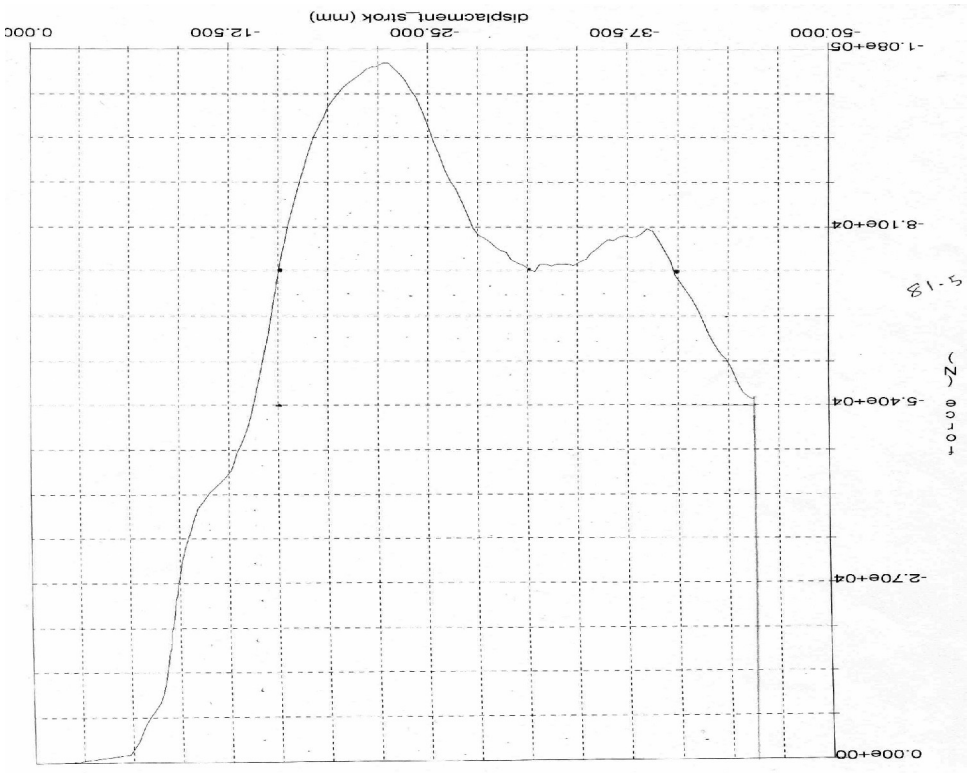

Fig.96 : Autographic record of Extrusion test(Al-Zr)

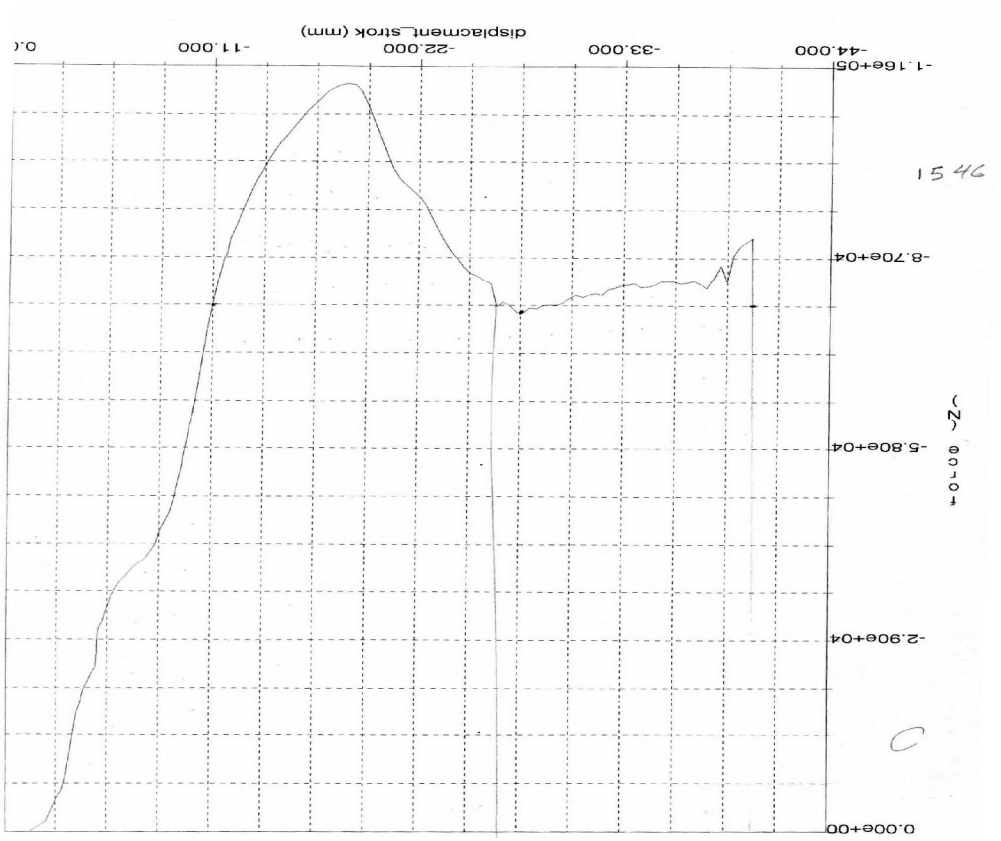

Fig 97 : Autographic record of Extrusion test(Al-Ti)

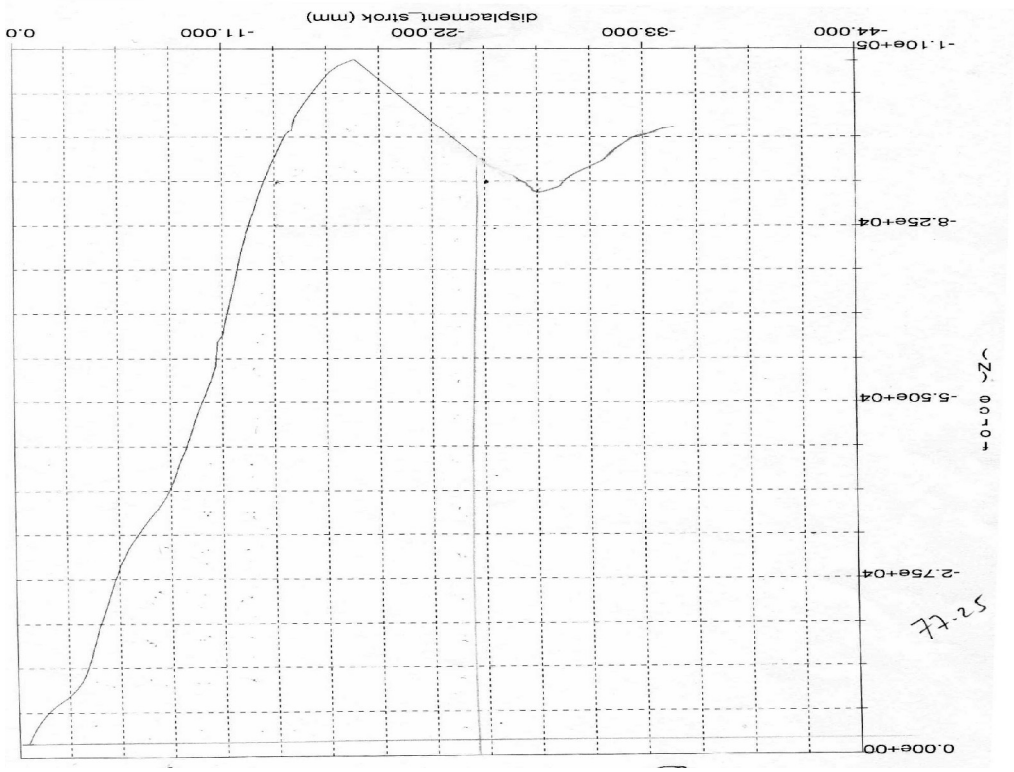

Fig 98 : Autographic record of Extrusion test(Al-Ti-Zr)

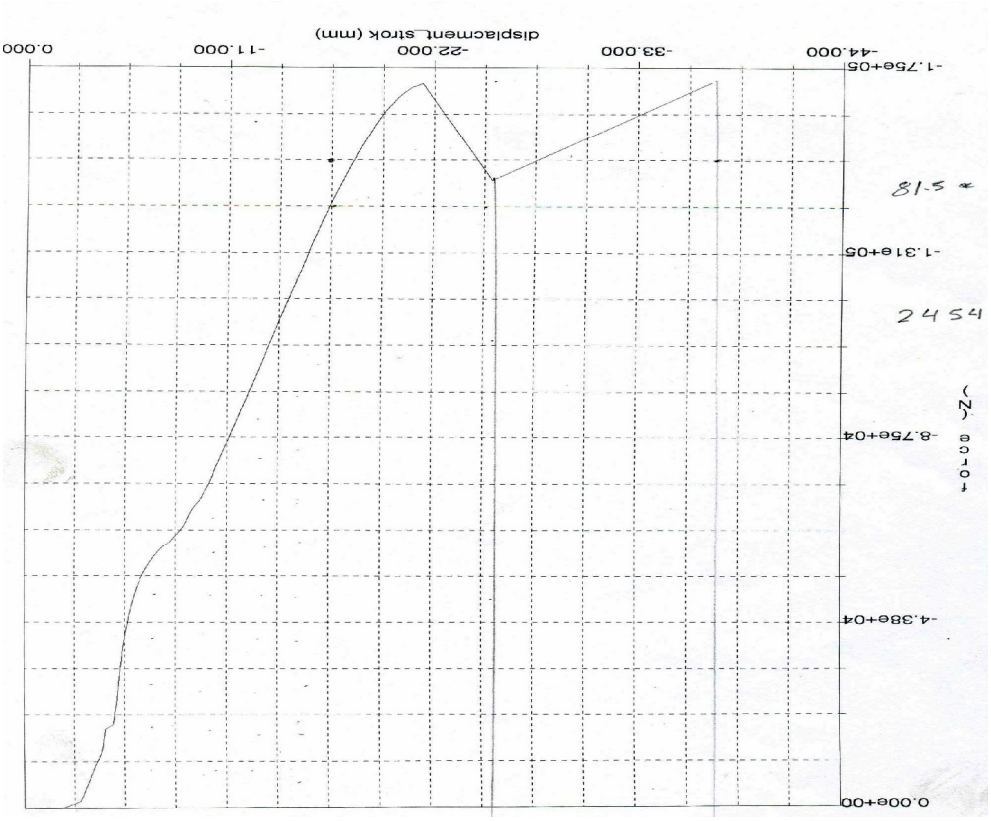

Fig 99 : Autographic record of Extrusion test(Al-T-B-Zr)

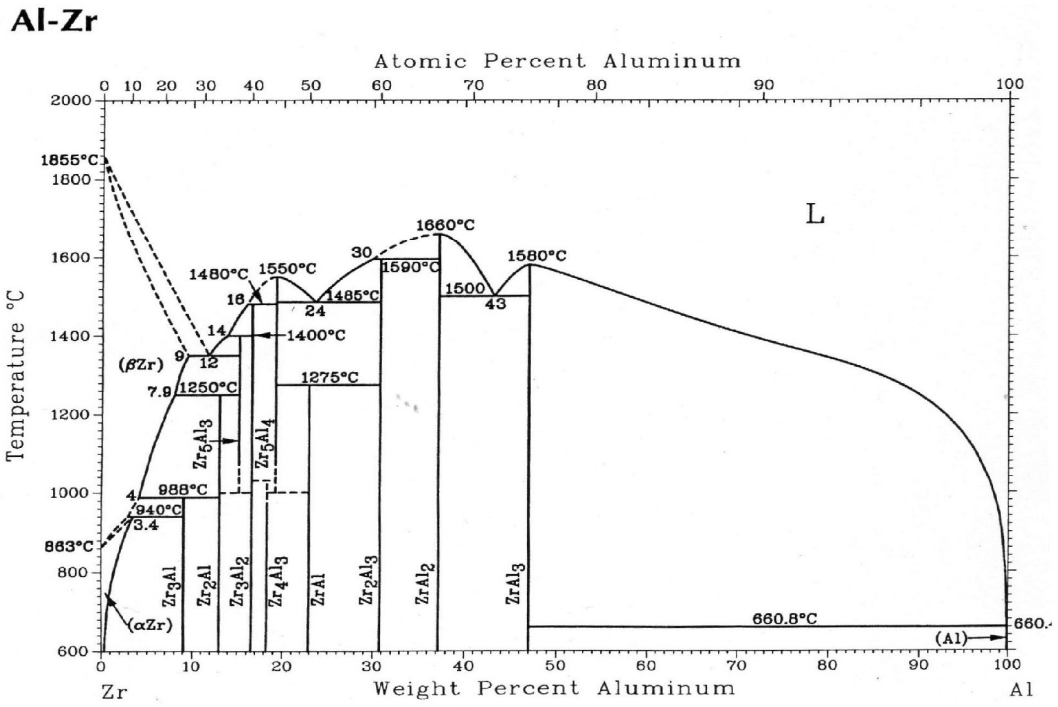

Fig. 100 : Phase diagram of Al-Zr alloy

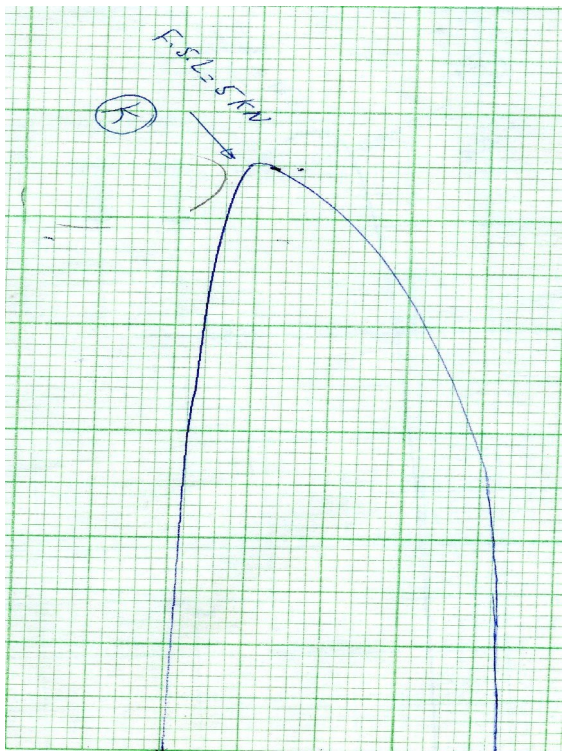

Fig. 101 : Autographic record of tensile test
(each square 50 N height and 0.2 mm width)

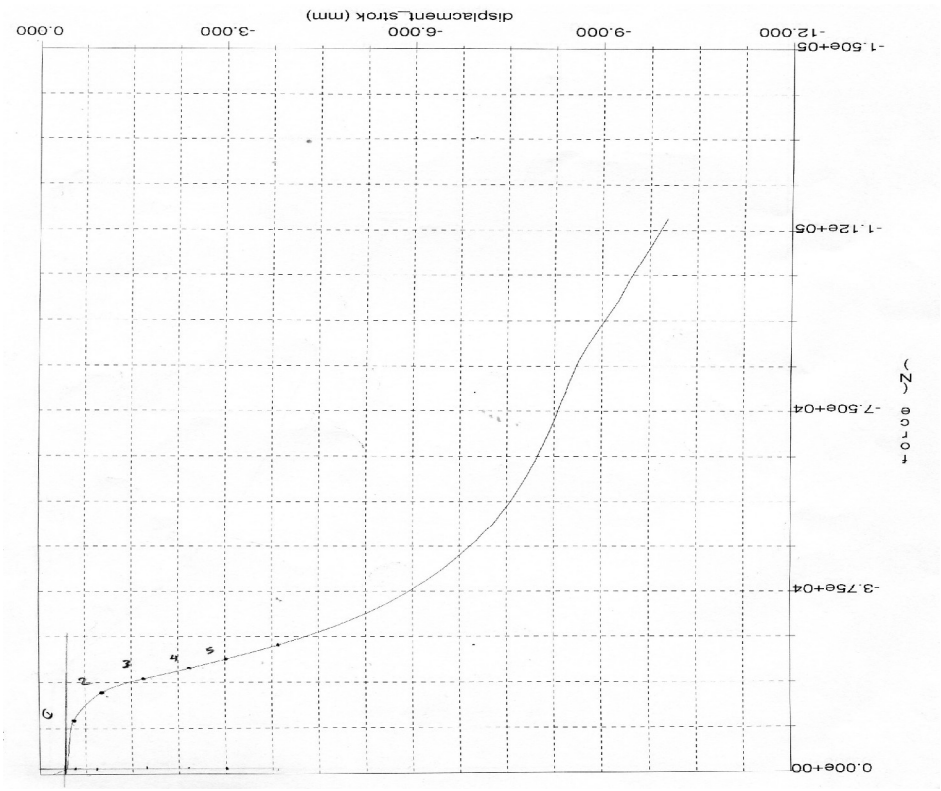

Fig. 102: Autographic record for upsetting process of (Al-T-B-Zr)

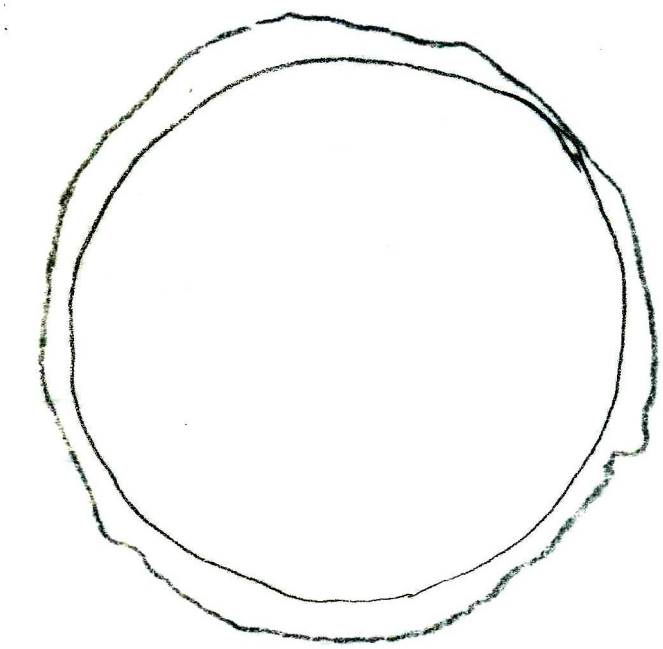

Fig. 103 : Mushrooming profile of (Al-Zr) at load 5N, S=35,t = 60 min

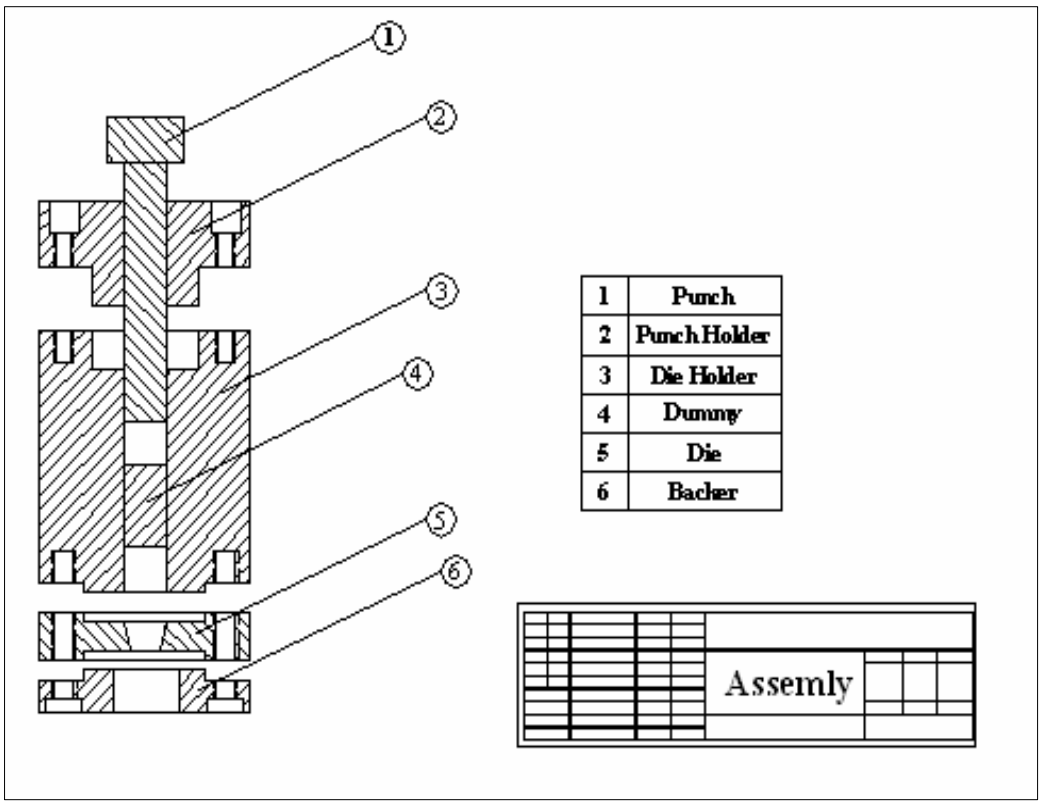

Fig. 104: Extrusion die assembly

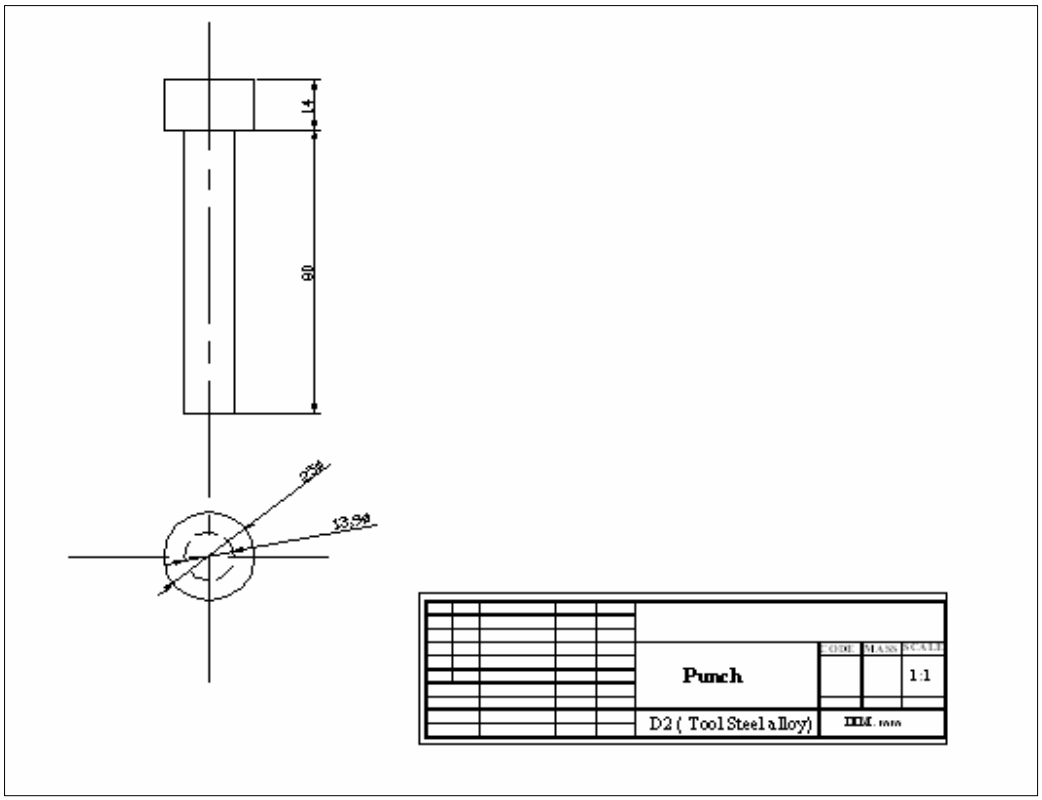

Fig. 105: Punch of extrusion die

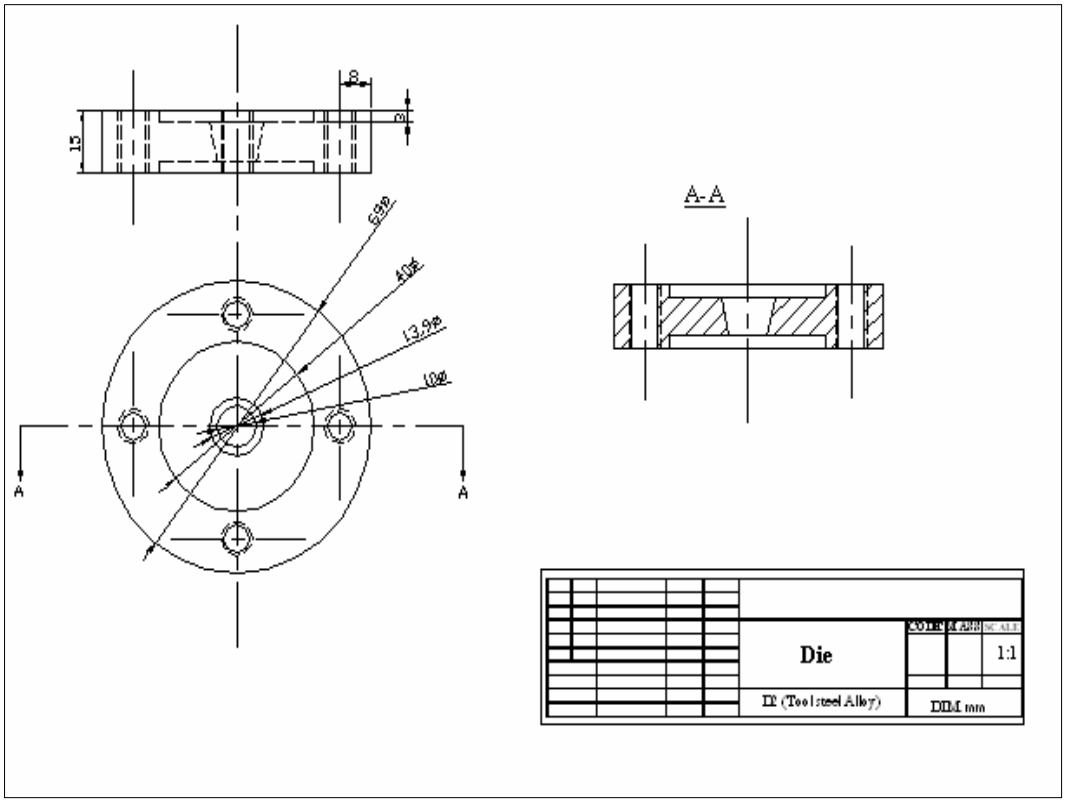

Fig:106: Extrusion die

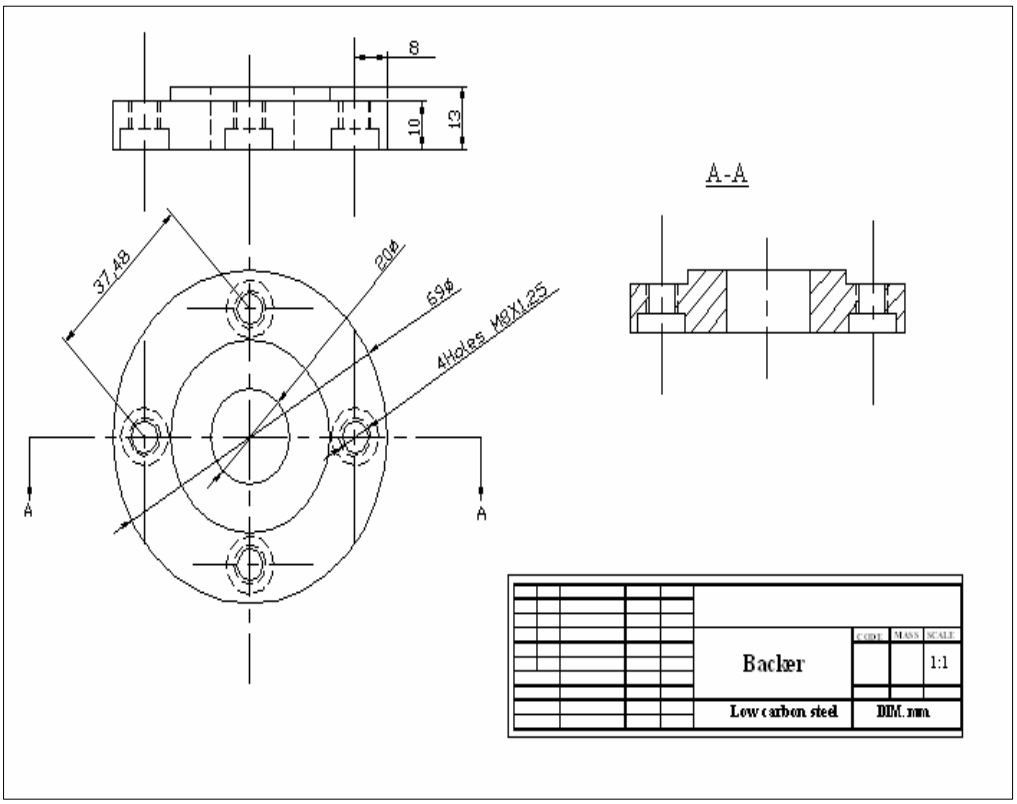

Fig. 107 : Backer

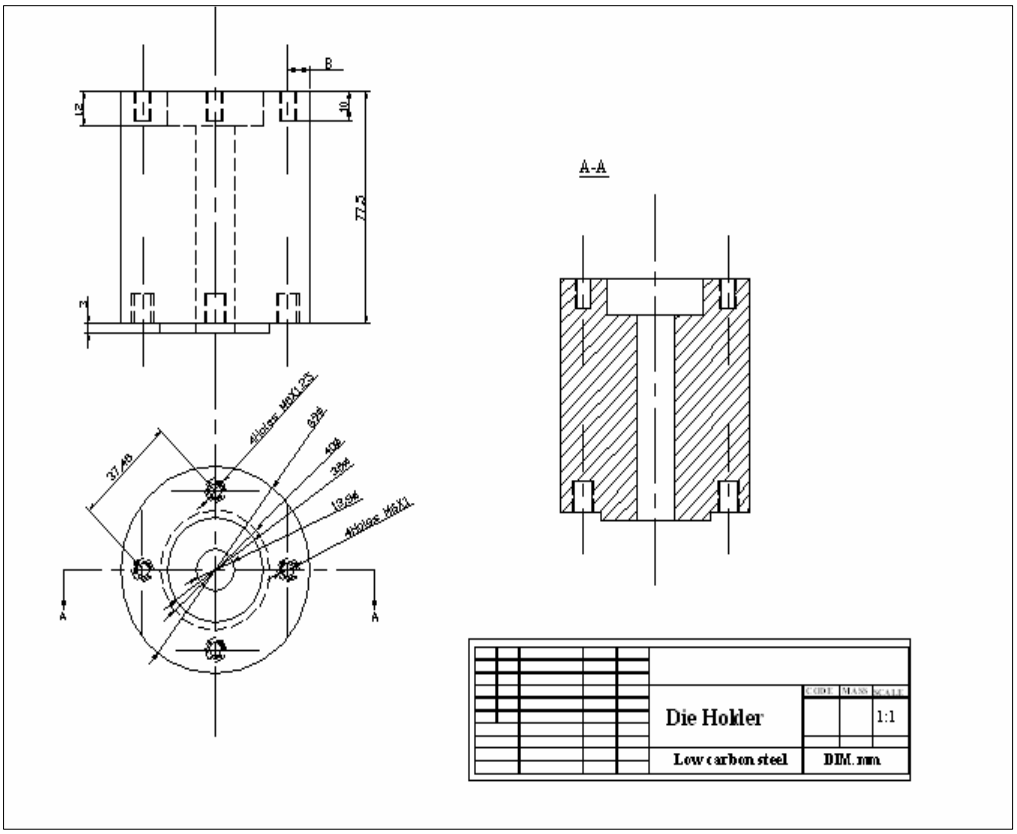

Fig. 108 : The container

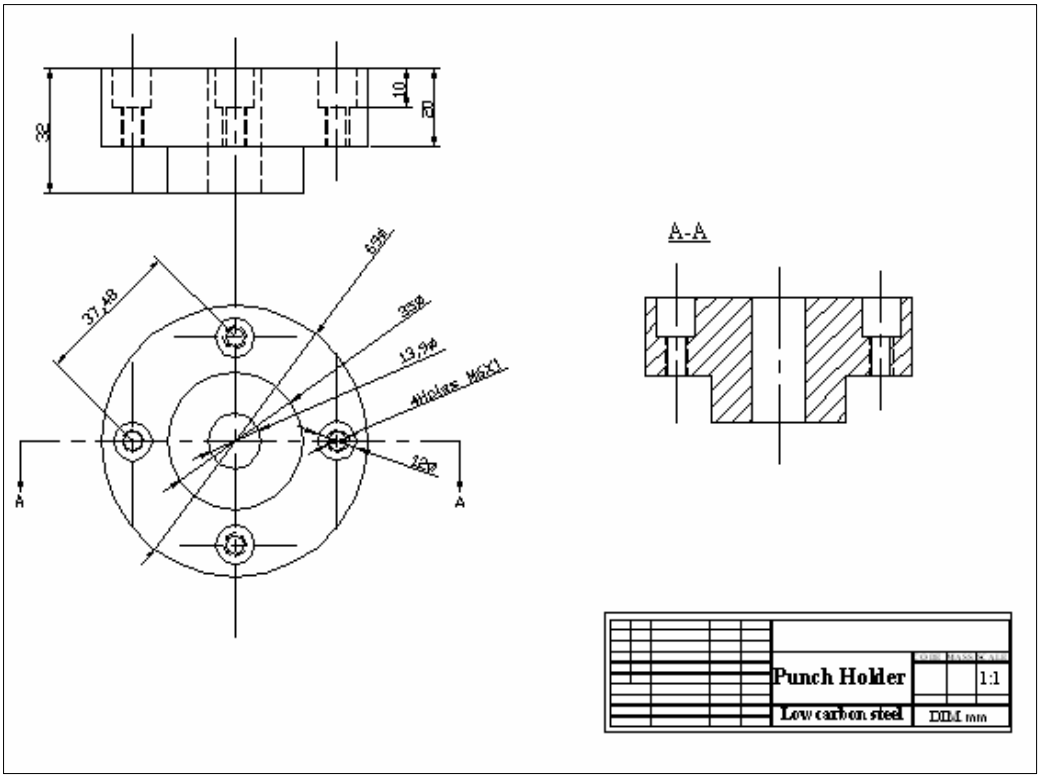

Fig.109 : Punch holder

Appendix (C) : MACRO GRAPH OF WEAR TEST

(N : microalloy number, s: speed , u : un extruded , N_1 : Al, N_2: Al-Ti, N_3: Al-Zr, N_4:Al-Ti-B, N_5: Al-Ti-B-Zr, N_6:Al-Ti-Zr)

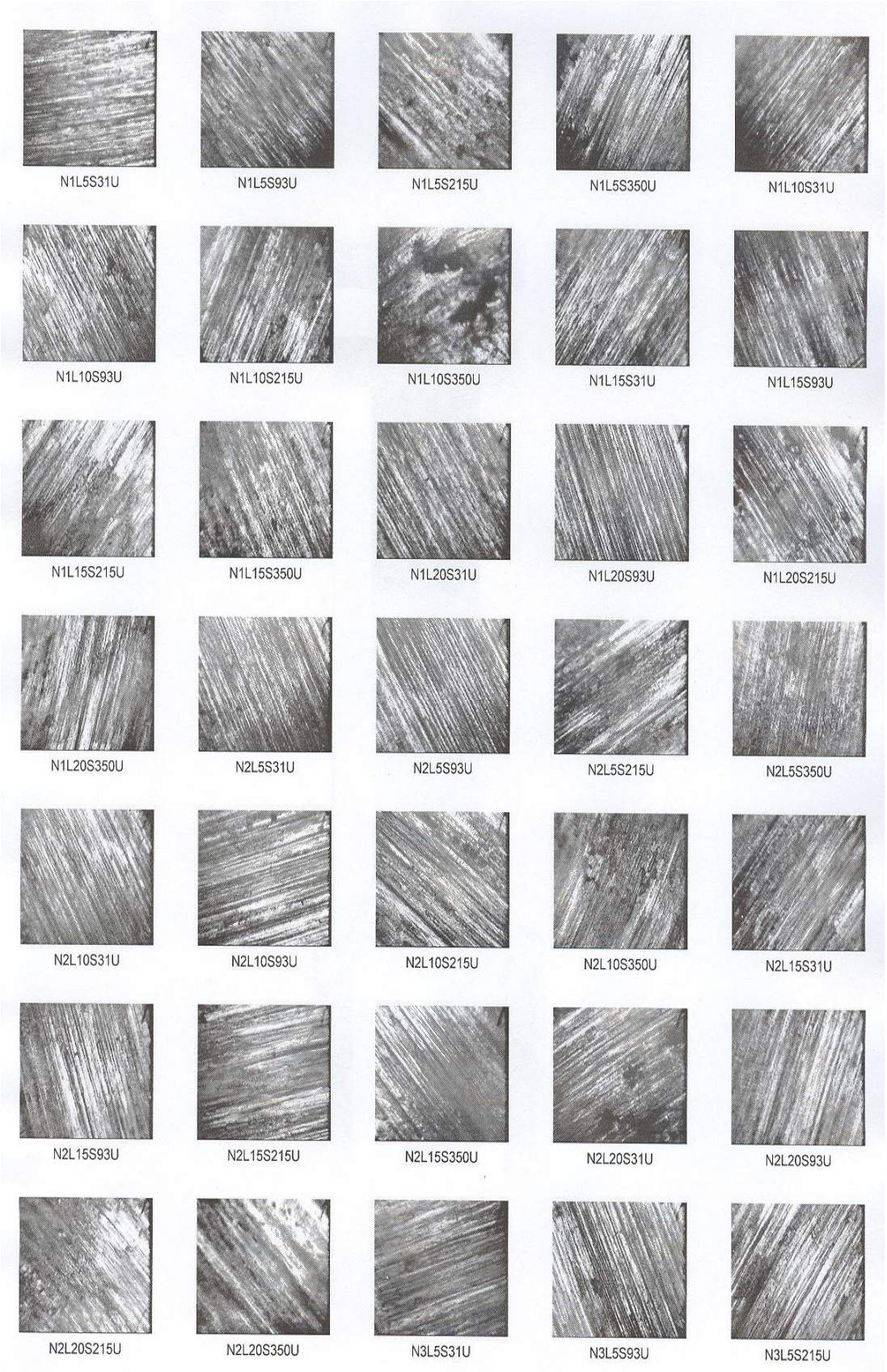

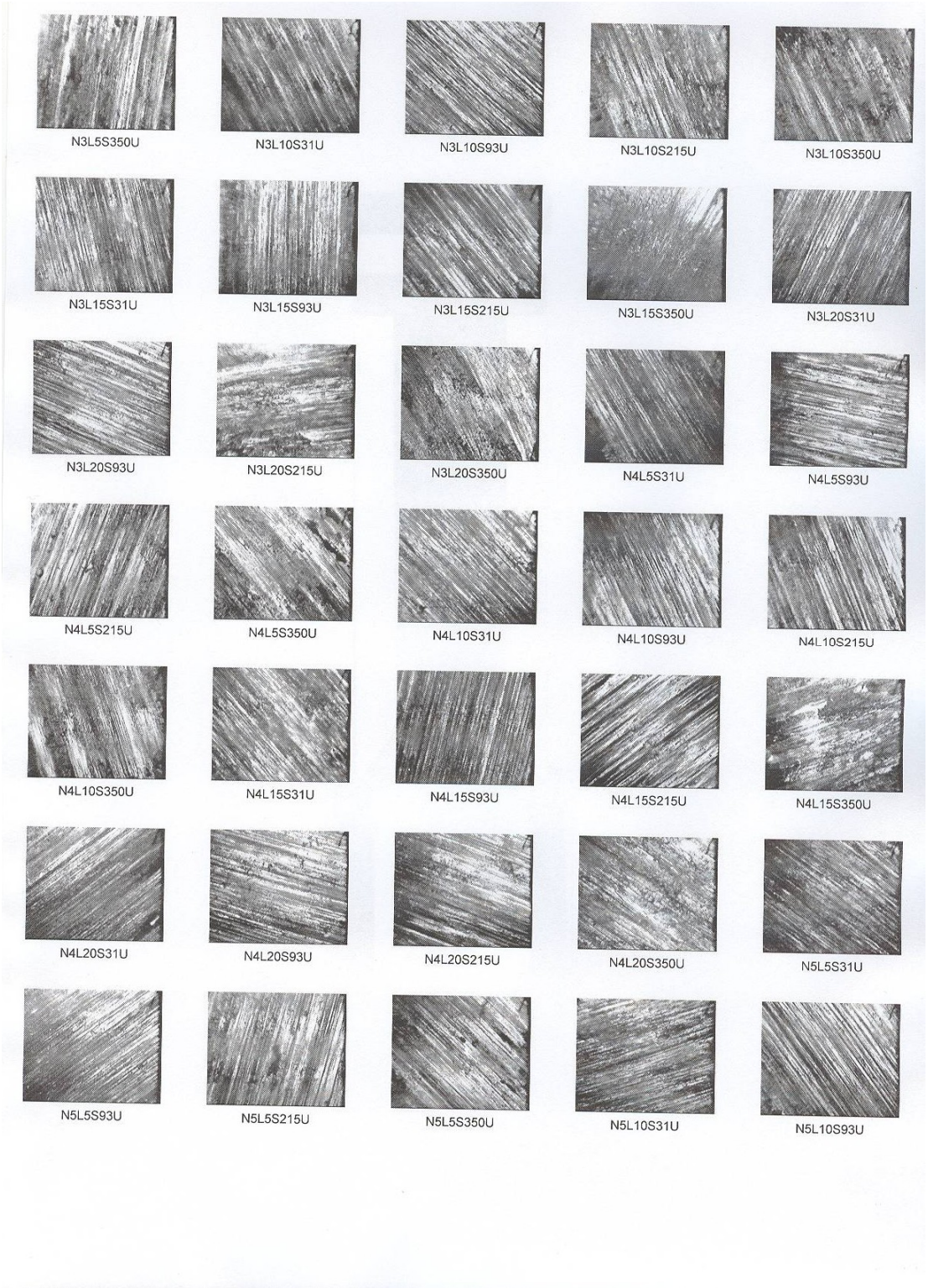

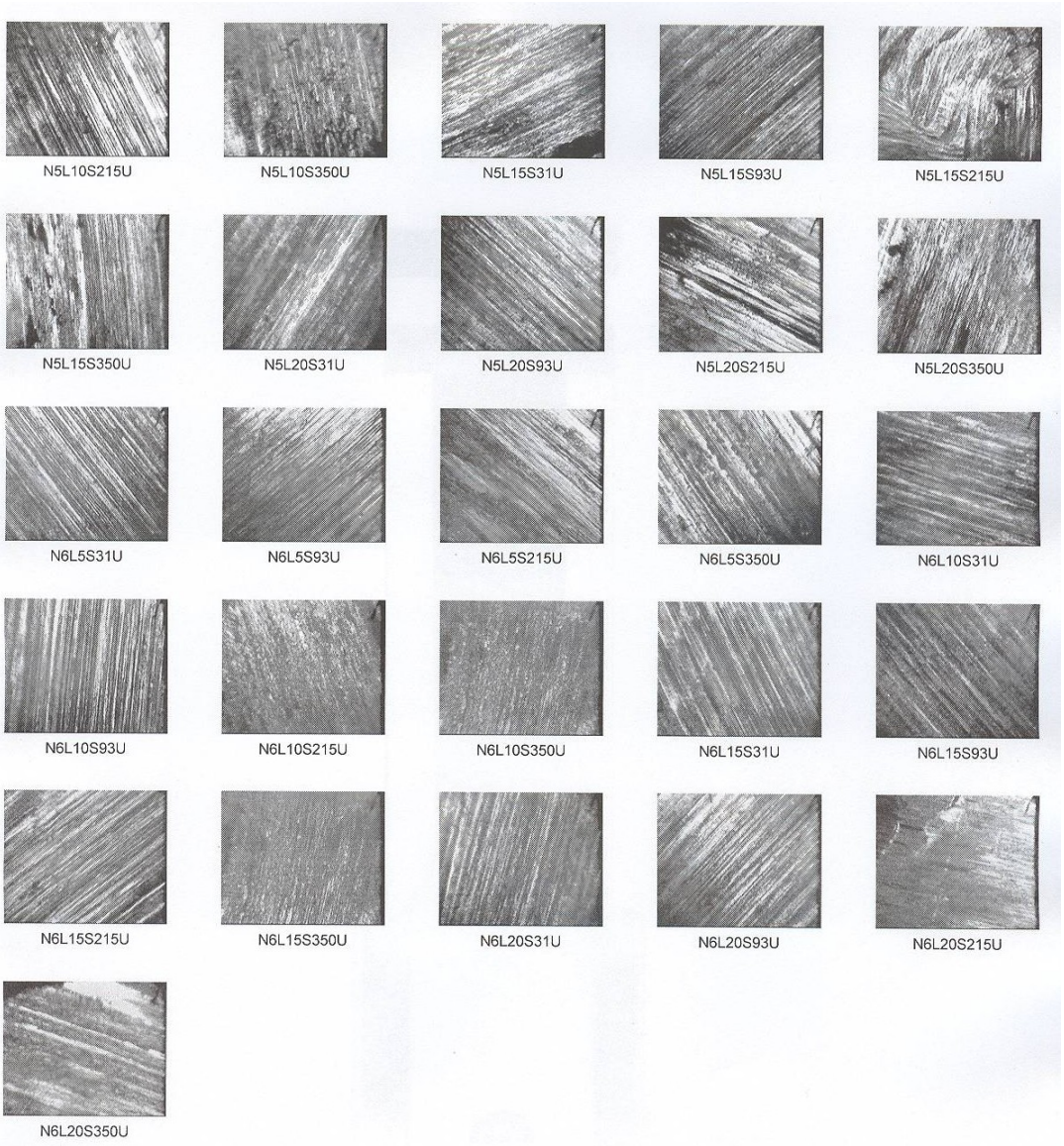

APPENDIX (D) : PROGRAMS AND REPORTS

Report (1) : FEM analysis using pro-engineer package.

(Pro/MECHANICA STRUCTURE Version 24.8(818
"Summary for Design Study "Analysis Punch
Tue Dec 19, 2006 01:53:43

Run Settings
Memory allocation for block solver: 128.0
...Checking the model before creating elements
These checks take into account the fact that AutoGEM will
automatically create elements in volumes with material
properties, on surfaces with shell properties, and on curves
.with beam section properties
.Generate elements automatically
...Checking the model after creating elements
No errors were found in the model
Pro/MECHANICA STRUCTURE Model Summary
(Principal System of Units: millimeter Newton Second (mmNs
Length: mm
Force: N
Time: sec
Temperature: C
Model Type: Three Dimensional
Points: 28
Edges: 108
Faces: 139
Springs: 0
Masses: 0
Beams: 0
Shells: 0
Solids: 58
Elements: 58

Standard Design Study
:"Static Analysis "Analysis1
Convergence Method: Single-Pass Adaptive
Plotting Grid: 4
(Convergence Loop Log: (01:53:44
>> Pass 1 <<
(Calculating Element Equations (01:53:44
Total Number of Equations: 600
Maximum Edge Order: 3
(Solving Equations (01:53:44
(Post-Processing Solution (01:53:44
(Checking Convergence (01:53:44
(Resource Check (01:53:44
Elapsed Time (sec): 0.83
CPU Time (sec): 0.77

Memory Usage (kb): 174380
Wrk Dir Dsk Usage (kb): 0
>> Pass 2 <<
(Calculating Element Equations (01:53:44
Total Number of Equations: 1581
Maximum Edge Order: 6
(Solving Equations (01:53:44
(Post-Processing Solution (01:53:44
(Checking Convergence (01:53:44
(Calculating Disp and Stress Results (01:53:45
because all external element edges lie
in regions that are constrained or where
.the stress is potentially singular
(Res ource Check (01:53:45
Elapsed Time (sec): 1.71
CPU Time (sec): 1.34
Memory Usage (kb): 174934
Wrk Dir Dsk Usage (kb): 2048
Total Mass of Model: 1.350952e-04
Total Cost of Model: 0.000000e+00
:Mass Moments of Inertia about WCS Origin
Ixx: 2.86936e-01
Ixy: 1.20983e-07 Iyy: 2.86936e-01
Ixz: -5.45550e-07 Iyz: -5.42041e-07 Izz: 5.88174e-03
:Principal MMOI and Principal Axes Relative to WCS Origin
Max Prin Mid Prin Min Prin
e-01 2.86936e-01 5.88174e-032.86936
WCS X: 8.38897e-01 -5.44290e-01 1.94108e-06
WCS Y: 5.44290e-01 8.38897e-01 1.92860e-06
WCS Z: -2.67809e-06 -5.61384e-07 1.00000e+00
:Center of Mass Location Relative to WCS Origin
(e-05, -1.81204e-04, 3.52878e+018.87441)
:Mass Moments of Inertia about the Center of Mass
Ixx: 1.18712e-01
Ixy: 1.20981e-07 Iyy: 1.18712e-01
Ixz: -1.22488e-07 Iyz: -1.40588e-06 Izz: 5.88174e-03
:Principal MMOI and Principal Axes Relative to COM
Max Prin Mid Prin Min Prin
e-01 1.18712e-01 5.88174e-031.18712
WCS X: 8.38896e-01 -5.44292e-01 1.08559e-06
WCS Y: 5.44292e-01 8.38896e-01 1.24602e-05
WCS Z: -7.69266e-06 -9.86191e-06 1.00000e+00
Constraint Set: ConstraintSet1
Load Set: LoadSet1
:Resultant Load on Model
in global X direction: -1.980360e-14
in global Y direction: -1.310063e-14
in global Z direction: -8.422000e+01
:Measures

```
max_beam_bending:   0.000000e+00
max_beam_tensile:   0.000000e+00
max_beam_torsion:   0.000000e+00
max_beam_total:     0.000000e+00
max_disp_mag:       2.643744e-05
max_disp_x:         4.646258e-06
max_disp_y:        -4.600077e-06
max_disp_z:        -2.643744e-05
max_prin_mag:      -1.508536e+00
max_rot_mag:        0.000000e+00
max_rot_x:          0.000000e+00
max_rot_y:          0.000000e+00
max_rot_z:          0.000000e+00
max_stress_prin:    9.451947e-01
max_stress_vm:      1.383595e+00
max_stress_xx:     -1.500639e+00
max_stress_xy:     -1.498138e-01
max_stress_xz:     -7.031695e-01
max_stress_yy:     -1.508478e+00
max_stress_yz:     -7.012053e-01
max_stress_zz:     -9.776341e-01
min_stress_prin:   -1.508536e+00
strain_energy:      9.818057e-04
(Analysis "Analysis1" Completed  (01:53:45
------------------------------------------------------------
:Memory and Disk Usage
Machine Type: Windows NT/x86
RAM Allocation for Solver (megabytes): 128.0
Total Elapsed Time (seconds): 1.75
Total CPU Time     (seconds): 1.39
Maximum Memory Usage (kilobytes): 174934
Working Directory Disk Usage (kilobytes): 2048
:(Results Directory Size (kilobytes
Analysis1\. 631
:(Maximum Data Base Working File Sizes (kilobytes
Analysis1.tmp\kel1.bas\. 2048
------------------------------------------------------------
Run Completed
Tue Dec 19, 2006   01:53:45
```

Program 2 : (Mat lab) program for 3D plotting wear results (mass loss, height loss, sliding velocity at different loads)

```
% Surface plots for mass losses for Wear Test, June 13,2007
%load masslossdata
for q=1:2
   %  load the input file which contain the following data:
   %   "rpm, time, Sliding
distance,pureAl,Al+Zr,Al+Ti+B,Al+Ti,Al+Ti+B+Zr,Al+Ti+Zr"
  S1={'Pure Al','Al+Zr','Al+Ti+B','Al+Ti','Al+Ti+B+Zr','Al+Ti+Zr'};
 % w=input('Sliding Distance Plots:1 ,Velocity vs.Time Plots:2 \n');
```

```
   w=2;
 %q=input('Non Extruded :1 ,Extruded :2 \n');
if q==2
      M5=M5E;
      M10=M10E;
      M15=M15E;
   end
 switch w
      case 1
         %input
         %x:nx1; y=1xn; z=length(y)xlength(x)
         x=M5(:,3);
         y=[5 10 15 20];
         s=input('pure Al=1,Al+Zr=2,Al+Ti+B=3,Al+Ti=4,Al+Ti+B+Zr=5,Al+Ti+Zr=6
\n \n');
         z=[M5(:,s+3),M10(:,s+3),M15(:,s+3),M20(:,s+3)]';
         xm=x(1):100:x(end);
         ym=y(1):1:y(end);
         [X1,Y1]=meshgrid(xm,ym);
         Z1=griddata(x,y,z,X1,Y1,'cubic');
         surf(X1,Y1,Z1), hold on
         xlabel('Sliding Distance (m)','Rotation',10);
         ylabel('Force(N)','Rotation',-20);
         zlabel('Mass Loss(g)');
         title(['Mass Loss Vs. Force & Sliding Distance for  ',char(S1(s))]);
      case 2
         % Surfafe plots MassLoss vs. Velocity,Time for different loads and materials
         %input
         %x:nx1; y=1xn; z=length(y)xlength(x)
  % s=input('pure Al=1,Al+Zr=2,Al+Ti+B=3,Al+Ti=4,Al+Ti+B+Zr=5,Al+Ti+Zr=6  \n
\n');
         for s=1:6
        for L=1:3
               figure;
               load Saf_masslossdata_NE
               load Saf_masslossdata_E
 % L=input('load 5N:1,load 10N:2, load 15N:3,load 20N:4 \n \n');
               H{1}=('load 5N');
               H{2}=('load 10N');
               H{3}=('load 15N');
               H{4}=('load 20N');
               if L==1
                  M=M5;
               elseif L==2
                  M=M10;
               elseif L==3
                  M=M15;
               else
                  M=M20;
               end
```

```
                x=M(1:4,2); % rotational velocity
                %       y=[91 212 438]; % time
                y=[31 93 215 350]; % time
                for i=1:length(x)
                   for j=1:length(y)
                      z(j,i)=[M(find(M(:,1)==y(j)& M(:,2)==x(i)),s+3)];
                   end
                end
                xm=x(1):1:x(end);
                ym=y(1):10:y(end);
                [X1,Y1]=meshgrid(xm,ym);
                Z1=griddata(y,x,z',Y1,X1,'cubic');
                surf(X1,Y1,Z1), hold on
                xlabel('Time(min)','Rotation',10,'fontsize',10,'fontweight','bold');
                ylabel('Rotational Speed (rev/min)','Rotation',-
25,'fontsize',10,'fontweight','bold');
                zlabel('Mass Loss(g)','fontsize',10,'fontweight','bold');
                if q==2
                   title(['Mass Loss Vs. Time & Rotaional Speed for  ',char(S1(s)),'
Extruded at ',char(H{L})],'fontsize',10,'fontweight','bold');
                else
                   title(['Mass Loss Vs. Time & Rotaional Speed for  ',char(S1(s)),' at '
,char(H{L})],'fontsize',10,'fontweight','bold');
                end
                axis([0 60 0 400 0 0.055]);
                for i=1:length(x)
                   for j=1:length(y)
                      plot3(x(i,1),y(1,j),z(j,i),'o',...
                         'MarkerFaceColor','k',...
                         'MarkerSize',7), hold on;
                   end
                end
                clear x y z xm ym X1 Y1 Z1;
             end
          end

    end
end
```

ABSTRACT IN ARABIC

دراسة تأثير إضافة بعض العناصر النادرة على السلوك الميكانيكي، قابلية التشكيل ومقاومة البلي للألمنيوم

إعداد
صفوان محمد أحمد القوابعة

المشرف
الأستاذ الدكتور عدنان إبراهيم زيد الكيلاني

ملخص

الألمنيوم ومعظم سبائكه تتجمد على شكل حبيبات كبيرة في غياب المنعمات و التي تؤدي إلى انخفاض الخصائص الميكانيكية وجودة السطح ، يمكن الحصول على حبيبات ناعمة نتيجة بإضافة بعض العناصر مثل التيتانيوم والبورون أثناء عملية الصهر قبل الانجماد. وبعد إجراء المسح والمراجعة للأبحاث المتعلقة بتنعيم الحبيبات تبين أنها تناولت تأثير المنعمات وهي التيتانيوم، البورون، الزركونيوم، الكروميوم، الليثيوم، المولبدنيوم ، الفانديوم على الناحية المتالورجية و قليل من المنشورة قد تناولت تأثير المنعمات على السلوك الميكانيكي، مقاومة الكلل ومقاومة البلي ولم يتضح أن هناك أي بحث قد تناول تأثير هذه المنعمات على قابلية الألمنيوم للتشكيل مما شكل أساس هذا البحث.

أصبحت إضافة هذه المنعمات من أساسيات سباكة الألمنيوم وسبائكه لزيادة المقاومة الميكانيكية ونعومة السطح حيث يستخدم التيتانيوم والتيتانيوم مع البورون لهذا الغرض. تمت في هذه الأطروحة دراسة تأثير إضافة عنصر الزركونيوم بنسبة 0.1 % الى الألمنيوم و الألمنيوم المنعم بالتيتانيوم او التيتانيوم + البورون (وهي النسبة المستخدمة في الصناعة) على البنية الميتالورجية والخواص الميكانيكية وقابلية التشكيل (من خلال عمليتي البثق و الانضغاط) إضافة إلى مقاومة البلي. حيث تم الحصول على النتائج ومناقشتها.

تبين من النتائج التي تم الحصول عليها أن إضافة التيتانيوم مع البورون أفضل من إضافته لوحده بالرغم من أن البورون كعنصر ليس منعما للحبيبات وكمية التيتانيوم هي ثلث الكميةالمستخدمة عند إضافته لوحده.كما وجد أيضا إن تأثير إضافة 0.1 % زركونيوم أدى إلى تسمم التركيبة الميتالورجية في حين إن إضافته إلى الألمنيوم المنعم باستخدام التيتانيوم أو التيتانيوم مع البورون قد تسبب في زيادة كفاءة التنعيم لكل منها. كما وجد أن إضافة التيتانيوم مع البورون إلى الألمنيوم قد أدى إلى تحسين في الصلادة والخواص الميكانيكية في حين إن إضافة التيتانيوم أدت إلى انخفاض في الخصائص الميكانيكية.

إن تأثير إضافة الزركونيوم إلى سبائك الألمنيوم المنعمة بالتيتانيوم أدت إلى انخفاض قيم الصلادة والخصائص الميكانيكية الأخرى ما عدا المطيلية ، في حين أن إضافته إلى سبائك الألمنيوم المنعمة بالتيتانيوم والبورون أدت إلى انخفاض قيم الصلادة والخصائص الميكانيكية ولوحظ ارتفاعا في القيمة القصوى لحمل للشد.

أدت عملية البثق إلى تنعيم أخر في الحبيبات لجميع السبائك، حيث ارتفعت قيم الصلادة أما بالنسبة إلى الخصائص الميكانيكية فقد ارتفعت قيم الإجهاد و القيمة القصوى للشد أما بالنسبة إلى المطيلية فقد تحسنت في سبائك الألمنيوم المنعمة بالتيتانيوم و سبائك الألمنيوم المنعمة بالتيتانيوم والبورون و سبائك الألمنيوم المنعمة بالتيتانيوم والبورون والزركونيوم وانخفضت في سبائك الألمنيوم المنعمة بالتيتانيوم والزكونيوم وسبائك الألمنيوم المنعمة بالزكونيوم.

إن تأثير هذه الإضافات على البلى والمعتمدة على فرضيات نقص الوزن وفرضية معامل البلى المقترح من قبل اركارد لم تعطي تفسيرا للنتائج لأنها لا تأخذ بعين الاعتبار التشكيل اللدن الذي يحدث في نهاية العينة لذا وضعت فرضية جديدة تأخذ هذا الأمر بعين الاعتبار، وقد كانت أكثر واقعية في تمثيل نتائج البلي لهذه السبائك.